



universität
wien

DISSERTATION

Titel der Dissertation

**Discovery and Mechanistic Characterization of Natural Products
Acting as PPAR γ Agonists or NF- κ B Inhibitors**

angestrebter akademischer Grad

Doktor der Naturwissenschaften (Dr. rer.nat.)

Verfasserin / Verfasser:	Nanang Fakhrudin
Matrikel-Nummer	0748883
Dissertationsgebiet (lt. Studienblatt):	Pharmazie
Betreuerin / Betreuer:	Univ.-Prof. Dr. Verena Dirsch

Wien, im Februar 2011

**For my wife and my children,
*"I am going back home"***

Don't ever let somebody tell you: "You can't do something".

You got a dream, you got to protect it.

If you want something, go..., get it!

(Will Smith, Pursuit of Happiness)

ABSTRACT

Atherosclerosis is an inflammatory disease which is initiated by accumulation of low-density lipoprotein cholesterol in the arterial wall that activate the endothelium and provoke local vascular inflammation finally leading to the formation of an atherosclerotic plaque. Nuclear factor kappa B (NF- κ B) and peroxisome proliferator-activated receptor gamma (PPAR γ) are among the transcription factors involved in the regulation of inflammation in the development of atherosclerosis. The aim of this study was to find natural compounds activating PPAR γ and/or inhibiting NF- κ B, thus having a potential antiatherosclerosis action. The selection of natural products or plants was based on ethnopharmacological and computational approaches.

Screening of natural compounds was performed using appropriate reporter gene assays in HEK-293 cells. Further mechanistic characterization of some of the identified compounds was performed in relevant cells models for vascular inflammation.

Three neolignans from *Magnolia officinalis* and 6 polyacetylenes from *Notopterygium incisum* were identified as activators of PPAR γ . All those compounds exhibited maximal activation of PPAR γ several folds lower than the full agonist pioglitazone, and with an activation pattern suggesting partial agonism. Interestingly, all compounds (except the neolignan magnolol) are selective agonists of PPAR γ . Moreover, plumericin and 4 benzofurans isolated from *Himantus suluensis* and *Krameria lappacea*, respectively, were discovered as NF- κ B inhibitors. These compounds inhibited TNF- α -induced NF- κ B activation in 293/NF- κ B-luc cells but showed distinct mode of actions. Plumericin significantly inhibited I κ B- α degradation, whereas KT8 (the most active compound among the 4 benzofurans) failed to do so, suggesting that plumericin targets the proteins upstream of I κ B- α degradation, whereas KT8 might target proteins downstream of I κ B- α within the NF- κ B pathway. These findings might contribute to the development of promising leads for an antiinflammatory therapy, and provide scientific evidence for the traditional use of the investigated plants against inflammatory diseases.

ZUSAMMENFASSUNG

Atherosklerose ist eine entzündliche Erkrankung, die durch Akkumulation von LDL-Cholesterin in der arteriellen Wand ausgelöst wird. Dies aktiviert das Endothel, ruft eine lokale Gefässentzündung hervor und führt in der weiteren Folge zur Bildung von atherosklerotischen Plaques. Nuclear factor-kappa B (NF- κ B) und der Peroxisome proliferator-activated receptor gamma (PPAR γ) sind Transkriptionsfaktoren, die an der Regulation dieser Entzündungsprozesse beteiligt sind. Das Ziel dieser Arbeit war es, Naturstoffe zu finden, die PPAR γ aktivieren und/oder NF- κ B inhibieren und dadurch eine potentiell antiatherosklerotische Wirkung besitzen. Die Auswahl des Naturstoffe erfolgte nach ethnomedizinischen Gesichtspunkten bzw. durch computer-gestütztes Modelling. Für die Identifikation von PPAR-Agonisten bzw. NF- κ B-Inhibitoren wurden entsprechende Luciferase-Reporter-Gen-Assays in HEK-293 Zellen durchgeführt. Die weitere Charakterisierung des Wirkmechanismus einiger identifizierter Substanzen erfolgte in ausgewählten für vasculäre Entzündung relevanten Zellmodellen.

Aus *Magnolia officinalis* and *Notopterygium incisum* wurden 3 Neolignane bzw. 6 Polyacetylene als Aktivatoren von PPAR γ identifiziert. All diese Substanzen zeigen eine maximale PPAR γ Aktivierung, die um ein Vielfaches unter der des vollen Agonisten Pioglitazon liegt. Ihr Aktivitätsmuster deutet auf einen partiellen Agonismus hin. Interessanterweise sind all diese Substanzen, ausser Magnolol, selektive Agonisten von PPAR γ . Ausserdem wurden Plumericin aus *Himantus succuba* und vier Benzofurane aus *Krameria lappacea* als NF- κ B Inhibitoren identifiziert. Diese Substanzen hemmen die TNF- α induzierte NF- κ B Aktivierung in 293/NF- κ B-luc Zellen aber zeigen unterschiedliche Wirkmechanismen. Plumericin hemmt den I κ B- α Abbau, während KT8 keinen Einfluss darauf hat. Das deutet darauf hin, dass Plumericin dem I κ B- α vorgeschaltete Proteine im NF- κ B Signalweg beeinflusst, während KT8 ein nachgeschaltetes Protein beeinflusst. Diese Ergebnisse könnten zur Entwicklung vielversprechender Leitsubstanzen zur Behandlung entzündlicher Erkrankungen beitragen, sowie die wissenschaftliche Grundlage für den traditionellen Gebrauch der untersuchten Pflanzen gegen Entzündungen darstellen.

A. CONTENTS

A. CONTENTS

Table of Contents

A. CONTENTS	1
B. INTRODUCTION	5
1. Background.....	5
1.1. Inflammation and atherosclerosis	5
1.2. Targeting inflammation in atherosclerosis	6
2. Aim of the work	7
3. Nuclear receptors	7
4. Peroxisome proliferator-activated receptors (PPARs)	8
4.1. Activators of PPARs.....	10
4.2. PPAR γ	11
4.3. PPAR γ and inflammation.....	12
4.4. PPAR γ activators	14
4.5. Natural products activating PPAR γ	15
5. NF- κ B and I κ B proteins.....	16
5.1. NF- κ B signalling.....	17
5.2. IKK in the NF- κ B signaling pathway.....	19
5.3. Role of NF- κ B in atherosclerosis	20
5.4 Inhibitors of NF- κ B	22
6. Drugs from nature targeting inflammation	24
C. MATERIALS AND METHODS	28
1. Materials	28
1.1. Products and supplier information	28
1.2. Culture medium and supplements	30
1.3. Commercially available kits.....	32
1.4. Reagents and buffers.....	32
1.5. Antibodies	35
1.6. Scientific software	36
1.7. Technical equipment.....	36
2. Methods	37

2.1. Identification of PPAR γ agonists.....	37
2.1.1. HEK-293 cells.....	37
2.1.2. Transient transfection.....	38
2.1.3. Luciferase reporter gene assay to detect PPAR γ activation.....	39
2.1.4. Data analysis.....	41
2.1.5. Preparation of charcoal-stripped FBS	42
2.1.6. DNA plasmid preparation.....	42
2.1.7. PPAR γ coactivator assay.....	43
2.1.8. Adipocyte differentiation assay	44
2.2. Identification of NF- κ B inhibitors	45
2.2.1. 293/NF- κ B-luc cells	45
2.2.2. Luciferase reporter gene assay to detect NF- κ B inhibition.....	45
2.2.3. IKK- β inhibition assay	46
2.2.4. Experiments with endothelial cells.	46
2.2.5. Experiments with vascular smooth muscle cells.....	50
2.2.6. Experiments with RAW 264.7 macrophages	51
2.2.7. Resazurin-staining assay.....	52
2.3. Statistics	53
C. RESULTS	55
1. Discovery of PPAR γ agonists	55
1.1. Optimization of transfection efficiency	55
1.2. Validation of the bioassay.....	56
1.3. Investigation of a PPAR γ -activating potential of plant extracts.....	57
1.4. Discovery of PPAR γ agonists guided by pharmacophore modeling.....	59
1.4.1. PPAR γ ligand binding assay	60
1.4.2. PPAR γ luciferase reporter gene transactivation	61
1.4.3. Coactivator recruitment assay	62
1.4.4. Molecular docking studies.....	63
1.4.5. Selectivity study.....	65
1.4.6. Adipogenic activity in 3T3-L1 preadipocytes	67
1.5. The effect of PPAR γ agonists on the NO production in macrophages	69
1.6. The effect of PPAR γ agonists on the migration of VSMC.....	70
1.7. Discovery of PPAR γ agonists by an ethnopharmacological approach.	70

1.7.1. Pharmacological evaluation of extracts in the PPAR γ -driven reporter gene assay	71
1.7.2. Discovery of PPAR γ agonists from <i>Notopterygium incisum</i>	71
2. Discovery of NF- κ B inhibitors	75
2.1. Validation of the bioassay	75
2.2. Investigation of NF- κ B inhibitors from plant extracts.....	76
2.2.1. Discovery of plumericin as a NF- κ B inhibitor	77
2.2.2. Discovery of NF- κ B inhibitors from <i>Krameria lappacea</i>	82
2.3. Identification of an IKK- β inhibitor by a virtual screening approach	84
D. DISCUSSION	88
1. Assay optimization and verification.....	88
2. Discovery of PPAR γ agonists and NF- κ B inhibitors from plant extracts	89
3. Discovery of neolignans as activators of PPAR γ	89
4. Examination of PPAR γ agonists in further cell models relevant for atherosclerosis..	92
5. Discovery of polyacetylenes as activators of PPAR γ	93
6. Discovery of plumericin as a NF- κ B inhibitor	94
7. Discovery of benzofurans as NF- κ B inhibitors.....	96
8. Discovery of a novel IKK- β inhibitor by ligand-based virtual screening	96
E. SUMMARY	99
F. REFERENCES	102
G. APPENDIX	125
1. SUPPLEMENTARY DATA	125
2. ABBREVIATIONS	146
3. PUBLICATIONS	150
4. CURRICULUM VITAE	154
5. ACKNOWLEDGMENTS	156

B. INTRODUCTION

B. INTRODUCTION

1. Background

1.1. Inflammation and atherosclerosis

Inflammation is the body's response to injury and constitutes to various chronic diseases and disorders including atherosclerosis. For years, efforts to understand the role of inflammation in atherosclerosis have flourished. Previously considered as mere lipid accumulation disease, atherosclerosis is now also seen as an inflammatory disease due to significant discoveries with respect to the underlying cellular and molecular mechanisms leading to atherosclerosis. Scientific evidence has demonstrated the presence of inflammatory markers during atherogenesis and suggested the association between inflammation and atherosclerosis [1, 2].

In atherosclerosis, hallmarks of inflammation occur hand-in-hand following lipid accumulation in the artery wall. Central events in acute as well as chronic inflammation are the emigration of leucocytes from the blood vessel to the site of injury and leukocyte activation. These events also occur in the initial steps of atherogenesis. Under normal condition, leukocytes poorly adhere to the endothelium surface. However, accumulation of cholesterol-containing low-density lipoproteins in the intima activates the endothelium, provokes a local vascular inflammation and initiates atherogenesis. This leads to the production and surface expression of adhesion molecules such as VCAM-1, ICAM-1 and E-selectin, and subsequent attachment of leukocytes to endothelial cells which form the inner layer at the blood vessel. Once attached to the endothelium via adhesion molecules, leukocytes start to translocate into the intima, a process that is supported by chemoattractant molecules such as MCP-1. The presence of chemoattractants in the intima attracts monocytes to migrate into the site of lesion in the intima and to differentiate into macrophages which produce proinflammatory proteins and growth factors. Monocytes further undergo a series of phenotypic

changes and engulf the oxidized LDL to differentiate into foam cells loaded with massive cholesterol accumulation. Foam cells produce a variety of growth factors and cytokines that induce VSMC proliferation and migration. In addition, metalloproteinases which are responsible for matrix degeneration are also produced. Eventually, an atherosclerotic plaque is formed and leads to narrowing of the artery. Therefore, atherosclerosis is appropriately regarded as an inflammatory process [3-6].

Proinflammatory proteins contribute not only to the development of atheroma but also to the complications of atherosclerosis. Exaggerated inflammatory activation can lead to local proteolysis, plaque rupture, and thrombus formation. These events indicate that inflammation plays a vital role in atherosclerosis [1, 7].

1.2. Targeting inflammation in atherosclerosis

The important role of inflammation in the progression of atherosclerotic plaques has been investigated and has gained increased interest [1]. Current understanding on the nature of atherosclerosis and its pathogenesis has led to the identification of novel therapeutic targets. There is a firm indication that targeting inflammation is a promising approach for chronic inflammatory diseases such as atherosclerosis [8, 9].

Many studies have suggested that interference with the transcription of proinflammatory genes can inhibit atherogenesis. Crucial transcription factors involved in inflammation are Nuclear Factor Kappa B (NF- κ B) with proinflammatory and Peroxisome Proliferator-Activated Receptor γ (PPAR γ) with antiinflammatory action. NF- κ B represents the predominant transcription factor in the inflammatory response including the regulation of leukocyte extravasation and activation. Expression of many genes involved in the inflammatory response such as those of chemokines (MCP-1, IL-8), cytokines (TNF, IL-1 β , IL-6/10/12, IFN- γ), mediator producing enzymes (COX-2, 5-LOX, iNOS), and adhesion molecules (e.g. E-Selectin, ICAM-1) [10-12] are also regulated by NF- κ B.

PPAR γ , a nuclear receptor which serves as a main transcriptional regulator of genes involved in glucose and lipid metabolism [13] [14], is expressed in VSMC, the endothelium and macrophages, large intestine, kidney and liver [15-17]. More importantly, this receptor is reported to interfere with vascular inflammation in the early development of atherosclerosis by dampening NF- κ B-regulated gene expression [18-20].

2. Aim of the work

Considering the important role of PPAR γ and NF- κ B in the regulation of inflammation, the main aim of this study was to identify and characterize natural products with a promising antiinflammatory profile by targeting PPAR γ and the NF- κ B signalling pathway. A computational and an ethnopharmacological approach were hereby used to identify novel PPAR γ agonists and NF- κ B inhibitors from medicinal plants. Further mechanistic characterization and validation of the active compounds were also performed in relevant cell for atherosclerosis.

3. Nuclear receptors

Nuclear receptors are ligand-dependent transcription factors which have an important role in development, endocrine signalling and metabolism. They bind to DNA as monomer, homodimer, or heterodimer and affect gene transcription in conjunction with a variety of cofactors or coactivators. The main function of nuclear receptors is to mediate transcriptional activity through the recruitment of positive or negative regulatory proteins, termed as coactivators or corepressors, respectively, in response to hormones and other metabolic ligands. The recruitment of corepressor complexes is a crucial step in mediating active repression of unliganded nuclear receptors whereas the recruitment of coactivator complexes mediates ligand-induced transcriptional activity. There are around 50 members of the nuclear receptor family in humans that regulate a complex genetic network in

which the physiological responses are defined by their coordinated activity. Some nuclear receptors are ligand-inducible transcription factors, while others lack identified ligands and are termed “orphan” receptors [21-23].

The activity of nuclear receptors is regulated by at least three different mechanisms: 1) binding of a small lipophilic ligand to the receptor and heterodimerization with its partner; 2) covalent modification, usually phosphorylation occurring at the cellular membrane or during the cell cycle; and 3) interactions with other transcription factors including nuclear receptors themselves [24]. Understanding of nuclear receptors has grown over the years and nuclear receptors have developed into a highly diverse family in terms of both their physiological role and molecular action. In the classical view, these receptors are activated by a unique high-affinity ligand with a dissociation constant in the nanomolar range, such as in the case of the estrogen receptor and the androgen receptor. More recently, some nuclear receptors so-called ‘metabolic receptors’, such as the PPARs have been identified and they are activated by numerous but low-affinity ligands with dissociation constants in the micromolar range [25].

4. Peroxisome proliferator-activated receptors (PPARs)

Peroxisome Proliferator-Activated Receptors (PPARs) are ligand-dependent nuclear receptors first identified and cloned in 1990. Initially, these receptors were found to be activated by phthalate ester plasticizers used in the plastics manufacture and the hypolipidemic agent fibrate that were found to increase the number of peroxisome in liver tissue and then were called “peroxisome proliferators” and the respective receptors peroxisome proliferator-activated receptors [26, 27]. The family of PPARs comprises three identified sub-types; PPAR α , PPAR β/δ and PPAR γ , and they have been found in human [28], monkey [29], mouse [30] and fish [31]. PPARs are encoded by distinct single-copy genes with different locations in the chromosome. In humans, PPAR α , β/δ and γ are encoded by chromosome number 22, 6 and 3 whereas in mice they are encoded by chromosomes 15, 17 and 6, respectively [28, 32, 33].

PPARs are expressed in different tissues and cell types and regulate distinct functions and activities. PPAR α is expressed in muscle, liver, heart and kidney where fatty acid catabolism is commonly taking place. PPAR α has a major role in the regulation of genes involved in lipid and lipoprotein metabolism [14, 34, 35]. PPAR γ is expressed in adipose tissue, lung and the large intestine, kidney, liver, heart and macrophages [16]. PPAR γ activation is closely related with increased insulin sensitivity and anti diabetes activity [36]. The last subtype, PPAR β/δ is ubiquitously expressed in various tissues and associated with lipid metabolism and energy expenditure [37].

Similar to other nuclear receptors, PPARs have a poorly conserved N-terminal domain (A/B) that functions in a ligand-independent manner and modulates receptor activity. As shown in **Figure 1a**, a variable hinge region (D) is located close to the DNA binding domain (C), followed by a highly conserved ligand-binding domain (LBD) (E), and a variable C-terminus (F). The LBD is important for hormone recognition, ensures a specific and selective physiologic response, and acts as a molecular switch that turns the receptor to a transcriptionally active state. A highly conserved DNA binding domain (C) which targets the receptor to a specific DNA sequence known as response element is located close to the N-terminal region. This domain comprises two zinc-finger-like structures with α -helical DNA binding motifs [38, 39]. **Figure 1b** shows that once activated by ligands, PPARs bind to the respective response elements located in the promoter region of their target genes and further form a heterodimer with another nuclear hormone receptor, the 9-cis retinoic acid receptor (RXR) [40]. The PPAR response element (PPRE) consists of two direct repeat sequences, separated by one nucleotide: AGGTCA n AGGTCA (“n” represents any nucleotide) [41]. Binding of PPAR/RXR heterodimers to PPRE triggers the recruitment of nuclear receptor coactivator proteins or cofactors [42, 43] and further results in a chromatin rearrangement that mediates initiation of the transcription of the target genes [44, 45].

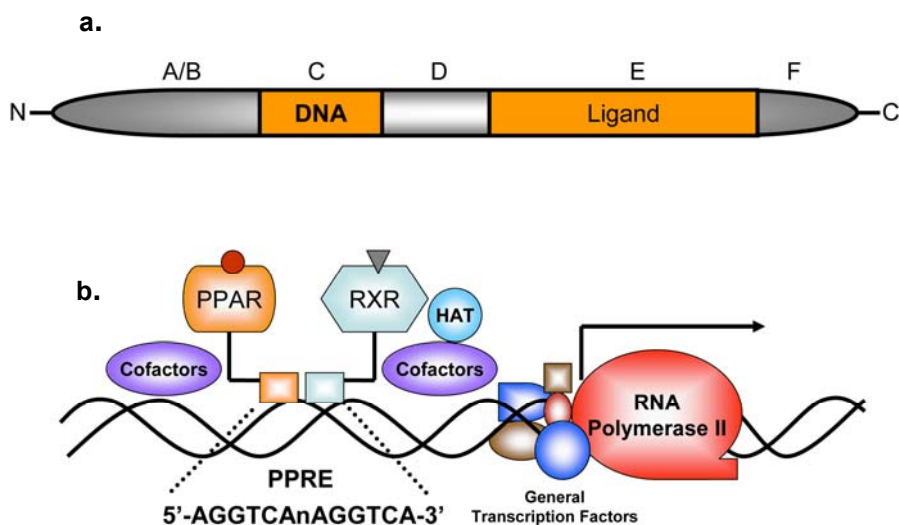


Figure 1. Functional domains of PPARs and their activation pathway. (a) The binding domains of PPARs. (b) PPAR activation upon ligand binding. Figure is adapted from [38, 39].

4.1. Activators of PPARs

Although the basic activation mechanism of PPARs is similar to that for the steroid hormone receptors, ligands of PPARs are chemically more diverse [46]. PPARs can be activated by various endogenous ligands such as linoleic acid, linolenic acid, eicosapentaenoic acid, docosahexanoic acid, hydroxyeicosatetraenoic acids (HETEs), leucotrienes, and eicosanoids [47, 48], and different synthetic ligands. PPAR α can be activated by synthetic fibrates, a clinically approved class of drug to treat dyslipidemia [49]. The synthetic antidiabetics, thiazolidinediones are activators of PPAR γ , whereas the synthetic compounds GW501516 [50] and GW0742 [51] are selective activators of PPAR β/δ . In contrast to PPAR α and γ , there is no PPAR β/δ activator approved for clinical use so far [48]. Recently, rosiglitazone, a thiazolidinedione activator of PPAR γ , has been withdrawn from the European market and has been alerted by the FDA due to increased cardiovascular risk [52-54]. **Figure 1** summarizes the variety of compounds that activate PPARs.

Table 1. Synthetic and endogenous compounds activating PPARs [48, 55]

Ligand class	PPARα	PPARβ	PPARγ
Synthetic agonists	GW7647	GW0742	Rosiglitazone
	WY14643	GW501516	Troglitazone
	Clofibrate	L165041	Pioglitazone
	Fenofibrate		JTT-501
	Cipofibrate		Muraglitazar
	Bezafibrate		Tesaglitazar
	Gemfibrozil		Farglitazar
	Muraglitazar		
	Tesaglitazar		
	Farglitazar		
Fatty acids	Docahexanoid acid	Docahexanoid acid	Docahexanoid acid
	Arachidonic acid	Arachidonic acid	Arachidonic acid
	Linoleic acid	Linoleic acid	Linoleic acid
Eicosanoids	15d-PGJ2	15d-PGJ2	15d-PGJ2
	Prostacyclin	Prostacyclin	Prostacyclin
	8-(R)HETE		8-(R)HETE
	13-(R/S)HODE		13-(R/S)HODE
	LTB ₄		9-oxoODE

4.2. PPAR γ

PPAR γ is one of the best characterized nuclear receptors and its ligands have been clinically developed as type 2 antidiabetic agents [36]. In contrast to PPAR α which is involved in the catabolism process, this receptor regulates anabolism processes such as gluconeogenesis and glucose transport. Predominantly expressed in insulin-responsive tissues such as adipose tissue, PPAR γ activation induces adipocyte differentiation (adipogenesis), glucose uptake and insulin sensitivity [56-58]. Excess glucose is stored in adipocytes as lipid. PPAR γ plays a significant role in the glucose transport and metabolism by controlling glucose uptake mediated by glucose transport proteins responsive to

insulin such as GLUT4 [59, 60]. Despite its major function in metabolism, recent studies showed that PPAR γ also plays a significant role in inflammation [18, 61-63] which will get special attention in the following chapter.

PPARs have a large T-shaped ligand-binding cavity with mainly hydrophobic pockets buried within the bottom half of the LBD. Rosiglitazone, a selective agonist of PPAR γ forms hydrogen bonds within the LBD and occupies about 40 % of the PPAR γ ligand-binding cavity [38, 64]. The large size of ligand-binding pocket allows binding of a broad range of ligands. Binding of different PPAR γ ligands to the PPAR γ LBD could lead to conformational changes in the LBD with distinct alterations in domain–domain-, receptor–coactivator- and receptor–DNA interactions. The ligands hereby occupy different portions of the LBD and may elicit recruitment of different coactivators [65]. On the contrary, GW9662, a PPAR γ antagonist, interacts with PPAR γ LBD with different binding mode, thus, induces distinct conformation change and transcriptional effects [65-67]. A recent study demonstrated that the difference in the loop conformation induced by binding of fatty acids to the PPAR γ LBD is linked with distinct degrees of transcriptional activity [67, 68]. Thus, ligands of PPAR γ with a broad range of structures and distinct activity have been identified [69].

4.3. PPAR γ and inflammation

PPAR γ is a negative regulator of inflammation through a crosstalk with inflammatory signalling pathways and transcription factors activating these pathways. This mechanism is termed transrepression and is illustrated in **Figure 2**. The mechanism involves interaction between the nuclear receptor and promoter-bound transcription factors, rather than sequence-specific direct interactions with DNA [70]. Ricote et al. have proposed different mechanisms of transrepression through direct interaction of activated PPAR with proinflammatory transcription factors (a), induction of inhibitors (e.g. via increased promoter activity of the I κ B gene) (b), regulation of kinase activities (e.g. JNK) necessary for the transcription activities of AP-1 and NF- κ B (c), competition for coactivators necessary for proinflammatory protein transcription (d), and inhibition of

corepressor shedding in the promoter of the proinflammatory proteins (e) [45]. In the latter point, PPAR γ interferes with the inflammatory signalling by inhibition of signal-dependent clearance of corepressor complexes from proinflammatory gene promoters through a SUMOylation-dependent pathway. Hereby, the recruitment of the proteasome machinery is blocked which is required for the clearance of the corepressor complex as a prerequisite for the transcription of proinflammatory proteins [71].

In the progression of atherosclerosis, increased expression of adhesion molecules is a critical step for further proinflammatory processes and a phenotypic feature of endothelial activation. The expression of adhesion molecules VCAM-1, ICAM-1 and E-selectin was inhibited by constitutive activation of PPAR γ [72]. The suppression of TNF- α -induced ICAM-1 expression by troglitazone, a PPAR γ agonist, was partly dependent on PPAR γ . Similar PPAR γ -dependent antiinflammatory activity was also observed in 15d-PGJ2- and ciglitazone-treated cells, but not with rosiglitazone treatment [73]. After infiltration of mononuclear macrophages in the intima, PPAR γ agonists were found to inhibit the formation of macrophage-derived foam cells by decreasing lipid inclusion, cholesterol and triglyceride level during the inflammation process. PPAR γ also antagonizes the transcription factors AP-1, STAT and NF- κ B, represses the activation of macrophages and inhibits the production of inducible nitric oxide synthase (iNOS) suggesting that PPAR γ could be a potential target for atherosclerosis in which inflammation events exert pathogenic effects [19, 74, 75].

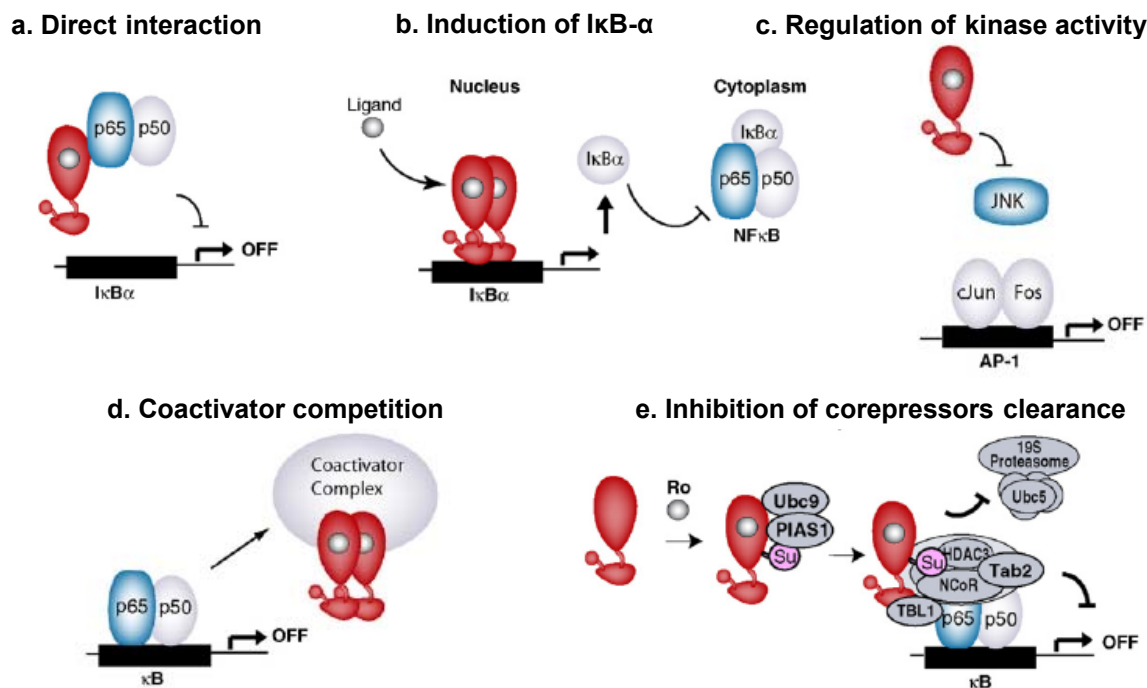


Figure 2. Transrepression mechanisms mediated by PPARs. (a) Direct interaction of PPAR with the p65 subunit of NF- κ B, (b) Induction of I κ B- α expression by PPAR activation. (c) Inhibition of c-Jun N-terminal kinase (JNK) MAPK activity by PPAR activation, (d) Competition for coactivators required for NF- κ B-mediated transcription, (e) Inhibition of corepressor shedding required for NF- κ B-mediated transcription. AP-1, activator protein-1; HDAC3, histone deacetylase 3; NCoR, nuclear-receptor corepressor complexes; TBL1, transducin- β -like 1, TBL1; TBL1-related protein, TBLR1; PIAS1, protein inhibitor of activated STAT1; Ubc5, ubiquitin-conjugating enzyme 5 ; Tab2, TAK1-binding proteins 2. Figure is adapted from [45].

4.4. PPAR γ activators

A broad range of compounds with a variety of structures has been found to activate PPAR γ . The most successful PPAR γ activators are thiazolidinediones which have been clinically used for years as type 2 anti diabetes agents acting via PPAR γ [76]. Thiazolidinediones have high affinity towards the PPAR γ LBD. Activation of PPAR γ by these compounds induces adipogenesis and increases insulin sensitivity [77]. Thiazolidinediones, however, display serious side effects such as weight gain, increased bone fracture, fluid retention, and heart failure [78], limiting their broad therapeutic potential and leading to a great interest in the discovery of novel ligands with more favourable properties. Thus, much effort has

been focused on the discovery and development of selective PPAR γ modulators as a safer alternative to the full agonists of PPAR γ [79, 80].

4.5. Natural products activating PPAR γ

For decades, natural products have inspired the discovery and development of modern drugs and provide a broad range of compounds with a variety of chemical structures and remain an important source of drug discovery [69]. So far, no natural product or any derivative has been approved as PPAR γ activators for the clinical use. However, considering the undesired side effects of the current PPAR γ agonists approved as drug, the discovery of PPAR γ agonists from natural resources is still of a great interest and promise.

Previous studies have shown that various plant extracts [81] and natural products isolated from plants [82-85] are PPAR γ activators. To date, different chemical structures originally isolated from plants have been discovered as PPAR γ ligands. Phenolic compounds isolated from the root of *Glycyrrhiza glabra* [86], the isoflavon genistein and biochanin from red clover extracts [87], kaempferol and quercetin from *Euonymus alatus* [85], naringenin from the flowers of *Sambucus nigra* L. [88], the plant fatty acids octadecadienoic acids (from the seeds of *Coix lacryma*) [89], (9 S,13 R)-12-oxo-phytodienoic acid (from *Chromolaena odorata*) [82], 12-O-methyl carnosic acid and α -linolenic acid (from stems and leaves of *Salvia officinalis*) [90] have been discovered as PPAR γ agonists. Some other compounds such as the monoterpene carvacrol from thyme oil [91], auraptene from the citrus fruit [92], citral from lemon grass [93] and commiphoric acid from *Commiphora mukul* [94] are activators of both PPAR α and γ . Moreover, there are several plant extracts that have been identified to activate PPARs but the active compounds have not determined yet [95, 96].

5. NF- κ B and I κ B proteins

NF- κ B has been first identified by Sen and Baltimore as proteins that bind to the enhancer sequence of the kappa light chain and immunoglobulin heavy chain in an electrophoretic mobility shift assay [97]. NF- κ B is a common name for a family of transcription factors consisting of 5 proteins (**Figure 3a**). Three proteins, p65 (RelA), c-Rel and RelB belong to the Rel family (also called NF- κ B1), whereas the other two proteins, p50 and p52 and their precursor p105 and p100, respectively, belong to the NF- κ B family (also called NF- κ B2). These proteins can form either a homodimer or a heterodimer and the complex of p65/p50 is the most common form often referred to as being “NF- κ B”. All NF- κ B proteins have a conserved 300-amino acid comprising sequence, namely the Rel Homology Domain (RHD). RHD is responsible for the DNA binding, interaction with I κ B proteins, dimerization and it also contains a nuclear localization sequence [98-100]. Although the transactivation domains which are required for efficient transcription of NF- κ B target genes are found only in the C terminal region of RelA, RelB and c-Rel, the p50 and p52 subunits can also be involved in the transactivation of NF- κ B target genes by heterodimerization with RelA, RelB, or c-Rel [101].

In unstimulated cells, NF- κ B complexes are kept inactive in the cytoplasm via noncovalent interaction with an inhibitory protein, called inhibitor of κ B (I κ B). I κ B has a core domain consisting of six to seven ankyrin repeats (ANK) which are important for the binding to the RHD of NF- κ B and thus covering the nuclear localization sequence (**Figure 3b**). I κ B exists in several isoforms: I κ B- α , I κ B- β , I κ B- ϵ and Bcl-3. Among those, I κ B- α is the most predominant and best studied [11, 102, 103]. Each isoform targets distinct combinations of RHD. For instances, I κ B- ϵ interacts with c-Rel homodimers and p65; I κ B- α and I κ B- β bind predominantly to p50:c-Rel and p50:p65 heterodimers; whereas Bcl-3 associates with p50 and p52 homodimers. Stimulation by all identified NF- κ B activators leads to degradation of I κ B- α . Contrary, I κ B- β is only degraded by specific activators (e.g. LPS and IL-1). This might cause variations in the NF- κ B activation pathway in a cell-type- and stimulus-specific manner [104]. Over 20 years of investigation, NF- κ B has turned out to be a vital transcription factor in numerous signaling pathways and many

biological processes including inflammation, cancer and the immune response [102, 105].

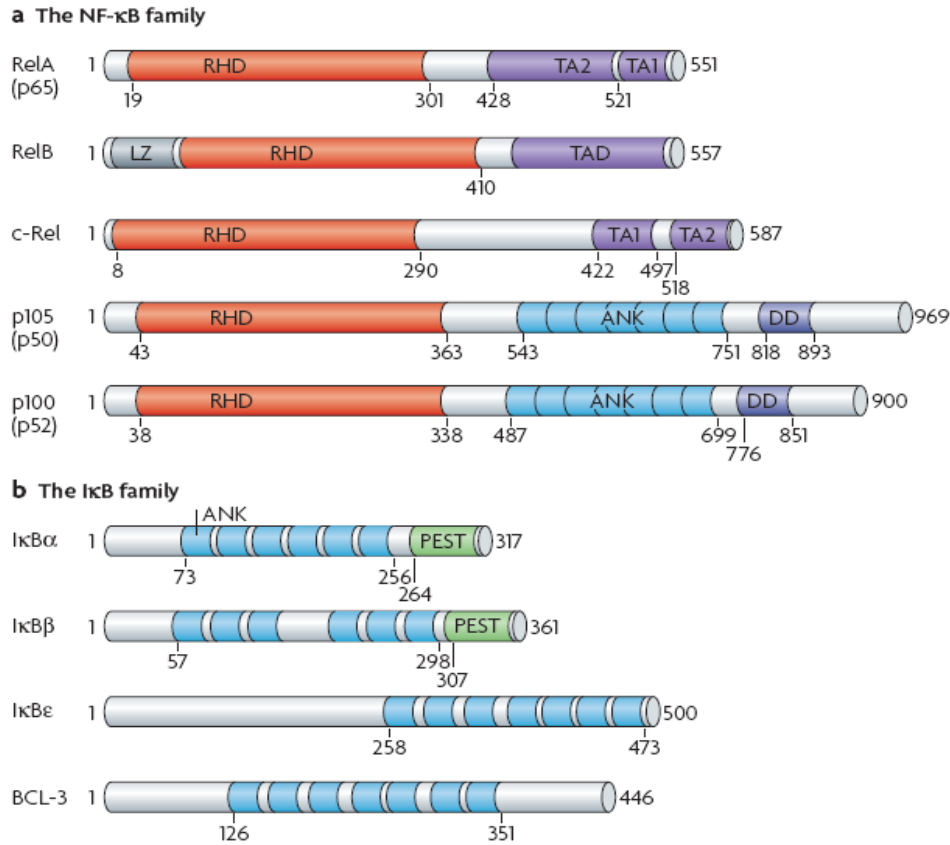


Figure 3. The mammalian NF- κ B and I κ B family members. a) NF- κ B consists of 5 proteins, and all proteins have an N-terminal Rel-homology domain (RHD) for DNA binding, dimerization, and also nuclear localization. b) Inhibitor of NF- κ B comprising 5 members that contain ankyrin-repeat motifs (ANK) in their C terminal. The figure is taken from [98].

5.1. NF- κ B signalling

Binding of NF- κ B to I κ B prevents the translocation of NF- κ B to the nucleus and maintains it in the inactive state. There are two NF- κ B signalling pathways which are commonly considered to occur upon cell stimulation, mainly by proinflammatory cytokines. In the classical pathway, stimulation of the cell leads to the phosphorylation of I κ B proteins at the two N-terminal serine residues by the I κ B kinase (IKK) complex, mainly by the IKK- β subunit. Phosphorylated I κ B proteins undergo polyubiquitination by ubiquitin ligase and further degradation by

the proteasome. The degradation of I κ B leads to translocation of unbound NF- κ B, mainly RelA-p50 dimers, from the cytoplasm to the nucleus and then to induction of the transcription of respective NF- κ B target genes. In the alternative pathway, the signal transduction to the nucleus is carried out by RelB-p52 dimers. The dimers of RelB-p52 do not bind to any I κ B, but they are derived from the larger precursor RelB-p100 in the cytoplasm. Upon activation by inflammatory stimuli, p100 in the RelB-p100 dimer is exclusively phosphorylated by IKK- α to form RelB-P52 heterodimers that translocate to the nucleus and mediate the transcription of inflammatory genes [102, 106-108]. These two pathways are described in **Figure 4**.

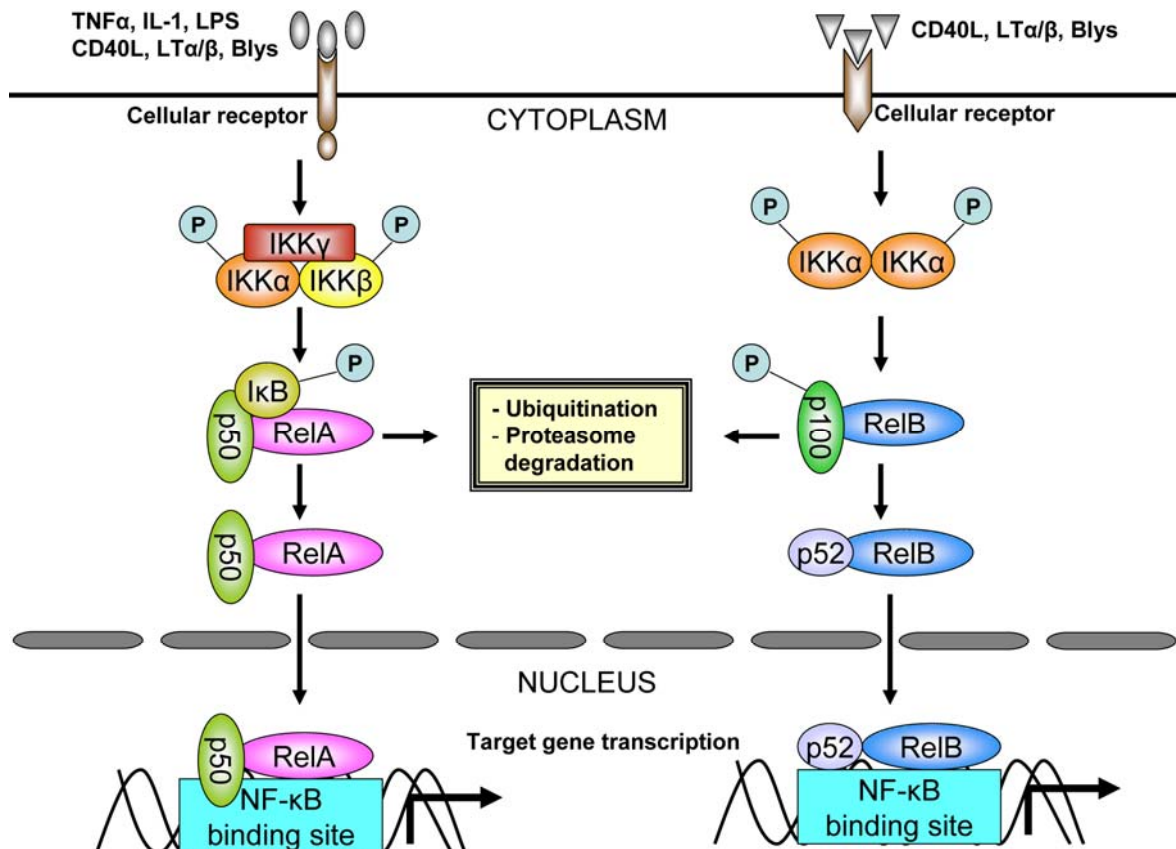


Figure 4. Two different signalling pathways that lead to the activation of NF- κ B and subsequent target gene expression. (a) Classical pathway and (b) Alternative pathway. Figure is modified from [103] and [105].

Ubiquitination and proteasomal degradation are responsible for the degradation of phosphorylated I κ B and subsequent translocation of NF- κ B to the nucleus [109]. Ubiquitin-mediated degradation controls the fate of short lived proteins and plays a key role in various basic cellular processes such as the modulation of the inflammatory response, the immune system, the biogenesis of subcellular organelles, differentiation of tissues, the cell cycle, cell division, modulation of cell membrane receptors, DNA repair and the control of transcription [110]. It is known that E3, an enzyme member of the ubiquitin–substrate ligase family is responsible for the recognition of phosphorylated human I κ B- α at the lysine residue. A polyubiquitin tree is formed by tagging activated ubiquitin moieties to the lysine residues. This complex is degraded by the 26S proteasome, an ATP-driven multi subunit proteolytic machine, followed by releasing free and reusable ubiquitin [110-112].

5.2. IKK in the NF- κ B signaling pathway

IKK is a protein complex comprising two catalytic subunits: IKK- α (also called IKK1) and IKK- β (also called IKK2), and one regulatory subunit IKK- γ (also called NF- κ B essential modulator or NEMO) [113]. IKK- α and IKK- β consist of 745 and 756 amino acids, respectively, and each has a N-terminal kinase domain, a leucine zipper (LZ) region and a C-terminal HLH domain (

Figure 5). The formation of homo- or heterodimers of IKK- α and IKK- β is mediated by binding via the LZ domains, whereas the kinase activity is determined by the HLH domain [104].

Although each IKK sub-type has similar structure and kinase activity, they have a subtly different response to inflammatory stimuli. In the NF- κ B classical pathway, IKK- β is the principal player for I κ B phosphorylation [114-117] whereas NEMO is required for the kinase activity of the complex [115, 118, 119]. IKK- α is not required for I κ B phosphorylation in the classical pathway [120-122] but it is responsible for kinase activity in the alternative pathway. In this pathway, IKK- α independent of IKK- β and IKK- β /NEMO, phosphorylates the p100-ReI κ B complex at the C-terminal region of p100. This leads to ubiquitination followed by degradation

of the p100 to generate p52-RelB that further translocates to the nucleus (see **Figure 4**) [123, 124].

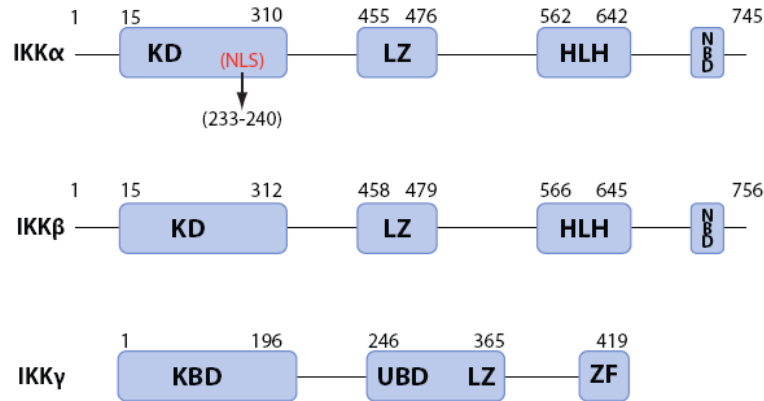


Figure 5. The domain structure of individual IKK subunits. The schematic representation of each IKK structure and the functional motifs are shown as indicated. HLH: helix loop helix motif, LZ: leucine zipper, KD: kinase domain, NBD: NEMO-binding domain, KBD: kinase-binding domain, NLS: nuclear localization signal, UBD: ubiquitin-binding domain, ZF: zinc finger. The figure is taken from [125].

IKK- β is an exquisitely serine-specific kinase phosphorylating both serine residues of I κ B which are required for *in vivo* activity [104]. However, previous studies showed that IKK- β also phosphorylated RelA/p65 at serine 536 [126] and p105 [127] which is important for p65 transcriptional activity and degradation of p105, respectively. Another protein which is phosphorylated by IKK- β is forkhead transcription factor FOXO3 [128]. Phosphorylation of this tumor suppressor protein by IKK- β provokes its translocation to the cytoplasm and further degradation which eventually induces tumorigenesis.

5.3. Role of NF- κ B in atherosclerosis

Inflammation is an important feature of vascular diseases including atherosclerosis. Atherosclerosis is initiated by modification of LDL into oxidized forms in the vessel wall. This leads to a local inflammation and results in the expression of adhesion molecules on the surface of endothelial cells and release of chemotactic factors. Monocytes are attracted on the site of inflammation and

once adherent to the activated endothelial layer, the monocytes transmigrate into the inner part of the arterial wall or intima [11, 129]. Inflammatory mediators, such as TNF- α , IL-1 β and CD40 ligands are also found in the atheroma and they activate proinflammatory pathways in the cells involved in atherosclerosis (**Figure 6**) [129, 130].

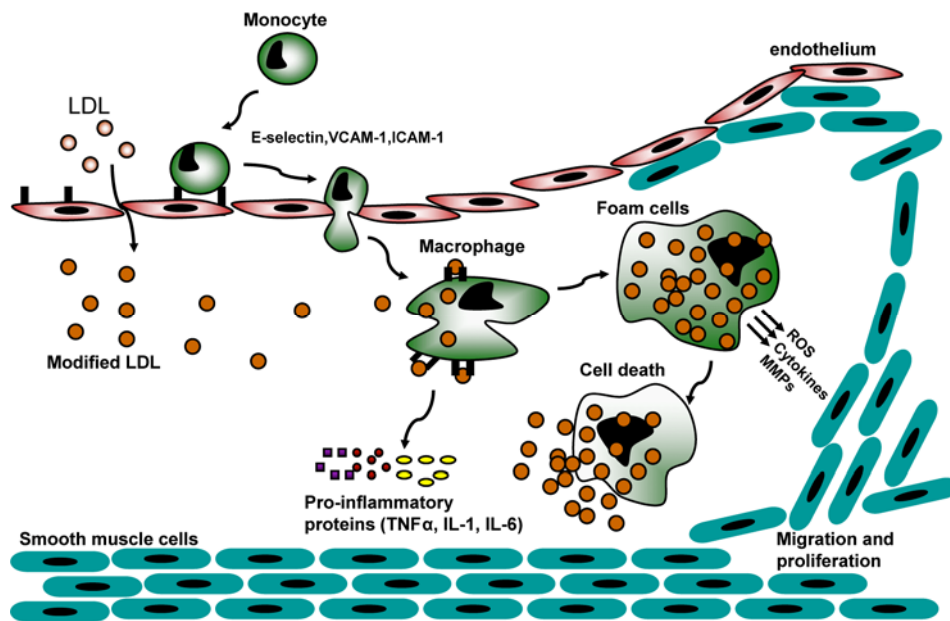


Figure 6. Schematic representation of the inflammatory responses regulated by NF- κ B in atherogenesis. The cell types involved and some events potentially affected by NF- κ B activation are indicated. The figure is adapted from [11].

According to de Winter et al., NF- κ B contributes to the development of atherosclerosis in three critical points. Firstly, NF- κ B regulates the expression of enzymes responsible for the generation of proinflammatory lipid mediators and LDL oxidation, such as COX-2 [131], phospholipase A2 [132] and lipoxygenase [133]. Secondly, NF- κ B regulates MCP-1, a cytokine that attracts monocytes from the artery lumen into the intima [134]. Thirdly, inflammatory mediators activating the NF- κ B pathway induce the expression of adhesion molecules such as VCAM-1, E-selectin and ICAM-1 [130, 135] that leads to the initiation of atherogenesis. The later stages of atherogenesis are characterized by the formation of a fibrotic

cap through proliferation and migration of vascular smooth muscle cells [11]. These events are partly regulated by NF- κ B [136, 137].

Adhesion molecules also facilitate the migration of lymphocytes and mast cells to the intima in response to chemoattractants. In the arterial intima, lymphocytes may encounter antigens such as oxidized LDL and then produce cytokines that influence the behaviour of other cells present in the atheroma, whereas mast cells are further degranulated and release the proinflammatory cytokine TNF- α [9, 129]. All these events, involving the activity of NF- κ B, further aggravate vascular inflammation.

5.4 Inhibitors of NF- κ B

Considering the pivotal role of NF- κ B in vascular inflammation, the inhibition of NF- κ B activation is a promising approach for disrupting the expression of many proteins that are involved in atherosclerosis. According to Gilmore and Herscovitch [138], NF- κ B activation can be inhibited through 3 strategies: (1) inhibition of the signal at the initiation phase by antagonizing the binding of ligands to the receptor (e.g. TNF receptor) which results in total abrogation of the downstream effect; (2) blocking a specific element of the activation pathway in the cytoplasm (e.g., targeting the recruitment of adaptor proteins such as TRADD to the receptor upon ligand binding, interference with the activation of the IKK complex, inhibition of I κ B phosphorylation and degradation); or (3) inhibiting the nuclear activity of freed NF- κ B subunits (e.g., blocking translocation of NF- κ B subunits to the nucleus, interfering with the binding of NF- κ B to DNA, alteration in the specificity and activity of NF- κ B subunits by modification of NF- κ B in the nucleus, or disturbing the interaction of NF- κ B subunits with the transcription apparatus and other transcription factors) [138, 139].

Numerous synthetic and nature-derived agents have been discovered as NF- κ B inhibitors [138]. Such inhibitors from natural products include parthenolide, butein, helenalin, panepoxydone, caffeic acid phenethyl ester, oridonin and ponocidin. Parthenolide is a sesquiterpene lactone from the medicinal plant Feverfew (*Tanacetum parthenium*) which has been reported to inhibit NF- κ B

activation via covalent modification of the cysteine 179 residue of IKK- β [140, 141]. Butein, a chalcone isolated from *Semecarpus anacardium* and *Dalbergia odorifera*, directly inhibited IKK activation by a mechanism similar to parthenolide and consequently the expression of the proteins regulated by NF- κ B [142]. Helenalin, the antiinflammatory sesquiterpene lactone from *Arnica montana* and *Arnica chamissonis* ssp. *foliosa*, demonstrates a distinct mechanism of action by selectively alkylating the p65 subunit of NF- κ B without affecting NF- κ B translocation to the nucleus and I κ B degradation [143]. Caffeic acid phenethyl ester inhibited the nuclear translocation of the p65 subunit without significantly affecting I κ B degradation. Whereas oridonin and ponicedin, the major diterpenoid constituents of *Isodon rubescens*, are NF- κ B inhibitors acting through direct interaction with the DNA-binding domain of NF- κ B. These compounds also inhibited NF- κ B translocation without affecting I κ B phosphorylation and degradation [144]. Some other plant-derived substances have been found as inhibitors of the NF- κ B pathway of which the mechanism of action is still unclear [138]. However, most of the natural terpenoid inhibitors of NF- κ B exert their NF- κ B inhibitory activity by targeting the IKK complex via their α - β -unsaturated carbonyl group [145].

Besides natural products, numerous synthetic inhibitors of NF- κ B have been discovered, including Dehydroxylmethylepoxyquinomicin (DHMEQ) [146] and 3-hydroxy-4,3',4',5'-tetramethoxychalcone [147]. DHMEQ was derived from the natural compound Epoxyquinomicin C, a 5,6-epoxycyclohexenone compound isolated from bacterium *Amycolatopsis* sp.[148]. Although DHMEQ has structural similarity with panepoxydon, it inhibited NF- κ B activation with a different mechanism of action. DHMEQ targets nuclear translocation of p65 DNA binding of NF- κ B components without affecting I κ B phosphorylation and degradation [149]. Further investigation revealed that the epoxycyclohexenone moiety of DHMEQ was responsible for its inhibitory activity by formation of a covalent bond at the cysteine residue 38 of p65 [150, 151].

Table 2 provides a representative list of NF- κ B inhibitors including a variety of natural and synthetic compounds. A more comprehensive list of natural-, synthetic- and protein-based inhibitors of NF- κ B can be seen in [138].

Table 2. Compound inhibiting of NF- κ B and their suggested mode of action [138]

Compounds	Origin	Targets	References
Calagualine	Natural product	TRAF2-NIK	[152]
Betaine	Synthetic	NIK/IKK	[153]
Thienopyridine	Natural product	IKK- β activity	[154]
BMS-345541	Synthetic	IKK- β activity	[155]
Capsaicin	Natural product	I κ B degradation	[156, 157]
1-Bromopropane	Synthetic	I κ B degradation	[158]
Cyclosporin A	Natural product	Proteasome	[159, 160]
Disulfiram	Synthetic	Proteasome	[161]
Alginic acid	Natural product	Nuclear translocation	[162]
Rolipram	Synthetic	Nuclear translocation	[163]
Artemisinin	Natural product	DNA binding	[164]
Raloxifene	Synthetic	RelA DNA binding	[165]
Gypenoside XLIX	Natural product	Transactivation	[166]
Chromene derivatives	Synthetic	Transactivation	[167]
Curcumin	Natural product	Antioxidant	[168]
Flavonoids	Natural product	Antioxidant	[169, 170]
Pyrrrolinedithiocarbamate	Synthetic	Antioxidant	[171]

6. Drugs from nature targeting inflammation

This work is part of the collaborative NFN (*Nationales Forschungsnetzwerk*) project with the topic: Drugs from Nature Targeting Inflammation (DNTI). It is an interdisciplinary network interlinking the knowledge and skills from different groups at different universities in Austria and aiming for the identification of novel antiinflammatory leads derived from natural products. The selection of investigated plants was based on an ethnopharmacological use and/or a computational approach. Plants that are traditionally used in Austria (summarized in the

VOLKSMED database [172] or in traditional Chinese medicine against inflammation are extracted and tested in selected *in vitro* inflammation models (functional or target-based). Hit extracts are subjected to bioassay guided fractionation in order to obtain the active compound. Alternatively, a natural product data base is screened *in silico* versus different pharmacophore models aiming to identify modulators of a variety of inflammatory mediators. Hits are then validated and confirmed in *in vitro* and cell-based models. The collaborative network between different research areas and expertises contributing in a synergistic way to the success of the project is depicted in **Figure 7**. The main partners in this collaboration were phytochemistry groups from the Departments of Pharmacognosy at the universities in Vienna, Graz and Innsbruck, and the Department of Pharmaceutical Chemistry, University of Innsbruck. The group from the Institute of Vascular Biology and Thrombosis Research, Medical University of Vienna was responsible for the *in vivo* experiments. A more detailed overview over the mission of the NFN/DNTI program, involved groups and the workflow can be seen at www.uibk.ac.at/pharmazie/pharmakognosie/dnti/.

During my thesis work, I have been involved in the project part “From cell-based assays to molecular mechanisms” with the major aim to identify and characterize natural products with a promising antiinflammatory profile in *in vitro* and cell-based models. Three major contributions of our project part within the DNTI-network are a) establishing methods, guiding fractionation and isolation of PPAR α and γ agonists and NF- κ B inhibitors; b) providing appropriate cell models and tools for validation of the compounds virtually identified as specific PPAR α and γ agonists as well as NF- κ B inhibitors; and c) studying the molecular mechanisms of active compounds in models of vascular inflammation.

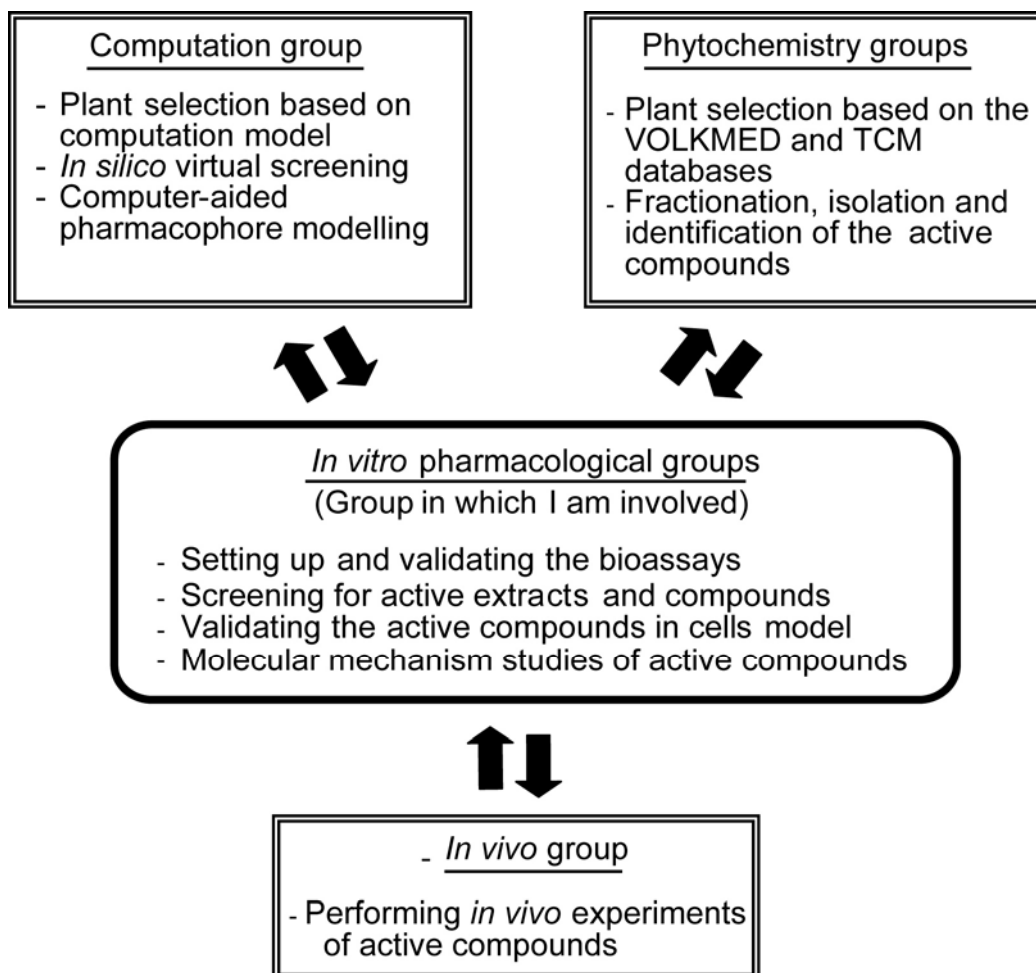


Figure 7. Overview of the collaboration within the DNTI project

C. MATERIALS AND METHODS

C. MATERIALS AND METHODS

1. Materials

1.1. Products and supplier information

<i>Name</i>	<i>Suppliers</i>
Cell culture material	
Benzylpenicillin	Lonza Group Ltd. (Basel, Switzerland)
Bovine brain extract	Lonza Group Ltd. (Basel, Switzerland)
Dulbecco's Modified Eagle Medium (DMEM)	Lonza Group Ltd. (Basel, Switzerland)
Foetal bovine serum	Lonza Group Ltd. (Basel, Switzerland)
Foetal bovine serum superior	Biochrom (Berlin, Germany)
Genitacin	PAA Laboratories (Pasching, Austria)
Gentamicin	Lonza Group Ltd. (Basel, Switzerland)
Hydrocortisone	Lonza Group Ltd. (Basel, Switzerland)
Hygromycin B	Roche (Basel, Switzerland)
Hypoxanthine-aminopterin-thymidine	Sigma (MO, USA)
L-glutamine	Lonza Group Ltd. (Basel, Switzerland)
Penicillin (potassium salt)-Streptomycin sulphate	Lonza Group Ltd. (Basel, Switzerland)
Recombinant human epidermal growth factor	Lonza Group Ltd. (Basel, Switzerland)
Trypsin	Invitrogen (CA, USA)
Compounds used as a positive control	
BADGE	Cayman (MI,USA)
GW0742	Cayman (MI,USA)
GW6471	Sigma (MO, USA)
GW7647	Cayman (MI,USA)
GW9662	Cayman (MI,USA)
IKK- β inhibitor IV	Calbiochem (Darmstadt, Germany)
Parthenolide	Alexis (PA, USA)
Pioglitazone	Molekula (Shaftesbury, UK)
Rosiglitazone	Cayman (MI,USA)
T0070907	Cayman (MI,USA)
Troglitazone	Cayman (MI,USA)

Biologicals and chemicals

Amphicillin (sodium salt)	Sigma (MO, USA)
ATP	Sigma (MO, USA)
Bacteriological agar	Sigma (MO, USA)
Bovine serum albumine	New England Biolabs (MA, USA)
Coenzyme A (trilithium salt)	Sigma (MO, USA)
Complete™	Roche Diagnostics, (Penzberg, Germany)
Dithiothreitol (DTT)	Fluka (MO, USA)
D-Luciferin (sodium salt)	Synchem (Flesberg, Germany)
DMSO	Fluka (MO, USA)
Gelatine	Fluka (MO, USA)
Kanamycin	Sigma (MO, USA)
LB broth	Sigma (MO, USA)
LPS	Sigma (MO, USA)
N-(1-Naphthyl)ethylenediamine 2 HCl	Sigma (MO, USA)
Oil red O	Fluka (MO, USA)
p-coumaric acid	Sigma (MO, USA)
PMSF	Sigma (MO, USA)
Poly-D-lysine	Sigma (MO, USA)
recombinant human PDGF-BB	Bachem (Weil am Rhein, Germany)
Recombinant human TNF- α	Sigma (MO, USA)
Reporter lysis 5X buffer	Promega (Wi, USA)
Resazurin (sodium salt)	Sigma (MO, USA)
Roti® Quant	Carl Roth (Karlsruhe, Germany)
SOC medium	Sigma (MO, USA)
Sulfanilamide	Fluka (MO, USA)
T-70 dekstran	Sigma (MO, USA)
TEMED	Fluka (MO, USA)
Triton® X-100	Sigma (MO, USA)

Plasmids

pSG5-PL-hPPAR α (hPPAR α)	Prof. Walter Wahli and Prof. Beatrice
pSG5-hPPAR-beta (hPPAR β)	Desvergne (Center for Integrative
pSG5-PL-hPPAR-gamma1 (hPPAR γ)	Genomics, University of Lausanne,
	Switzerland)
pCMX-mPPARgamma (mPPAR γ),	Prof. Ronald M. Evans (Howard Hughes

pCMX-mPPARalpha (mPPAR α), and tk-PPREx3-luc	Medical Institute, California, USA)
pEGFP-N1	Clontech (CA, USA)
Miscellaneous	
Fugene [®] HD	Roche (Basel, Switzerland)
Gel blotting paper	Whatman plc (Kent, UK)
Immuno-blot [™] PVDF Membrane (0.2 μ m)	BIO-RAD Laboratories (CA, USA)
Norit A charcoal	Sigma (MO, USA)
Precision Plus Protein [™] Standard	BIO-RAD Laboratories (CA, USA)

Table 3. Products and supplier information

1.2. Culture medium and supplements

Name	Components	Amount
HEK-293, RAW 264.7, and VSMC growth medium	DMEM (phenol red free)	500 ml
	Penicillin (potassium salt)	100 U/ml
	Streptomycin sulphate	100 μ g/ml
	L-glutamine	2 mM
	Foetal bovine serum	10 %
	New born bovine serum (for VSMC)	10 %
Experiment medium for PPAR assays	DMEM (phenol red free)	500 ml
	Penicillin (potassium salt)	100 U/ml
	Streptomycin sulphate	100 μ g/ml
	L-glutamine	2 mM
	Charcoal-stripped FBS	5 %
293/NF- κ B-luc growth medium	DMEM (phenol red free)	500 ml
	Penicillin (potassium salt)	100 U/ml
	Streptomycin sulphate	100 μ g/ml
	L-glutamine	2 mM
	Foetal bovine serum	10 %
	Hygromycin B	100 μ g/mL

Experiment medium for 293/NF- κ B-luc	DMEM (phenol red free)	500 ml
	Penicillin (potassium salt)	100 U/ml
	Streptomycin sulphate	100 μ g/ml
	L-glutamine	2 mM
	Foetal bovine serum	0.1 %
HUVECtert growth medium	EBM medium with phenol red	500 ml
	Penicillin (potassium salt)	100 U/ml
	Streptomycin sulphate	100 μ g/ml
	Amphotericin B	50 pg/ml
	Gentamicin	50 ng/ml
	Foetal bovine serum (superior)	10 %
	Benzylpenicillin	100 U/ml
	Bovine brain extract	0.4 %
	Hydrocortisone	4-15 pg/ml
	Recombinant human epidermal growth factor	0.5 - 4 ng/ml
EA.hy926-heNOS-Luc (for eNOS promoter activity assay)	DMEM without phenol red	500 ml
	Penicillin (potassium salt)	100 U/ml
	Streptomycin sulphate	100 μ g/ml
	L-glutamine	2 mM
	Foetal bovine serum	10 %
	Hypoxanthine	100 μ M
	Aminopterin	0.4 μ M
	Thymidine	16 μ M
	Geneticin	400 μ g/ml
Freezing medium	Growth medium	50 %
	DMSO	10 %
	Foetal bovine serum	40 %
Bacterial growth medium (agar plate)	LB broth	20 %
	Agar	1.5 %
	Ampicillin or kanamycin	50-60 μ g/ml
Charcoal-stripped FBS	FBS	500 ml
	Norit A charcoal	0.25 %

T-70 dekstran	0.0025 %
sucrose	0.25 M
MgCl ₂	1.5 mM
HEPES pH 7.6	10 mM

Table 4. Culture medium and supplements

1.3. Commercially available kits

Name	Supplier
ELISA-based (K-LISA™) IKK-β activity assay (Catalogue number CBA044)	Calbiochem (Darmstadt, Germany)
LanthaScreen™ TR-FRET Peroxisome Proliferator Activated Receptor gamma Coactivator Assay (Catalogue number PV4548)	Invitrogen (CA, USA)
LanthaScreen™ TR-FRET PPARγ Competitive Binding Assay (Catalogue number PV4894)	Invitrogen (CA, USA)
peqGOLD Plasmid Miniprep Kit I (Catalogue number 12-6943-01)	PeqLab (Erlangen, Germany)
PureYield™ Plasmid Midiprep System (Catalog number A2495)	Promega (Wi, USA)

Table 5. Commercially available kits

1.4. Reagents and buffers

Name	Components	Amount
Calcium phosphate- based transfection	NaHPO ₄ (stock solution)	5.25 g in 500 ml H ₂ O
	CaCl ₂	2 M
	2x HBS	8.0 g NaCl
		6.5 g HEPES (sodium salt)
		10 ml NaH ₂ PO ₄ stock solution
	<i>PH adjusted to 7.04 with diluted NaOH or HCl and filled up to 500 ml. To transfect the cells in a 10 cm disk, 720 µl 2x HBS, 94 µl CaCl₂ 2 M, ddH₂O to a final volume of 1500 µl was needed</i>	
5 X reporter lysis buffer	Luciferase lysis buffer	diluted 1:5 in ddH ₂ O

Lysis buffer (protein extraction for gel electrophoresis)	HEPES	50 mM
	NaCl	50 mM
	NaF	50 mM
	Na ₄ P ₂ O ₇ x 10 H ₂ O	10 mM
	EDTA (pH 7.5)	5 mM
	Complete™ (tablet)	solved in 2 ml ddH ₂ O
	PMSF	0.1 M in isopropanol
	Triton® X-100	10 % in ddH ₂ O
<i>Prior to use, complemented with 1x Complete™, 1 % Triton X-100 and 1 mM PMSF (0.1 M stock diluted in isopropanol)</i>		
10 X Resazurin stock	Resazurin (sodium salt)	diluted 1 mg/ml in PBS
<i>Prior to use, the stock was diluted in PBS 1:10 and further diluted 1:10 with the growth medium in the well plates.</i>		
Griess assay reagent	Solution A:	
	N-(1-Naphthyl)ethylenediamine 2 HCl	0.1 %
	Solution B: Sulfanilamide	
		1 % in 0.5 % H ₃ PO ₄
<i>Solution A and B was mixed prior to use (1:1).</i>		
PBS	MgCl ₂ x 6 H ₂ O	0.1 g
	KH ₂ PO ₄	0.2 g
	NaCl	8.0 g
	CaCl ₂ x 2 H ₂ O	0.1 g
	KCl	0.2 g
	Na ₂ HPO ₄	1.15 g
	Aqua dest.	ad 1000 ml and the pH was adjusted to 7.4
Trypsin/EDTA	EDTA	0.02 %
	Trypsin	0.05 %
	PBS	1000 ml
Gelatine 0.1 %	Gelatine	1 g
	Aqua dest.	ad 1000 ml
<i>The solution was autoclaved prior to use.</i>		

Table 6. Reagents and buffers

1.5. Western blot solutions and buffers

Name	Components	Amount
3x SDS sample buffer	Bromophenol blue	15.0 mg
	2-Mercaptoethanol	15 ml
	Glycerol	30.0 ml glycerol
	SDS	6.0 g
	TRIS-HCl solution 0.5 M, pH 6.8	37.5 ml
	Aqua dest.	ad 100 ml
	<i>Prior to use, the 3x stock solution was mixed with 2-mercaptoethanol (15 %). This 3x stock solution was added to the cell lysates (3x dilutions).</i>	
Blotting buffer 5x	Glycine	72.9 g
	TRIS-base	15.17 g
	Aqua dest.	ad 1000 ml
Blotting buffer 1x (prior to use)	5x blotting buffer	200 ml
	Methanol	200 ml
	Aqua dest.	ad 1000 ml
Electrophoresis buffer 5x	Glycine	72.0 g
	TRIS-base	15.0 g
	SDS	5.0 g
	Aqua dest.	ad 1000 ml
TBS-T pH 8.0	NaCl	11.1 g
	Tris-base	3.0 g
	Tween-20	1 ml
	ddH ₂ O	ad 1000 ml
Resolving gel 10 %	PAA solution 30 %	2.5 ml
	SDS 10 %	75 µl
	1.5 M TRIS-base pH 8.0	1.875 ml
	Aqua dest.	3.05 ml
	APS	37.5 µl
	TEMED	7.5 µl

Stacking gel	PAA solution 30 %	640 µl
	SDS 10 %	75 µl
	1.5 M TRIS-base pH 6.8	375 µl
	Aqua dest.	2.62 ml
	APS	18.8 µl
	TEMED	3.75 µl
ECL (Home-made)	Tris-base (1 M; pH 8.5)	0.5 ml
	ddH ₂ O	4.5 ml
	p-coumaric acid (90 mM in DMSO)	11 µl
	Luminol (0.25 M in DMSO)	25 µl
	H ₂ O ₂ 30 % (prior to use)	3 µl
Stripping solution	NaOH	0.5 M

Table 7. Western blot solutions and buffers

1.5. Antibodies

Target	Dilution	Source	Supplier
Goat IgG	1:2500	Rabbit	New England Biolabs (MA, USA)
Human CD106/VCAM-1 (FITC)	1:10	Mouse	Neomarkers (CA, USA)
Human CD54/ICAM-1 (FITC)	1:10	Mouse	eBioscience (CA, USA)
Human CD62/e-selectin (FITC)	1:10	Mouse	eBioscience (CA, USA)
IκB-α	1:1000	Rabbit	Cell signalling Technology (MA, USA)
Mouse IgG	1:2500	Goat	Upstate (MA, USA)
Mouse IgG1 (isotype control, FITC)	1:10	Mouse	Dako (Copenhagen, Denmark)
Rabbit IgG	1:2500	Goat	Cell signalling Technology (MA, USA)
α-tubulin	1:500	Mouse	Santa Cruz (CA, USA)

Antibodies were diluted in 5 % BSA in TBS-T. Anti-IκBα and secondary antibodies were diluted in 5 % milk powder in TBS-T.

Table 8. Antibodies

1.6. Scientific software

<i>Name</i>	<i>Supplier</i>
Cell Profiler	Broad Institute, MA, USA
XFLUOR4 Version 4.51	Tecan (Männedorf, Switzerland)
XFLUOR4GENIOSPRO Version 4.63	Tecan (Männedorf, Switzerland)
EndNote X, version 1.01	Thomson ResearchSoft (CA, USA)
Cell Quest Pro version 5.2	BD Biosciences (San Diego, CA, USA)
Vi-Cell™ XR 2.03	Beckman Coulter (CA, USA)
GraphPad PRISM™, version 4.03	GraphPad Software, Inc. (CA, USA)
Irfan View for windows version 4.27	Irfan Skiljan (Wiener Neustadt, Austria)
AIDA™(Advanced Image Data Analyzer),version 4.06	Raytest GmbH (Straubenhardt, Germany)

Table 9. Scientific software

1.7. Technical equipment

<i>Name</i>	<i>Supplier</i>
Bacterial incubator	Edmund Buehler (Hechingen, Germany)
Eluator™ Vacuum Elution Device	Promega (Wi, USA)
FACSCalibur™ BD Biosciences	Pharmingen (CA, USA)
Fluorescence Microscope Olympus BX51	Olympus Europa GmbH (Hamburg, Germany)
LAS-3000™ Luminescent Image Analyzer	Fujifilm (Tokyo, Japan)
Light Microscope Olympus CKX31	Olympus Europa GmbH (Hamburg, Germany)
Mini Trans-Blot™ Electrophoretic Transfer Cell	BIO-RAD Laboratories (CA, USA)
Olympus Live View Digital SLR Camera E-330	Olympus Europa GmbH (Hamburg, Germany)
Power supply Power Pac™ HC	BIO-RAD Laboratories (CA, USA)
Tecan GENios Pro	Tecan (Mannedorf, Switzerland)
Tecan Sunrise	Tecan (Mannedorf, Switzerland)
Vac-Man® Laboratory Vacuum Manifold	Promega (Wi, USA)
Vi-Cell™ XR Cell Viability Analyzer	Beckman Coulter (CA, USA)

Table 10. Technical equipment

2. Methods

2.1. Identification of PPAR γ agonists

2.1.1. HEK-293 cells

2.1.1.1. Origin

Human Embryonic Kidney 293 (HEK-293) cells are originally derived from human embryonic kidney cells by transformation with sheared fragments of adenovirus (Ad)5 DNA comprising the early region 1 (E1) transforming sequences integrated into chromosome 19. This transformation generated a cell line with respective characteristics, including the elaboration of a virus-specific tumour antigen. The cells are easy to grow and to maintain and exhibit a typical adeno-transformed cell phenotype with a tendency to divide continuously after reaching confluence [173, 174]. They have been widely used in cell biology and yield a high transfection efficiency favourable for many researchers.

2.1.1.2. Culture

HEK-293 cells were grown in a 150 cm² flask containing 20 ml culture medium in a cell incubator (5 % CO₂ / 37 °C humidified air). Culture medium was replaced with the fresh culture medium every three days.

2.1.1.3. Passaging

The confluent cells were split and sub-cultured twice a week. To make a new passage of cells, confluent cells were washed once with 10 ml prewarmed PBS. The PBS was then replaced by 2 ml of prewarmed trypsin. Cells were incubated for 1-2 minutes allowing the trypsinization process to detach cells from the bottom of the cultivation flask. 8 ml prewarmed culture medium was added to terminate the trypsin reaction process. 500 μ l of the cells suspension was subjected to ViCell™ for counting. To start a new passage of cells, 2 x 10⁶ – 4 x 10⁶ cells were seeded in a new 150 cm² flask.

2.1.1.4. Thawing

A vial of frozen cells was preincubated in the water bath at 37 °C until approximately half of it defrosted. The thawed solution was then transferred to a 50 ml Falcon tube containing prewarmed 15 ml culture medium and immediately centrifuged at 1400 rpm (or 412 g) for 4 minutes at 20 °C. The supernatant was discarded and the pellet was resuspended in 20 ml prewarmed culture medium by up and down pipetting. Cell suspension was transferred to a 150 cm² flask and incubated in 5 % CO₂ / humidified air incubator at 37 °C. The medium was replaced with the fresh culture medium after 2 days.

2.1.1.5. Preparation of cells for transfection

6 x 10⁶ HEK-293 cells were seeded in a 100 mm dish containing 10 ml culture medium and incubated in the cell incubator overnight. To distribute the cells evenly in the dish, the disk was gently moved back and forth. The cells were then incubated overnight and used for transfection (approximately 60-70 % confluence).

2.1.2. Transient transfection

In this study, the transfection method used for introducing DNA into the cells was the calcium phosphate precipitation method. In a 2 ml eppendorf tube, the plasmid DNA (diluted in ddH₂O) was mixed with 720 µl 2x HBS and 94 µl CaCl₂ 2 M and ddH₂O to a final volume of 1500 µl. This mixture was incubated at room temperature for 20-30 minutes to allow DNA-calcium phosphate complex formation. This complex was used to transfect the overnight grown 6 x 10⁶ HEK-293 cells (approximately 60-70 % confluence) in a 100 mm culture dish. 8 µg of PPAR γ receptor expression plasmid, 8 µg reporter plasmid (tk-PPREx3-luc), and 4 µg green fluorescent protein plasmid (pEGFP-N1) as internal control were used for the transfection. In every transfection, the total DNA and the ratio tk-PPREx3-luc: PPAR γ :EGFP were kept 12 µg and 2:2:1, respectively. Cells were maintained in the culture medium containing calcium phosphate-DNA complexes in the incubator

for 6 hours. The medium was then removed by applying vacuum and cells were washed once with 10 ml of prewarmed PBS followed by addition of 2 ml prewarmed trypsin after discarding the PBS. To accomplish cell detachment, they were incubated in the cell incubator for 1-2 minutes. Trypsinization was terminated by addition of 8 ml prewarmed culture medium. The detached cell suspension was centrifuged in a 50 ml falcon tube at 1400 rpm (412 g) for 4 minutes at 20 °C. The supernatant was discarded and replaced with DMEM containing 5 % charcoal-stripped FBS (*experiment medium*). The cells were resuspended and filtered through a cell strainer to exclude clotted and coagulated cells.

To count the number of viable cells, 500 µl cell suspension was subjected to the ViCell[®] cell counter. The desired amount of transfected cells was transferred to a multichannel pipette reservoir and distributed by using a multichannel pipette into a 96-well plate, at 5×10^4 cells per well in 150 µl medium. The cells were incubated in the cell incubator for 60 minutes to allow attachment to the plate prior to treatment.

Another transfection method that was also performed during the optimization process of transfection efficiency was with FuGENE[®] HD. The method was performed according to the manufacturer's instruction. Cell seeding and DNA amount was the same as previously described for the calcium phosphate transfection.

2.1.3. Luciferase reporter gene assay to detect PPAR γ activation

Test compounds (dissolved in DMSO) were prediluted in the *experiment medium* to obtain a four times higher compound concentration than the desired concentration. The transiently transfected cells in a 96-well plate containing 150 µl *experiment medium* were treated with 50 µl prediluted respective compounds and an equal concentration of DMSO was also prepared as a control. To avoid cell detachment, the cells were treated wisely by dropping the compounds solution along the wall of the well. Gentle shaking was applied to equally distribute the compounds throughout the well prior to a 18 hours incubation in the cell incubator. Untransfected cells were also included in each experiment for background

normalization. **Figure 8** shows a typical setting of the experiments performed in a 96-well plate.

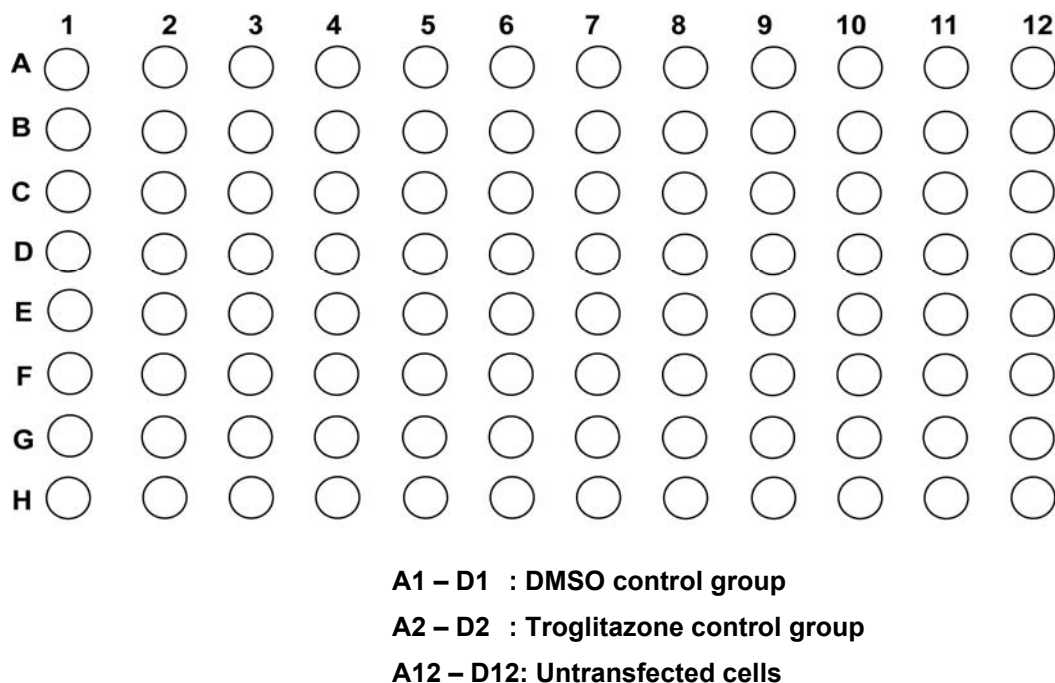


Figure 8. The setting of PPAR γ luciferase reporter gene transactivation assay in a 96-well plate. Each sample was tested in a quadruplet and the activation values were corrected for the background of the untransfected group and were correlated to DMSO-treated control.

After 18 hours of incubation, the treatments were terminated by removing the medium from the plates using a vacuum pump, and the plates were immediately stored at -80 °C until analysed. To determine the luciferase activity, the plates were taken out from the -80 °C freezer, and the cells were lysed by addition of 50 μ l luciferase lysis buffer per well supplemented with 1 mM DTT. To accelerate cell lysis, the plate was agitated on a horizontal plate shaker for 10 minutes. 40 μ l of cell lysate was transferred to a black bottom 96-well plate using a multichannel pipette for EGFP-derived fluorescence and luminescence measurements in a Tecan GeniosPro using XFluor GeniosPro Version: V 4.63 software. Measurement parameters on the Tecan GeniosPro are listed below.

EGFP-derived fluorescence measurement

Measurement mode	: Fluorescence
Excitation wavelength	: 485 nm
Emission wavelength	: 520 nm
Gain	: Optimal
Number of reads	: 1
Integration time	: 1000 μ s
Lag time	: 0 μ s
Mirror selection	: 40 ms

Luminescence measurements

Measurement mode	: Luminescence
Integration time (manual)	: 2000 ms
Attenuation	: None
Plate definition file	: GRE96fb
Part of the plate	: A1 - H12
Time between move and integration	: 50 ms
Well kinetic number	: 1
Well kinetic interval (minimal)	: 2020 ms
Injector A volume	: 50 μ l
Injector A speed	: 200 μ l/s
Injector B volume	: 50 μ l
Injector B speed	: 200 μ l/s
Injection mode	: Standard

2.1.4. Data analysis

The values obtained from the EGFP-derived fluorescence and the luminescence measurements of the reporter gene transfected cells were corrected for background of the untransfected cells. To account for differences in cell number and/or transfection efficiency, the luminescence values were further normalized to the EGFP-derived fluorescence. The activation value of each tested compound was determined by comparison of its normalized luminescence value to that of the DMSO control. The formula used to calculate PPAR activation was as follows.

$$\text{Luciferase activity} = \frac{\text{luminescence signal}}{\text{EGFP-derived fluorescence}}$$

$$\text{PPAR activation} = \frac{\text{luciferase activity upon treatment with test compound}}{\text{luciferase activity of DMSO control}}$$

The diploma student Christian Maier and Ursula Bauer and also our technicians Elisabeth Geiger and Judith Benedics also partly contributed to the screening of natural products for PPAR γ agonists. They worked under my guidance.

2.1.5. Preparation of charcoal-stripped FBS

Charcoal-stripped FBS was prepared to remove the androgens and other hormones which can interfere with our assays and give rise to high background levels. The protocol was according to Hibberts, et al [175] with several modifications. Norit A charcoal and T-70 dextran were mixed and incubated in a solution containing 0.25 M sucrose / 1.5 mM MgCl₂ / 10 mM HEPES pH 7.6 at 4 °C overnight. The mixture was centrifuged at 500 g for 10 minutes and the supernatant was discarded and replaced with equal volume of FBS. This solution was mixed and incubated under gentle shaking at 4 °C overnight. Following 10 minutes centrifugation at 750 g, the serum was filtered and stored at -20 °C. This charcoal-stripped FBS was used for a supplement in the *experiment medium* instead of regular FBS.

2.1.6. DNA plasmid preparation

All DNA plasmids were subjected to amplification by using JM109 competent *Escherichia coli* (Sigma-Aldrich). Prior to amplification and purification, the plasmids were subjected to a miniprep plasmid preparation using peqGOLD Plasmid Miniprep Kit (PeqLab). The plasmids were digested with appropriate restriction enzymes and the fragments were observed in a gel electrophoresis to

confirm validity of the plasmids. DNA plasmid amplification, extraction and purification were done with PureYield™ Plasmid Midiprep System (Promega). A vacuum-based purification method was performed with the procedure according to the manufacturer's instruction.

2.1.7. PPAR γ coactivator assay

The coactivator binding assay was performed using The LanthaScreen™ TR-FRET PPAR γ coactivator assay kit (Invitrogen) according to the manufacturers' protocol. Test compounds dissolved in DMSO or solvent vehicle were incubated together with fluorescein-labelled TRAP220/DRIP-2 coactivator peptide [176], human PPAR γ LBD tagged with GST, and a terbium-labelled antiGST antibody. In this assay, the binding of an agonist to the PPAR γ LBD results in a conformational change leading to recruitment of the coactivator TRAP220/DRIP-2 peptide. This recruitment brings the fluorescein attached to the coactivator peptide and the terbium attached to the GST antibody in close spatial proximity, and excitation of the terbium at 340 nm results in a FRET and a consequent partial excitation of the fluorescein observed at 520 nm. The 520 nm signals were normalized to the signals obtained from the terbium emission at 495 nm and thus the 520 nm/495 nm ratios were used as a measure for the TRAP220/DRIP-2 coactivator recruitment potential of the tested compounds. The measurements were performed with a Tecan GeniosPro plate reader. The binding curve was generated by plotting the emission ratio against log [ligand] using an equation for a sigmoidal dose response (varying slope) provided by GraphPad™ Prism® 4.0 [177]. **Figure 9** illustrates the plate setting of the experiments and the measurement parameters of the assay in the Tecan GeniosPro instrument is described below.

Measurement mode	: Fluorescence
Excitation wavelength	: 340 nm
Emission wavelength	: 495 nm and 520 nm (first and second measurement, respectively).

Gain	: Optimal
Number of reads	: 10
Integration time	: 200 μ s
Lag time	: 0 μ s
Mirror selection	: Dichroic
Plate definition file	: GRE96fb

	1	2	3	4	5	6	7	8	9	10	11	12	13	14	15	16	17	18	19	20	21	22	23	24
A																								
B																								

A1-B1 : No PPAR-LBD Control
A2-B2 : Negative (DMSO) Control
A3-B24 : Tested compounds (each in a duplicate)

Figure 10. The setting of a coactivator recruitment experiment in a 384-well plate

2.1.8. Adipocyte differentiation assay

3T3-L1 preadipocyte cells were cultured in a DMEM supplemented with 10 % new born bovine serum (NBS), and at confluency differentiated to adipocytes in a DMEM supplemented with 10 % foetal bovine serum, 1 μ g/mL insulin, as well as potential PPAR γ agonists. Briefly, the confluent cells (day 2) were kept for additional two days in DMEM 10 % NBS, before PPAR agonists in DMEM and insulin were added (day 0). Every two days, the medium was renewed until day 7 or 8. To estimate lipid accumulation, Oil Red O staining was performed. Cells were fixed in 10 % formaldehyde for 1 hour and stained with Oil Red O for 10 minutes. Excessive dye was washed off and then photos were taken. The bound dye was solubilized by 100 % isopropanol and photometrically quantified at 550 nm. The investigation of adipogenesis in this study was performed by Dr. Elke Heiss.

2.2. Identification of NF- κ B inhibitors

2.2.1. 293/NF- κ B-luc cells

2.2.1.1. Origin

The origin of this cell line is the same as for HEK-293. 293/NF- κ B-luc cells were created by transfecting HEK-293 cells with pNF- κ B-luc (Panomics P/N LR0051) and a hygromycin resistance gene. The hygromycin-resistant clone is capable of producing luciferase upon TNF- α stimulation. 293/NF- κ B-luc cells are appropriate to study the activity of the NF- κ B transcription factor at the cellular level. They preserve a chromosomal integration of a luciferase reporter gene construct regulated by multiple copies of the NF- κ B response elements (Panomic, Catalog No. RC0014).

2.2.2.2. Transient transfection

293/NF- κ B-luc cells were seeded as HEK-293 and were transiently transfected with 4 μ g pEGFP-N1 for 6 hours. Transfected cells were harvested by trypsinization, reseeded in a 96-well plate at a density of 4×10^5 cells/well in the *experiment medium* and incubated overnight.

2.2.2. Luciferase reporter gene assay to detect NF- κ B inhibition

The luciferase reporter gene assay to detect NF- κ B inhibitors was performed in a similar manner to that used for the identification of PPAR γ agonists. The transiently transfected cells were pretreated with the respective compounds for 30 minutes prior to stimulation with 2 ng/ml TNF- α for 4 hours. The experiments were performed in a 96-well plate with the setting similar to that of the PPAR γ agonist assay. Parthenolide (5 μ M), a potent NF- κ B inhibitor, was used as a positive

control. Obtained luminescence values were again normalized to EGFP-derived fluorescence and related to the DMSO control group.

The diploma students Olivia Schrammel and Anna Grzywacz and also our technicians Elisabeth Geiger and Judith Benedics contributed to the NF- κ B inhibitors investigation from the plant extracts. They worked under my guidance.

2.2.3. IKK- β inhibition assay

The IKK- β activity was measured with the ELISA-based (K-LISA™) IKK- β activity assay (Calbiochem) with the conditions recommended by the manufacturer. Test compounds dissolved in DMSO or solvent vehicle were incubated with GST-I κ B- α and human recombinant IKK- β in an assay buffer containing ATP / MgCl₂. GST-I κ B- α , a 50-amino acid peptide that includes the Ser32 and Ser36 IKK- β phosphorylation sites is used as a substrate. 30 minutes incubation at 30 °C with human recombinant IKK- β in a glutathione-coated 96-well plate, allows substrate phosphorylation. The phosphorylated GST-I κ B- α substrate was subsequently detected using antiphospho I κ B- α (Ser32/Ser36) as first antibody, followed by the HRP-conjugated secondary antibody. The colour development of the HRP substrate was monitored at 450 nm on a Tecan GeniosPro plate reader. The absorbance intensity was used as a measure for the IKK- β activity. The presence of IKK- β inhibitors inhibits the phosphorylation step and leads to a lower absorbance intensity.

2.2.4. Experiments with endothelial cells.

2.2.4.1. Origin of HUVECtert

HUVECtert, a human umbilical vein cell expressing telomerase reverse transcriptase, was provided by Prof. Hannes Stockinger (Department of Molecular Immunology, Center for Physiology, Pathophysiology and Immunology, Medical University of Vienna, Austria) [178]. This immortalized cell line was derived from parental primary cell (human umbilical endothelial cell) by introducing the catalytic

subunit of human telomerase (hTERT). HUVECtert displays morphogenetic and functional characteristics of the parental cells, and exhibits a survival advantage beyond the hurdling of replicative senescence since it is more resistant to programmed cell death [179, 180].

2.2.4.2. Treatment and cell lysates preparation

HUVECtert were seeded at a density of 5×10^6 cells per well in a 6-well plate for 3 days. The culture medium was then replaced with 1.3 ml fresh medium. After 30 minutes preincubation with the tested substances, the cells were stimulated with TNF- α 10 ng/ml for 10 minutes. The medium was removed and the plate was immediately put on ice and washed with ice-cold PBS. In each well, 100 μ l lysis buffer was added and the cells were scraped using cell scraper after 5 minutes incubation on ice. The cell lysates were put into eppendorf tubes and then centrifuged at 13.000 rpm (or 16.060 g) in 4 °C for 20 minutes. 5 μ l of the cell lysates was put into a small eppendorf containing 45 μ l ddH₂O for protein quantification using Bradford assay. The rest of the cell lysates was used for western blot analysis to analyze the expression of the protein of interest.

2.2.4.3. Protein quantification using the Bradford method

The Bradford assay is a colorimetric-based protein determination by measuring the absorbance maximum shift of Coomassie Brilliant Blue G-250 from 465 nm (red) to 595 nm (blue) in acidic condition when binding to protein. The absorbance linearly correlates with the protein concentration of the sample. Diluted cell lysates (1:10 in ddH₂O) were transferred to a 96-well plate in triplicate besides a serial dilution (50 - 500 μ g/ml) of BSA for standard curve. Bradford reagent (Roti[®] Quant) was diluted (1:3) in ddH₂O, and 190 μ l were added to the 10 μ l cell lysate per well [181]. After 5 minutes of agitation on a plate shaker at room temperature, the absorbance was measured at 595 nm in a Tecan Sunrise micro plate reader.

2.2.4.4. Gel electrophoresis

SDS-polyacrylamid gel electrophoresis was performed to separate proteins in the cell lysates according to their size. 3 x SDS sample buffer containing 2-mercaptoethanol was added to the cell lysates followed by 5 minutes heat denaturation at 95 °C. This led to the breakup of the tertiary protein structures to the linear primary structures. In addition, the anion part of the SDS was able by average to bind two amino acid residues of the protein which significantly increased negative charge of the proteins and abrogated differences in the mass/charge ratio during separation process. Like this, the smaller size protein migrates faster than the bigger one from the cathode to the anode through the polyacrylamid polymers upon application of an electric field. In the separation process, 15 - 30 µg protein was loaded per well, run in a Mini-PROTEAN™ 3 Cell System (BIO-RAD) connected to a Power supply Power Pac™ HC (BIO-RAD) and separated at 25-30 mA per gel for 70 minutes.

A Mini Trans-Blot™ Electrophoretic Transfer Cell System (BIO-RAD) was run at 100 V for 90 minutes to transfer the proteins to a PVDF membrane (BIO-RAD) previously equilibrated with methanol and subsequently blotting buffer for 5 minutes. The membranes were incubated in 5 % fat-free milk powder in TBS-T for 1 hour to block unspecific protein binding sites, followed by three times washing for 10 minutes with TBS-T.

2.2.4.5. Protein detection

The antibodies against the protein of interest were diluted as described in **Table 8**. The membranes were incubated with the specific primary antibodies at 4°C over night. After three washes with TBS-T for 10 minutes on a shaker, the incubation with species-specific horseradish peroxidase-conjugated secondary antibody was performed for 2 hours at room temperature. The membranes were then washed three times with TBS-T for 10 minutes. In the meantime, ECL-solution was prepared and immediately added to the membrane after washing. The presence of p-coumaric acid in ECL-solution enhances the chemiluminescence light produced by oxidation of luminol by H₂O₂ catalyzed by

Horseradish peroxidase. The reaction is accompanied by a light emission at 428 nm which can be detected as a luminescent image in the LAS-3000 instrument and yields bands. AIDA software was used to quantify the band densitometrically. In order to incubate with another primary antibody of interest, the membranes were stripped with 0.5 M NaOH solution for 10 minutes followed by three washes for 10 minutes in TBS-T. Then, the other primary antibody can be added and the membranes were preprocessed as just described.

Anna Grzywacz partly contributed in this assay by performing one experiment under my guidance to investigate the effect of plumericin on I κ B- α degradation.

2.2.4.6. Analysis of adhesion molecules

2.2.4.6.1. Flow cytometry

Flow cytometry is a method for measuring the properties of individual particles using the principle of light excitation, scattering and emission of fluorochrome particles. Once particles are injected to a flow cytometer, they are randomly distributed in a three-dimensional space, thus, allowing the analysis of their relative granularity, relative size, and relative fluorescence intensity. In contrast to spectrophotometer which measure whole particles in a volume of sample, flow cytometer measures the fluorescence intensity per particle or cell. This method is generally used for investigation of surface protein and antigen expression, membrane potential, cell cycle and apoptosis. In our instrument, the cells were illuminated with an argon laser (488 nm) and the signals from fluorescence-labelled antibodies were detected by a detector on a FACSCaliburTM instrument.

2.2.4.6.2. Staining of VCAM-1, ICAM-1 and E-selectin

HUVECTert were seeded at a density of $4 \times 10^5 - 5 \times 10^5$ cells per well overnight, or $2 \times 10^5 - 3 \times 10^5$ cells per well for two days in a 6-well plate containing 2 ml or 4 ml culture medium, respectively. The medium was replaced

with 2 ml fresh medium 1 hour prior to pretreatment with respective compounds followed by TNF- α (10 ng/ml) stimulation for 14 hours for VCAM-1 and ICAM-1 investigation or 5 hours for E-selectin. The stimulation was terminated by removing the medium and the cells were harvested by trypsinization, then transferred to FACS tubes and spun down at 1400 rpm (or 412 g) at 4 °C for 4 minutes. Cell pellets were washed and resuspended in a PBS containing 1 % BSA and spun down. This step was done twice and yielding washed cell pellets. To stain the cells, 10 μ l of the respective FITC-labelled antibody (anti-VCAM-1, -ICAM-1 and -E-selectin as well as isotype-control) were added to the cell pellet and incubated at the room temperature for 1 hour. After incubation, the cells were washed, spun down and resuspended twice in a PBS containing 2 % BSA followed by a final spinning down to obtain pellets. 300 μ l PBS containing 2 % BSA were added to the cell pellets and the stained cells were immediately analysed in a FACSCaliburTM instrument in the FL-1 channel. Analysis of VCAM-1 and ICAM-1 was performed from the same cell pellet, whereas E-selectin was analysed in a separate experiment.

2.2.5. Experiments with vascular smooth muscle cells

Vascular smooth muscle cells (VSMC) used in this study were isolated from three different aortas of male Sprague-Dawley rat and the identity was verified by fluorescence microscope using a monoclonal anti α -smooth muscle actin. The isolation and verification were performed by Cornelia Schreiner, a fellow graduate student in our laboratory, according to [182].

2.2.5.1. Culture of VSMC

The cells were grown in a phenol red-free Dulbecco's modified Eagle's medium (DMEM) supplemented with 100 U/ml penicillin and 100 μ g/ml streptomycin, 2 mM glutamine and 10 % NBS and incubated in the cell incubator. The cell passaging was done twice a week in a 150 cm² flask containing 20 ml culture medium.

2.2.5.2. Wound healing assay

A number of 2.5×10^4 cells was seeded in 6-well plates previously marked with a straight line at the bottom. The cells were incubated in 4 ml medium per well in the cell incubator for 72 hours. The confluent cell layer was then perpendicularly scratched with a blue tip along the plate bottom, which caused a wounding area (can be seen under the microscope). The cells were washed twice with PBS and incubated with 2 ml starvation medium in the incubator for 24 hours. Prior to stimulation, a picture of cells along the line was captured and the cells were pretreated with the test compounds for 30 minutes. Cell migration was stimulated with 2 ng/ml PDGF-BB for 21 hours. Cell pictures following stimulation were captured again and the migration area was calculated with Irfan View, CellProfiler and Microsoft Paint software.

2.2.6. Experiments with RAW 264.7 macrophages

Raw 264.7 cells are a macrophage-like cell line. They were established from a tumour induced by intraperitoneal injection of Abelson murine leukaemia virus in a male BALB/c mouse [183]. These cells have been commonly used in medical researches for inflammation, metabolic and apoptosis studies. The cells for the experiments were obtained from the ATCC.

2.2.6.1. Culture of RAW 264.7

Raw 264.7 cells were grown in a 150 cm² flask containing 20 ml culture medium in the cell incubator. Culture medium was replaced with the fresh culture medium every three days. Once reaching confluence, the cells were harvested and reseeded at a density of 2×10^6 – 4×10^6 cells in a 150 cm² flask containing 20 ml culture medium.

2.2.6.2. Seeding of Raw 264.7 cells

RAW 267.4 cells were seeded in a 96-well plate at a density of 8×10^5 cells per well and incubated for 28 hours. Prior to 30 minutes pretreatment with respective test compounds (prediluted in 50 μ l medium) and subsequent stimulation with 30 ng/ml LPS (diluted in 50 μ l medium) per well, the medium was replaced with 100 μ l fresh medium per well. 18 hours after LPS stimulation, 100 μ l supernatant was transferred to a new 96-well plate for determination of NO production (Griess assay), whereas the cells were used for a resazurin assay to account for differences in cell number and/or cytotoxic effect of the test compounds.

2.2.6.3. Griess assay

Griess assay is based on a diazotization reaction initially described by Griess [184]. The reaction occurs between NO_2^- , a breakdown product of physiological NO, with sulphanilamide to form a diazonium salt. The diazonium salt reacts with N-1-naphthylethylenediamine in acidic condition to generate a pink-coloured azo dye which can be spectrophotometrically quantified at 550 nm [185]. This method can identify NO_2^- in biological systems and tissue culture medium. To measure NO produced by the RAW 267.4 macrophages, 100 μ l cell supernatant was transferred to a non-sterile 96-well plate and mixed with 100 μ L of a 1:1 mixture of 1 % sulphanilamide in 5 % phosphoric acid and 0.1 % naphthylethylenediamine in water. These two components were freshly mixed prior to the measurement. The absorbance of generated colour was spectrophotometrically measured in a Tecan Sunrise instrument at 550 nm [185].

2.2.7. Resazurin-staining assay

The resazurin-staining assay was performed for normalization accounting for cytotoxic effects of the test compounds and/or differences in cell number. Resazurin is a water-soluble, membrane permeable and non toxic blue dye which can be converted by reductase activity of living cells to resorufin, a highly

fluorescence pink product. This method is fast, simple, accurate and sensitive and has been used to test antimicrobial activity, bacterial contamination and cell viability [186, 187]. In this assay, treated cells in 96-well plates were removed from the incubator into the laminar flow hood and the medium was reduced to 90 μ l per well. 10 μ l resazurin solution (0.1 mg/ml) in PBS was added to each well and the plates were returned to the cell incubator for an additional 2 hours incubation. The plates were fluorometrically measured in a Tecan GeniosPro plate reader according to the following program parameters. For background correction, each measurement included a blank containing culture medium without cells.

Measurement parameter for resazurin-staining assay

Measurement mode	: Fluorescence Top
Excitation wavelength	: 535 nm
Emission wavelength	: 590 nm
Gain (Manual)	: 20
Number of reads	: 10
Integration time	: 2000 μ s
Lag time	: 0 μ s
Mirror selection	: Dichroic 2
Plate definition file	: GRE96ft.pdf
Time between move and flash	: 40 μ s

2.3. Statistics

The statistical analyses were done using GraphPad Prism software, version 4.03. The statistical differences among the treatments were compared using oneway ANOVA followed by Benferroni's or Dunnett's t-tests for comparison all pairs of column and comparison to control, respectively. The bars in the figure represent means \pm standard error of mean (SEM) or standard deviation (SD).

C. RESULTS

C. RESULTS

1. Discovery of PPAR γ agonists

1.1. Optimization of transfection efficiency

HEK-293 cells have been widely used as a cell model for transfection-related experiments. These cells are easy to transfect and have a good capability to highly express proteins introduced through the transfected DNA plasmids. In order to obtain a high transfection efficiency in this study, two transfection methods: Fugene[®] HD and CaPO₄, were compared. **Figure 11** shows the comparison of transfection efficiency among these two methods. The CaPO₄ method produced higher transfection efficiency compared to Fugene[®] HD in HEK-293 cells with achieving up to 90 % efficiency. Thus, this method was further used to transfect the HEK-293 cells in the whole study.

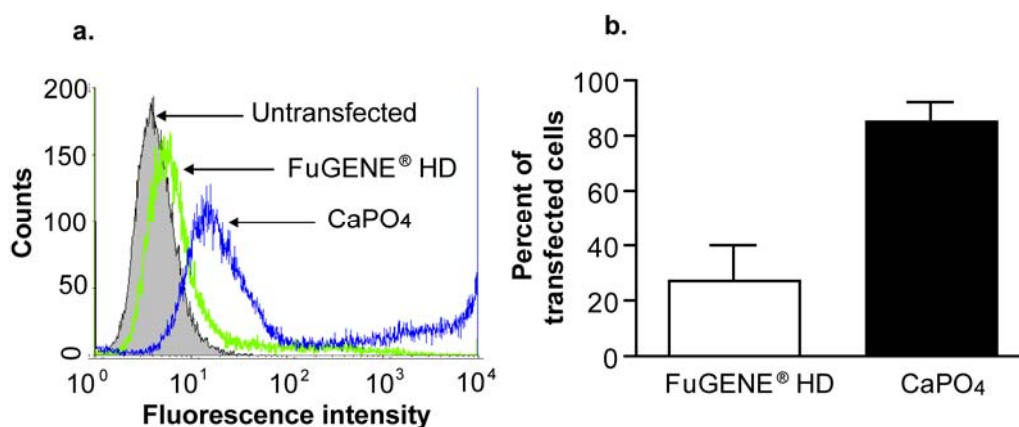


Figure 11. Optimization of transient transfection method in HEK-293 cells. (a) Comparison of the Fugene[®] with the CaPO₄ transfection method in HEK-293 cells. Representative result from two independent experiments are shown. (b) Quantification of transfection efficiency is expressed as % transfected cells. HEK-293 cells were transiently transfected with 12 μ g EGFP with the respective method for 6 hours. The EGFP level was determined by FACS analysis after 18 hours incubation. The bars shown are means \pm SEM from two independent experiments.

1.2. Validation of the bioassay

Transfection of HEK-293 cells with the PPAR γ expression plasmid, PPRE and EGFP resulted in transiently transfected cells responsive to the presence of PPAR γ agonists. The functionality of the method was validated by use of the known PPAR γ agonist, troglitazone. **Figure 12a** demonstrates that troglitazone dose dependently induced PPAR γ activation. To assess whether the activation of PPAR γ is due to the binding of the agonist to the receptor, the cells were pretreated for 30 minutes with GW9662, a PPAR γ antagonist, prior to troglitazone treatment. Indeed, GW9662 was able to block PPAR γ activation by troglitazone (**Figure 12b**), indicating that the activation is due to PPAR γ activation.

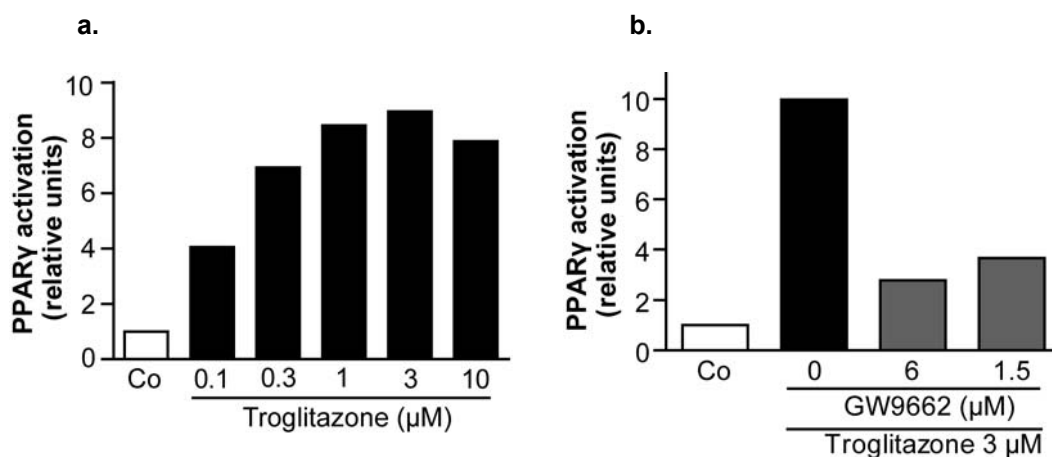


Figure 12. Validation of the bioassay using PPAR γ agonist and antagonist. (a) Dose-response of the transfected cells upon treatment with the PPAR γ agonist troglitazone. (b) Inhibition of troglitazone-induced PPAR γ activation by the PPAR γ antagonist, GW9662. HEK-293 cells were transiently cotransfected with a plasmid encoding full-length PPAR γ , a reporter plasmid containing PPRE coupled to a luciferase reporter and EGFP as internal control. The cells were stimulated with the indicated concentrations of troglitazone (a) or GW9662 followed by troglitazone (b) for 18 hours. Luciferase activity was measured and normalized by the EGFP-derived fluorescence, and the result was expressed as fold induction compared to the control DMSO (Co). The data show the mean of one experiment performed in a quadruplet and are representative of two independent experiments with similar result.

DMSO is commonly used to prepare the tested sample stock solutions. In our study, most of the samples were also diluted in DMSO. Therefore, the effect of

DMSO on this bioassay was evaluated. We found that DMSO in the concentration range from 0.1 % to 1 % did not significantly influence PPAR γ -mediated reporter gene transactivation (data not shown).

As we additionally performed screening to find novel PPAR α agonists, the functionality of the method was also validated. Treatment with a known PPAR α agonist, GW7647 induced PPAR α activation in concentration-dependent manner, and this activation was blocked in the presence of specific PPAR α antagonist GW6471 (**Supplementary Figure 1**). The identification and characterization of compounds activating PPAR α from the active plant extracts is on going. Therefore, we are focusing on the identification of PPAR γ agonists in this section.

1.3. Investigation of a PPAR γ -activating potential of plant extracts

To identify novel PPAR γ agonist from natural sources, 511 plant extracts were tested for their PPAR γ activation potency in a PPAR γ -mediated reporter gene transactivation assay. Plant extracts were obtained from the collaborative partners within the NFN (*Nationales Forschungs Netzwerk*) project “Drug from Nature Targeting Inflammation (DNTI)”, or from collaboration partners at the Department outside the DNTI. The plants were chosen for investigation based on ethnopharmacological and computational approaches. The extracts were initially tested at least in two independent experiments in the concentration of 10 $\mu\text{g/ml}$. The concentration was lowered to 3 $\mu\text{g/ml}$ or 1 $\mu\text{g/ml}$ if cytotoxicity was observed, as indicated by the lower value of EGFP-derived fluorescence. The extracts with more than 1.5 fold activation compared to control DMSO were considered active and marked with “+” **Figure 13** shows one representative experiment comparing the activity of several extracts (indicated with different numbers). In this representative experiment, sample number 720 was considered active.

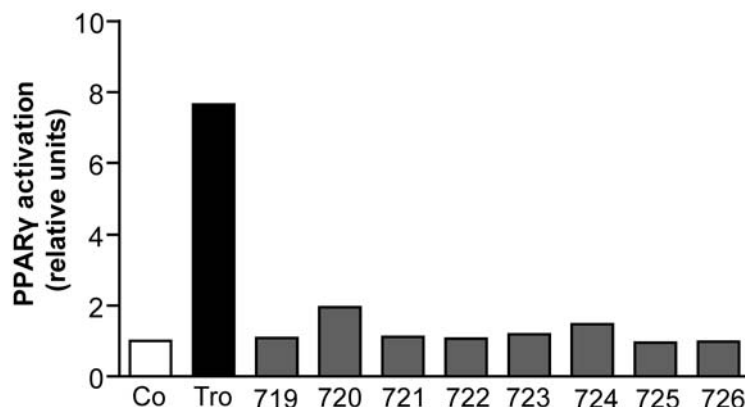


Figure 13 Representative experiment comparing the activity of the tested samples in the PPAR γ -driven reporter gene assay. Tested samples (719-726) were applied at 10 μ g/ml and troglitazone (Tro, 5 μ M) was used as a reference agonist to activate PPAR γ . The data shown are means from one representative experiment (out of two) each performed in a quadruplet. Sample number 720 which is inducing more than 1.5 fold activation compared to control (DMSO treatment) was considered active in this experiment.

From the list of the tested extracts, several plants, that were considered as most relevant, were selected for further separation and identification of the active compounds (**Table 11**). In the following section, the discovery of PPAR γ agonists from *Notopterygium incisum* (active plant originating from the ethnopharmacological approach) and *Magnolia officinalis* (active plant originating from the computational approach) will be presented. Others plants are also currently under investigation, but will not be presented in detail.

Table 11. The active plants selected for further isolation and identification of PPAR γ agonists.

Selected active plant	Current state with the identification of the bioactive compounds
<i>Albizia julibrissin</i>	Sub fractions
<i>Arisaema</i> sp.	Fatty acids
<i>Echinacea pallida</i>	Polyacetylenes
<i>Magnolia officinalis</i>	Neolignans
<i>Melampyrum</i> sp.	Sub fractions
<i>Notopterygium incisum</i>	Polyacetylenes
<i>Peucedanum ostruthium</i>	Sub fractions, fatty acids

1.4. Discovery of PPAR γ agonists guided by pharmacophore modeling

To identify novel natural product-derived PPAR γ ligands, a pharmacophore-based virtual screening approach was performed. This virtual screening work was done by the group of Prof. Gerhard Wolber (Institute of Pharmacy, Department of Pharmaceutical Chemistry, Freie Universität Berlin) and Dr. Daniela Schuster (Department of Pharmaceutical Chemistry and Centre for Molecular Biosciences Innsbruck, University of Innsbruck). The pharmacophore model generation and experimental validation were described previously [188, 189] and the best pharmacophore model for PPAR γ partial agonists was selected [190]. Virtual screening of the 3D multi-conformational natural product databases was performed. Highly scored virtual hits were obtained from the chemical class of neolignans. Dieugenol and tetrahydrodieugenol, both are small molecular weight neolignans representing dimers of the abundant natural phenylpropanoid eugenol, were selected from the hit list for further investigation. The highly similar magnolol, which is also a major compound in the traditional Chinese herbal remedy magnolia bark (hòu pò) [191], has also been selected for pharmacological evaluation. The compounds were obtained from the group of Prof. Judith Rollinger and Prof. Hermann Stuppner (Institute of Pharmacy/Pharmacognosy, University of Innsbruck). The structures of the respective compounds are presented in **Figure 14**.

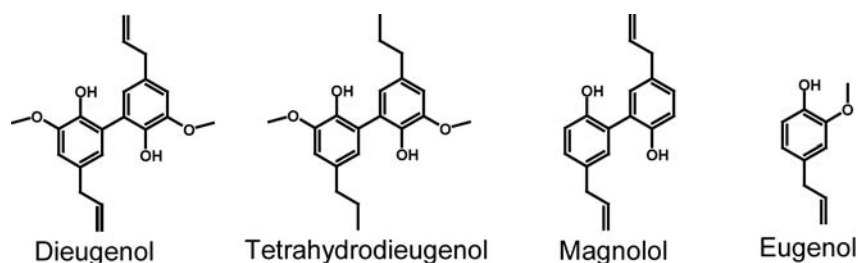


Figure 14. Chemical structures of the compounds selected for pharmacological testing.

1.4.1. PPAR γ ligand binding assay

The LanthaScreen™ TR-FRET PPAR γ competitive binding assay was used to validate the binding of predicted hits obtained from the virtual screening to the purified PPAR γ LBD. In this assay, stronger binding of the tested compound to the PPAR γ LBD leads to a stronger displacement of the fluorescently labelled ligand (Fluormone™ Pan-PPAR Green, Invitrogen) and subsequent decreasing of the FRET signal. Pioglitazone, a selective PPAR γ agonist in clinical use, was used as a positive control. **Figure 15** shows dose-response studies with the predicted hits.

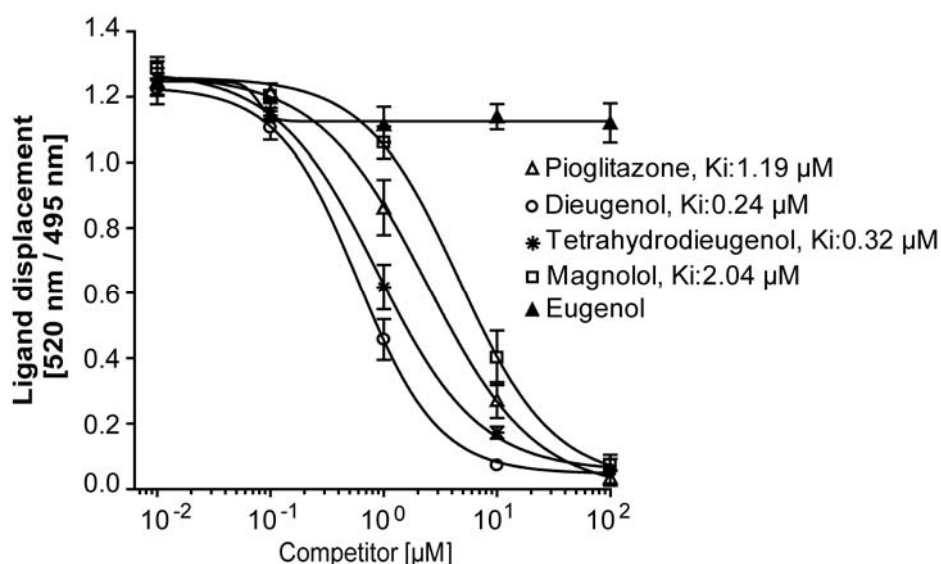


Figure 15. PPAR ligand binding potential of neolignans. Serial dilutions of the tested compounds were prepared in DMSO and mixed with a buffer solution containing a fluorescently-labelled PPAR γ agonist, terbium-labelled anti-GST antibody and the PPAR γ LBD tagged with GST. Following 1 hour of incubation, the ability of the tested compounds to bind to the PPAR γ LBD and thus to displace the fluorescently labelled ligand was estimated from the decrease of the emission ratio 520 nm/495 nm upon excitation at 340 nm. K_i : inhibition constant. Each data point represents the mean \pm SEM from three independent experiments performed in duplicate. The data were analyzed with GraphPad Prism software using settings for nonlinear regression with sigmoidal dose response and variable slope.

Figure 15 indicates that dieugenol, tetrahydrodieugenol and magnolol showed binding properties similar to pioglitazone, while eugenol failed to bind to the PPAR γ LBD (up to concentration of 100 μ M). Interestingly, dieugenol and tetrahydrodieugenol bound to the PPAR γ LBD with a higher affinity (K_i : 0.24 μ M

and 0.32 μM , respectively) than pioglitazone (K_i : 1.19 μM), whereas magnolol showed a slightly lower affinity (K_i : 2.04 μM).

1.4.2. PPAR γ luciferase reporter gene transactivation

To evaluate the functionality of the neolignans as PPAR γ agonists in intact cells, we next performed PPAR γ luciferase reporter gene assays. HEK-293 cells were cotransfected with a PPAR γ expression plasmid, a PPAR luciferase reporter plasmid (tk-PPREx3-luc), and EGFP as an internal control. Dieugenol, tetrahydrodieugenol and magnolol concentration-dependently induced PPAR γ activation in a concentration range similar to pioglitazone (**Figure 16**). Dieugenol and tetrahydrodieugenol showed maximal activation or saturation response in the same concentration range as pioglitazone (about 1 μM), indicating again similar binding affinities to PPAR γ . However, the maximal activation achieved by dieugenol and tetrahydrodieugenol was several folds lower than the full agonist pioglitazone, suggesting a partial agonism of the neolignans.

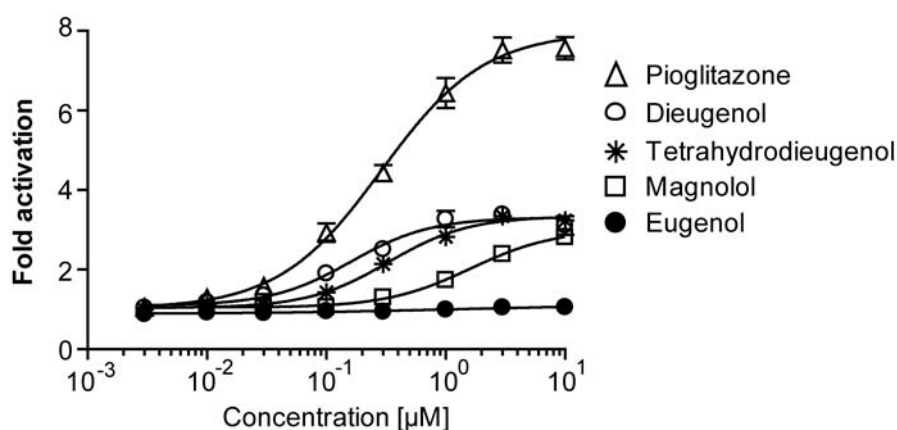


Figure 16. The activity of the neolignans towards PPAR γ in luciferase reporter transactivation assay. HEK-293 cells were transiently cotransfected with a reporter plasmid containing PPRE coupled to the luciferase reporter, PPAR γ expression plasmid, and EGFP as internal control. Upon stimulation with the indicated concentrations of the respective compounds for 18 hours, luciferase activity was measured and normalized by the EGFP-derived fluorescence. The result is presented as fold induction compared to the DMSO control. The data shown are means \pm SEM from three independent experiments performed in quadruplet. The data were analyzed with GraphPad Prism software using settings for nonlinear regression with sigmoidal dose response and variable slope.

1.4.3. Coactivator recruitment assay

Transcriptional regulation by the PPAR γ proteins is associated with a conformation change of the receptor and recruitment of coactivator proteins such as CBP, SRC-1, TRAP220, p300, upon binding of ligands to the PPAR γ LBD [192]. Therefore, a TRAP220/DRIP-2 coactivator recruitment assay was performed to investigate whether differences in the coactivator recruitment potential of the formed ligand-receptor complex is the reason for the lower maximal activation achieved by the neolignans in the luciferase reporter gene assay. Indeed, dieugenol, tetrahydrodieugenol and magnolol just partially induced the recruitment of the TRAP220/DRIP-2 coactivator peptide to the PPAR γ LBD, whereas the full agonist pioglitazone induced a several folds higher activation (**Figure 17**). Eugenol, as expected, failed to induce the recruitment of the coactivator peptide.

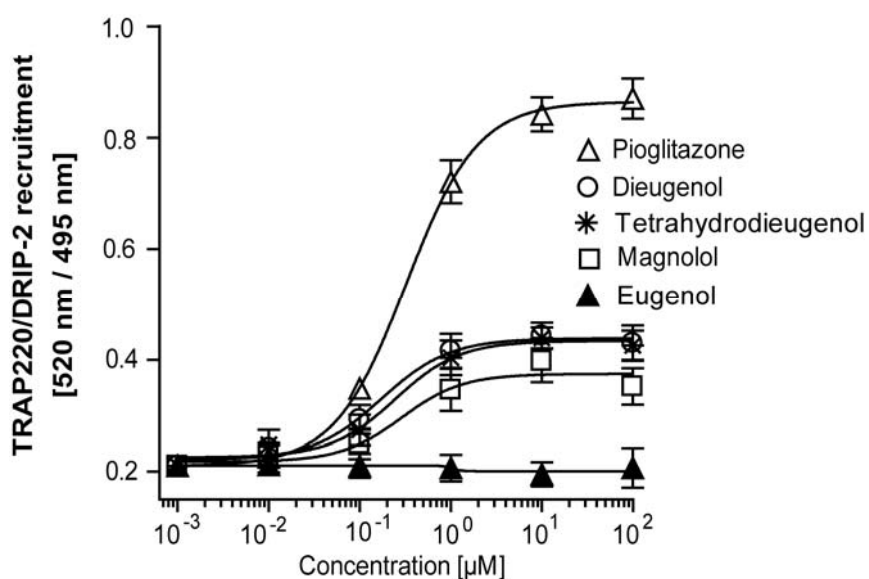


Figure 17. The effect of neolignans on PPAR γ coactivator recruitment. The recruitment of the TRAP220/DRIP-2 coactivator peptide by the PPAR γ -ligand complex formed with the test compounds was measured as described in details in the Materials and Methods section. The respective concentrations of test compounds were prepared in DMSO and then mixed with the PPAR γ LBD tagged with GST in a buffer solution containing fluorescein-labelled TRAP220/DRIP-2 coactivator peptide and terbium-labelled anti-GST antibody. The emission at 520 nm and 495 nm after excitation at 340 nm was measured after 1 hour incubation. The TRAP220/DRIP-2 coactivator recruitment potential of the respective compounds was determined by emission ratio at 520 nm/495 nm. The data shown are means \pm SEM from three independent experiments performed in duplicate. The data were analyzed with GraphPad Prism software using settings for nonlinear regression with sigmoidal dose response and variable slope.

In line with the result from the luciferase reporter gene assay, the maximal activation or saturation response induced with dieugenol, tetrahydrodieugenol, magnolol, and pioglitazone was achieved at the similar concentration range. However, the maximal activation induced with dieugenol, tetrahydrodieugenol, and magnolol was again several times lower than that of the full agonist pioglitazone.

Taken together, dieugenol, tetrahydrodieugenol, and magnolol show a high binding affinity against the PPAR γ LBD in a concentration range similar to that of the clinically used agonist pioglitazone. However, the binding of these neolignans to the PPAR γ LBD obviously induced different conformation of the ligand-receptor complex than the one induced with the full agonist pioglitazone. Consequently, these neolignans display partial agonism with respect to tk-PPREx3 promoter activation and TRAP220/DRIP-2 coactivator recruitment [177].

1.4.4. Molecular docking studies

To obtain a deeper mechanistic understanding of the neolignan binding to the PPAR γ LBD, the putative binding modes of these neolignans *in silico* were investigated by docking them into the PPAR γ binding pocket. This study was done by the group of Prof. Gerhard Wolber and Dr. Daniela Schuster. The initial docking of dieugenol, tetrahydrodieugenol, and magnolol to the PPAR γ binding pocket demonstrated that these neolignans did not completely occupy the large ligand binding pocket, and thus leave spaces and hydrogen bond possibilities for a second ligand. Based on a recent study by Itoh et al. [193] showing that a fatty acid bound to the LBD in a dimeric way, it has been assumed in these docking studies that the agonistic activity of magnolol, dieugenol, and tetrahydrodieugenol is also due to the simultaneous binding of two copies of neolignans to the LBD.

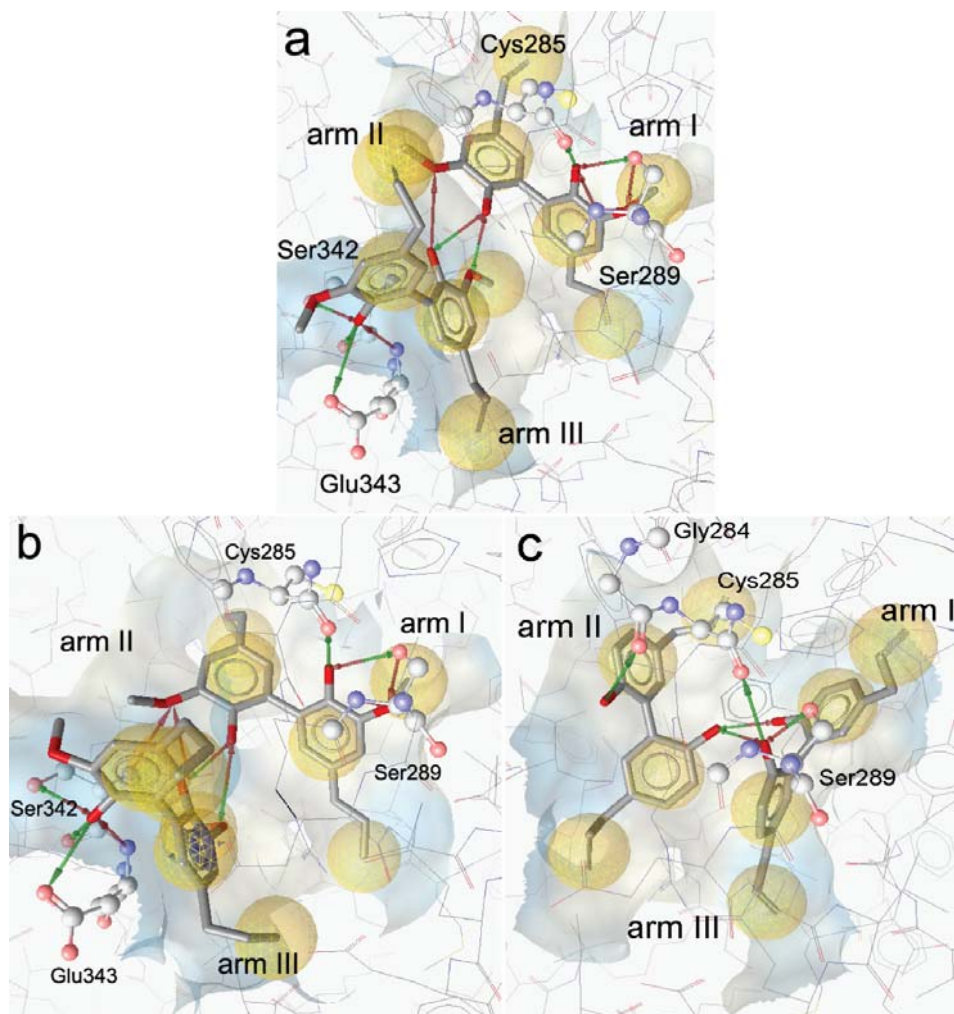


Figure 18. Putative interactions between the PPAR γ ligand binding domain and the neolignans dieugenol (a), tetrahydrodieugenol (b), and magnolol (c), visualized using LigandScout software. The colours represent hydrophobic interaction (yellow sphere), hydrogen bond donor (green arrow), hydrogen bond acceptor (red arrow) and aromatic interaction (blue rings). The ligand binding pocket is illustrated as a surface coloured based on the hydrophobicity/lipophilicity.

Docking of dieugenol into the PPAR γ ligand binding pocket demonstrated several hydrogen bonds between the binding site and the two dieugenol ligands (Figure 18a). A hydrogen bond network is formed between Ser289 and Cys285 with one 2-methoxyphenol moiety of the dieugenol located next to arm I. Several hydrogen bonds are also established by the second part of the ligand dimer by interaction of its 2-methoxyphenol moieties with residues Ser342 and Glu343. Another hydrogen bond network is also formed between both ligands involving the other 2-methoxyphenol group of this copy of dieugenol. Additionally, hydrophobic

contacts to the binding pocket are also established by the phenyl, vinyl and methoxy moieties of both molecules. Similar to dieugenol, the docking of two molecules of tetrahydrodieugenol to the ligand binding pocket resulted in the prediction of a binding mode with similar protein-ligand interactions (**Figure 18b**).

The best prediction for the binding of magnolol is presented in **Figure 18c**. One copy of the molecule situated between arm I and arm III whereas another copy of the ligand dimer located between arm II and arm III. The molecule of magnolol oriented towards arm I, and hydrogen bonds are formed between the hydroxyl group of magnolol and residues Cys285 and Ser289. The hydroxyl group of magnolol also forms a hydrogen bond with the hydroxyl group of the second magnolol molecule of the dimer. Another hydrogen bond is formed by the remaining hydroxyl group of the latter ligand with residue Gly284. Additionally, several hydrophobic interactions are established by interaction of both molecules with the three arms of the binding pocket. The higher affinity of dieugenol and tetrahydrodieugenol compared to magnolol in the ligand binding assay could be explained by the putative binding modes for the three compounds. Dieugenol and tetrahydrodieugenol have more interactions with the PPAR γ binding pocket than magnolol [177].

1.4.5. Selectivity study

To determine the selectivity of the neolignans on PPAR γ over the other two PPAR subtypes, the luciferase reporter gene assay using the respective receptor types expression plasmids was performed. In this experiment, the expression plasmid for PPAR γ was replaced with an expression plasmid for PPAR α or PPAR β/δ . In order to exclude species specific differences and to assess the activity of neolignans also in a murine model, the compounds were also evaluated for their potential to activate mouse PPAR γ (mPPAR γ). Selective agonists of PPAR α , PPAR β/δ and PPAR γ (GW7647, GW0742, and pioglitazone, respectively) were used to verify the selectivity of the test system. As shown in **Table 12**, dieugenol, tetrahydrodieugenol, and magnolol activated PPAR γ 3.58-fold (EC_{50} of 0.62 μ M), 3.34-fold (EC_{50} of 0.33 μ M) and 3.03-fold (EC_{50} of 1.62 μ M),

respectively. The neolignans exhibited a comparable potency of action also in the mouse PPAR γ model indicated by a high similarity in the profile of activation seen with human PPAR γ . Consistent with the results obtained from the aforementioned experiments, eugenol failed to activate any of the PPAR subtypes. Pioglitazone, the positive control, demonstrated an 8.05-fold activation (EC_{50} of 0.26 μ M) and a 6.80-fold activation (EC_{50} of 0.22 μ M) at human PPAR γ and mouse PPAR γ , respectively. Interestingly, dieugenol, and tetrahydrodieugenol selectively activated PPAR γ without affecting the other two PPAR subtypes. Magnolol was not equally specific, as it also activated PPAR β/δ at higher concentrations.

Table 12. The activity of the neolignans towards all subtypes of human PPAR (α , β/δ , γ), as well as towards mouse PPAR γ , determined in luciferase reporter transactivation assay*.

	PPAR α		PPAR β/δ		PPAR γ		mPPAR γ	
	EC_{50} (μ M)	maximal fold activation	EC_{50} (μ M)	maximal fold activation	EC_{50} (μ M)	maximal fold activation	EC_{50} (μ M)	maximal fold activation
GW7647	0.0016	3.09	-	-	-	-	-	-
GW0742	-	-	0.0015	22.47	-	-	-	-
Pioglitazone	-	-	-	-	0.26	8.05	0.22	6.80
Dieugenol	n.d.	n.d.	n.d.	n.d.	0.62	3.58	0.93	2.93
Tetrahydrodieugenol	n.d.	n.d.	n.d.	n.d.	0.33	3.34	0.38	2.98
Magnolol	n.d.	n.d.	11.41	2.45	1.62	3.03	1.14	2.81
Eugenol	n.d.	n.d.	n.d.	n.d.	n.d.	n.d.	n.d.	n.d.

* HEK-293 cells were transiently cotransfected with a reporter plasmid containing PPRE coupled to the luciferase reporter, a respective PPAR subtype expression plasmid, and EGFP as internal control. Upon stimulation with the indicated concentrations of the respective compounds for 18 hours, luciferase activity was measured and normalized by the EGFP-derived fluorescence. The result is presented as fold induction compared to the DMSO vehicle control, and n.d. denotes not detected (up to 30 μ M). To verify the specificity of the respective assays, selective agonists for PPAR α (GW7647), PPAR β/δ (GW0742), and PPAR γ (pioglitazone), were used. GraphPad Prism software version 4.03 (GraphPad Software Inc, USA) with non linear regression (sigmoidal dose response) was used to calculate the EC_{50} and maximal fold activation. The data shown are means of three independent experiments performed in triplicate. Note: mPPAR (mouse PPAR), PPAR (human PPAR)

In order to obtain compounds with possibly higher activity and to get insights into the underlying structure-activity relationship, 31 magnolol derivatives were synthesized (**Supplementary Figure 2**) and tested in the luciferase reporter gene assay (

Supplementary Table 2). Concerning PPAR γ activation, unfortunately, none of the derivatives demonstrated an impressively increased activity in comparison with magnolol. Three compounds (number 753, 754 and 775) demonstrated slightly higher PPAR γ activation.

Apart from that, we were able to identify honokiol, another neolignan with a high structural similarity and isolated from the same *Magnolia officinalis* extract, as an activator of all three PPAR subtypes (PPAR pan-agonist). The honokiol-induced activation of PPAR β/δ higher (up to 4.90 fold activation, EC₅₀ 6.25 μ M) than that of PPAR α and PPAR γ . The activation profile and the EC₅₀ in respective PPAR subtypes are shown in **Supplementary Figure 3**.

1.4.6. Adipogenic activity in 3T3-L1 preadipocytes

The effectiveness of neolignans in activating PPAR γ was then confirmed in a relevant cell model endogenously expressing PPAR γ . As it is widely accepted that PPAR γ is a key factor in adipocyte differentiation [194], the adipogenic potential of the compounds in preadipocytes (3T3-L1 cells) was investigated. Rosiglitazone, a potent PPAR γ agonist was used as positive control in this experiment [195].

Accumulated lipid droplets in the cells due to adipogenesis could be visualized and subsequently quantified by Oil Red staining. In this experiment, dieugenol, tetrahydrodieugenol, and magnolol treatment at 10 μ M led to the differentiation of 3T3-L1 preadipocytes to adipocytes, whereas eugenol did not exert adipogenic activity (**Figure 19**). Moreover, the adipogenic potential of dieugenol, tetrahydrodieugenol, magnolol, and rosiglitazone was significantly reduced by addition of the PPAR γ antagonist BADGE [195], demonstrating PPAR γ dependency of the effect (**Figure 19b**).

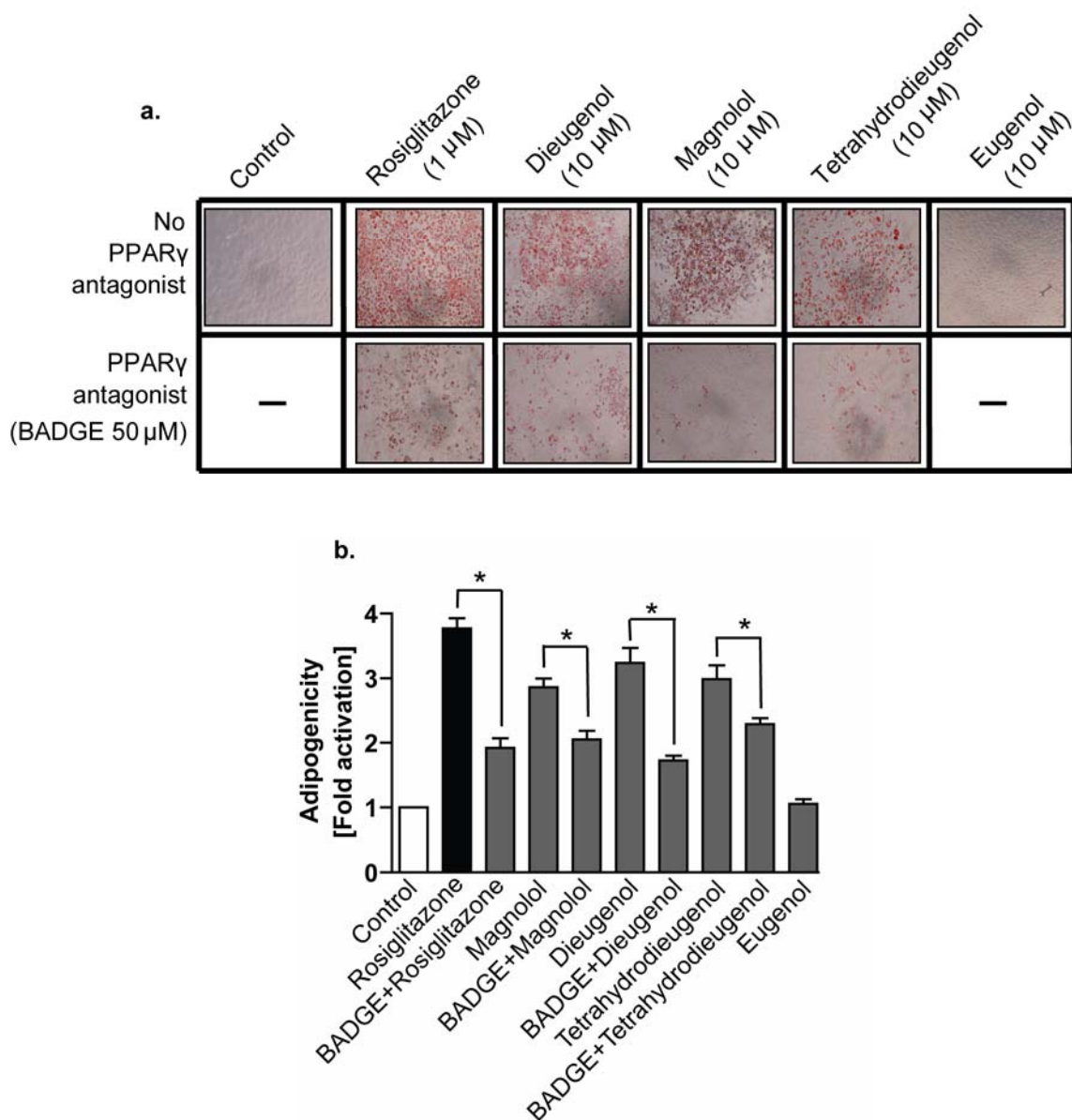


Figure 19. Induction of adipocyte differentiation by the neolignans. (a) Preadipocytes (3T3-L1) were differentiated to adipocytes with 1 μ M rosiglitazone, 50 μ M BADGE or 10 μ M of the neolignans as described in the Materials and Methods section. To visualize the accumulated lipids, Oil Red O staining was performed and representative photos of one experiment out of three are depicted. (b) The dye accumulated in the cells was solubilised by 100% isopropanol and photometrically quantified at 550 nm. The data shown are means \pm SEM from three independent experiments. *, $p < 0.05$ (one-way ANOVA followed by Bonferroni's post-test).

1.5. The effect of PPAR γ agonists on the NO production in macrophages

In atherogenesis, nitric oxide (NO) produced by activated macrophages is increased in response to cytokines at the site of inflammation. Agonists of PPAR γ have been reported to inhibit NO production [196]. Therefore, rosiglitazone, a selective PPAR γ agonist, was tested in RAW 264.7 macrophages for NO production inhibitory activity.

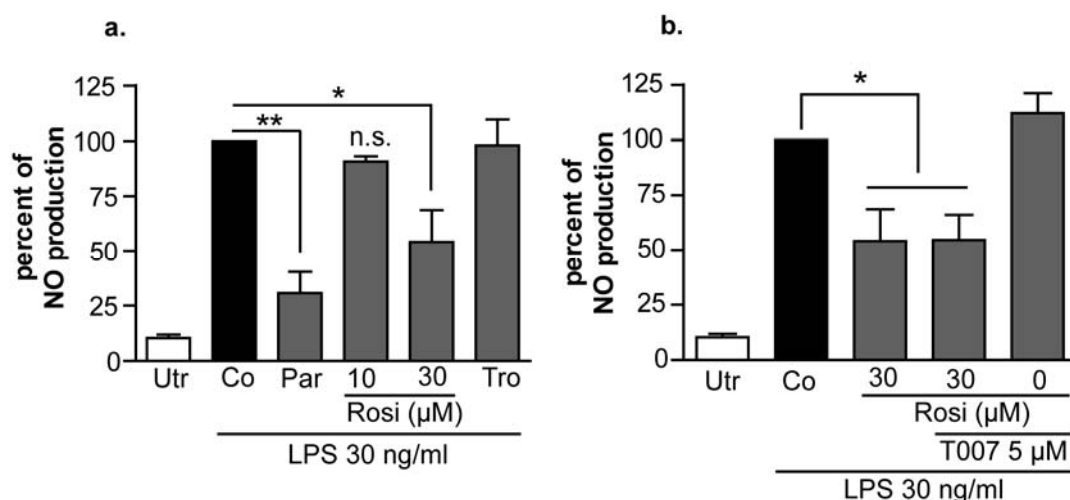


Figure 20. Influence of PPAR γ agonists on LPS-induced NO production in macrophages. (a) Inhibition of LPS-induced NO production by rosiglitazone (Rosi) and troglitazone (Tro, 10 μ M). (b) Effect of the PPAR γ antagonist T0070907 on the inhibition of LPS-induced NO production by rosiglitazone. RAW 264.7 cells were pretreated with indicated concentrations of compounds for 30 minutes prior to stimulation with LPS for 18 hours. The NO released in the medium was measured using the Griess assay and the values were normalized to the cell viability analyzed with the resazurin cell viability assay. The values are relative to the DMSO treatment (Co), and Utr denotes the untreated cells. The data shown are means \pm SEM from three independent experiments. *, $p < 0.05$; **, $p < 0.01$; n.s., not significant (one-way ANOVA followed by Dunnett's post-test).

Parthenolide, a NF- κ B inhibitor capable of inhibiting NO production was used as a positive control. In this experiment, rosiglitazone was able to inhibit LPS induced NO production at relatively high concentration of 30 μ M (Figure 20a). However, pretreatment with antagonist of PPAR γ , T0070907, failed to reverse the effect, suggesting that the effect is independent of PPAR γ (Figure 20b). In addition, treatment with another PPAR γ agonist troglitazone (10 μ M) did not inhibit the NO production. In our experiment, the three neolignan activators of PPAR γ failed to inhibit the NO production at concentration of 10 μ M (data not shown).

1.6. The effect of PPAR γ agonists on the migration of VSMC.

Migration of VSMC contributes to the development of atherosclerosis [197]. Although PPAR γ is expressed in VSMC [17], little data exist regarding inhibition of VSMC migration by PPAR γ agonists. Here, the effects of the selective PPAR γ full agonists pioglitazone and troglitazone on VSMC migration was investigated using the wound healing assay (**Figure 21**). Upon PDGF-BB stimulation for 21 hours, VSMC migrated to the scratched area. Pioglitazone and troglitazone treatment did not show a significant inhibition of VSMC migration at 10 μ M concentration. Similar effects were also observed upon treatment with the three neolignans. This suggests the lack of responsiveness of this model to PPAR γ agonists.

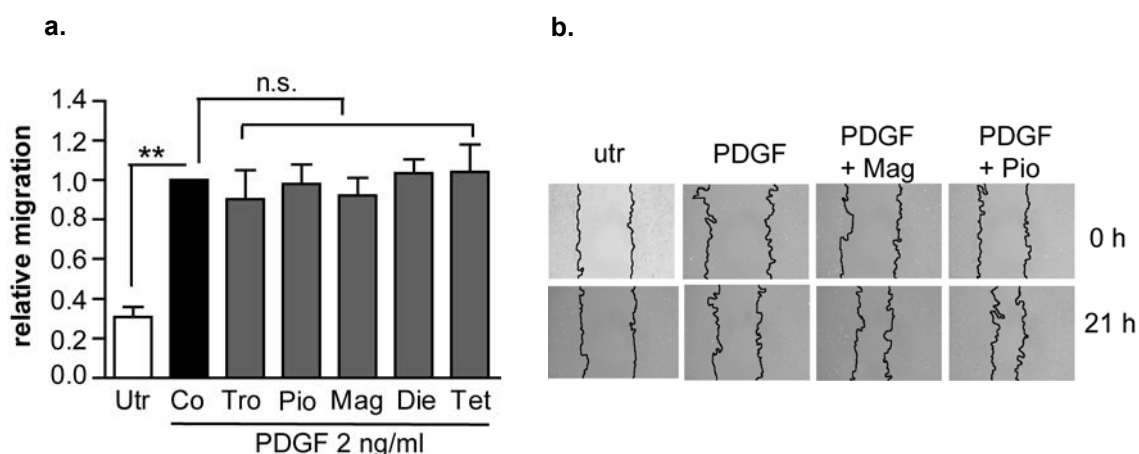


Figure 21. Influence of PPAR γ agonists on VSMC migration. (a) The effect of pioglitazone (Pio), troglitazone (Tro), magnolol (Mag), dieugenol (Die), and tetrahydrodieugenol (Tet) on PDGF-BB-induced migration. (b) Representative pictures of the wound healing assay. VSMC were serum-starved for 24 hours and then scratched before pretreatment with the respective compound at 10 μ M for 30 minutes, followed by stimulation with 2 ng/ml PDGF-BB for 21 hours. Pictures were captured at 0 and 21 hours of stimulation. The cell free scratched areas in the pictures were calculated by subtracting cell free area from both time points at the same location using Cellprofiler software. The arbitrary values were normalized to the DMSO control (Co), and Utr denotes the untreated cells. The bars represent means \pm SEM from three independent experiments. **, $p < 0.01$; n.s., not significant (one-way ANOVA followed by Dunnett's post-test).

1.7. Discovery of PPAR γ agonists by the ethnopharmacological approach.

In this section, the utilization of an ethnopharmacological approach to select plants for the screening of PPAR γ agonists is described. Plants traditionally used against inflammatory diseases were subjected to the PPAR γ -driven reporter gene

transactivation assay to find potential plant extract that activate PPAR γ (**Supplementary Table 1**). Among the active plants, several from the most promising were subjected to a bioassay guided fractionation to isolate the active compounds. Here, the results obtained with *Notopterygium incisum*, will be presented.

1.7.1. Pharmacological evaluation of extracts in the PPAR γ -driven reporter gene assay

The tested extracts were obtained from the groups of Prof. Brigitte Kopp and Prof. Gottfried Reznicek (Department of Pharmacognosy, University of Vienna), Prof. Rudolf Bauer (Institute of Pharmaceutical Sciences/Pharmacognosy, University of Graz) and from the group of Prof. Hermann Stuppner and Prof. Judith Rollinger (Institute of Pharmacy/Pharmacognosy, University of Innsbruck). For the screening assays, the extracts were initially tested at concentration of 10 μ g/ml in the PPAR γ -driven reporter gene transactivation assay as described in the Methods section. The extracts that exhibit more than 1.5 fold activation compared to the vehicle control (DMSO treatment) were considered active, and thus, marked with “+”. A representative result of the screening assay was previously shown in **Figure 13**.

1.7.2. Discovery of PPAR γ agonists from *Notopterygium incisum*

The dichloromethane extract of *Notopterygium incisum* roots and rhizomes was identified to activate PPAR γ in our screening. The activation achieved by the extract at concentration of 10 μ g/ml was around 2-fold compared to vehicle control (**Figure 23**). Bioassay-guided isolation from this plant extract led to the discovery of six polyacetylene activators of PPAR γ . The six identified compounds are: falcarindiol, 8-acetoxylfalarinol, 9-epoxy-falcarindiol, crithmundiol, 9-heptadecene-4,6-diyne-1-ol, and (2Z,9Z)-2,9-heptadecadiene-4,6-diyne-1-ol (**Figure 22**).

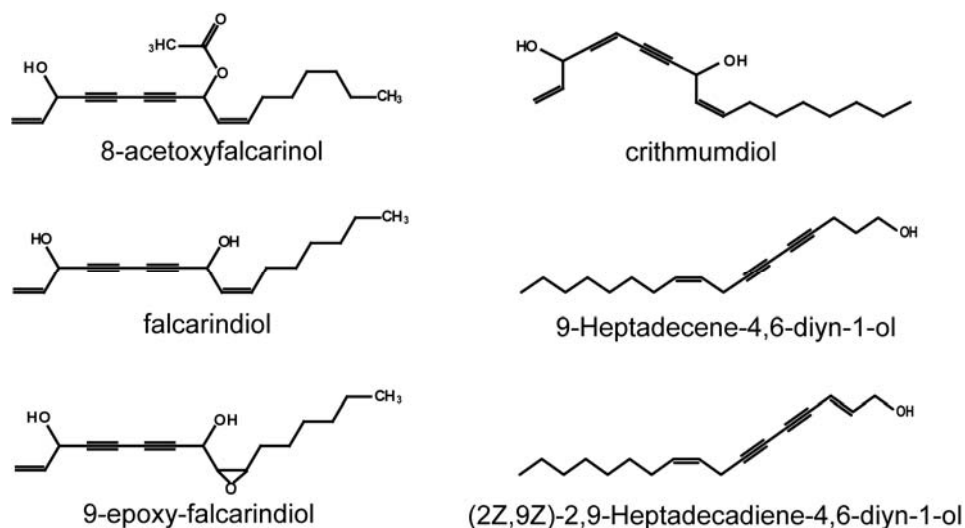


Figure 22. Chemical structures of the polyacetylene activators of PPAR γ .

To evaluate the functionality of the polyacetylenes as PPAR γ agonists in intact cells, they were subjected to the PPAR γ -driven luciferase reporter gene assay. All polyacetylenes activated PPAR γ in a concentration-dependent manner (**Figure 23**). The activation achieved by the compounds at a concentration of 10 μ M was around 2-fold compared to vehicle control and several folds lower than that of the full agonist pioglitazone (1 μ M).

To determine the EC₅₀, the polyacetylenes were tested in a broader concentration range. Furthermore, the selectivity of action over the other two PPAR subtypes was determined. Verification of the selectivity of the test system was achieved by using selective agonists of PPAR α , β/δ , and γ (GW7647, GW0742, and pioglitazone, respectively). As shown in **Table 13**, 8-acetoxylfincarinol, faltarindiol, 9-epoxy-faltarindiol, crithmumdiol, 9-heptadecene-4,6-diyn-1-ol and (2Z,9Z)-2,9-heptadecadiene-4,6-diyn-1-ol activated PPAR γ 2.36-fold (EC₅₀ of 3.59 μ M), 2.29-fold (EC₅₀ of 4.25 μ M), 1.88-fold (EC₅₀ of 2.03 μ M) and 2.29-fold (EC₅₀ of 4.58 μ M), 1.921 fold (EC₅₀ of 11.31 μ M), and 1.73-fold (EC₅₀ of 4.18 μ M), respectively, whereas pioglitazone, the positive control, demonstrated 7.96-fold activation (EC₅₀ of 0.31 μ M). The pattern of PPAR γ activation shown by the polyacetylenes was similar to the previously described

neolignans, thus, it suggests partial agonism. Interestingly, all polyacetylenes selectively activated PPAR γ without affecting the other two PPAR subtypes.

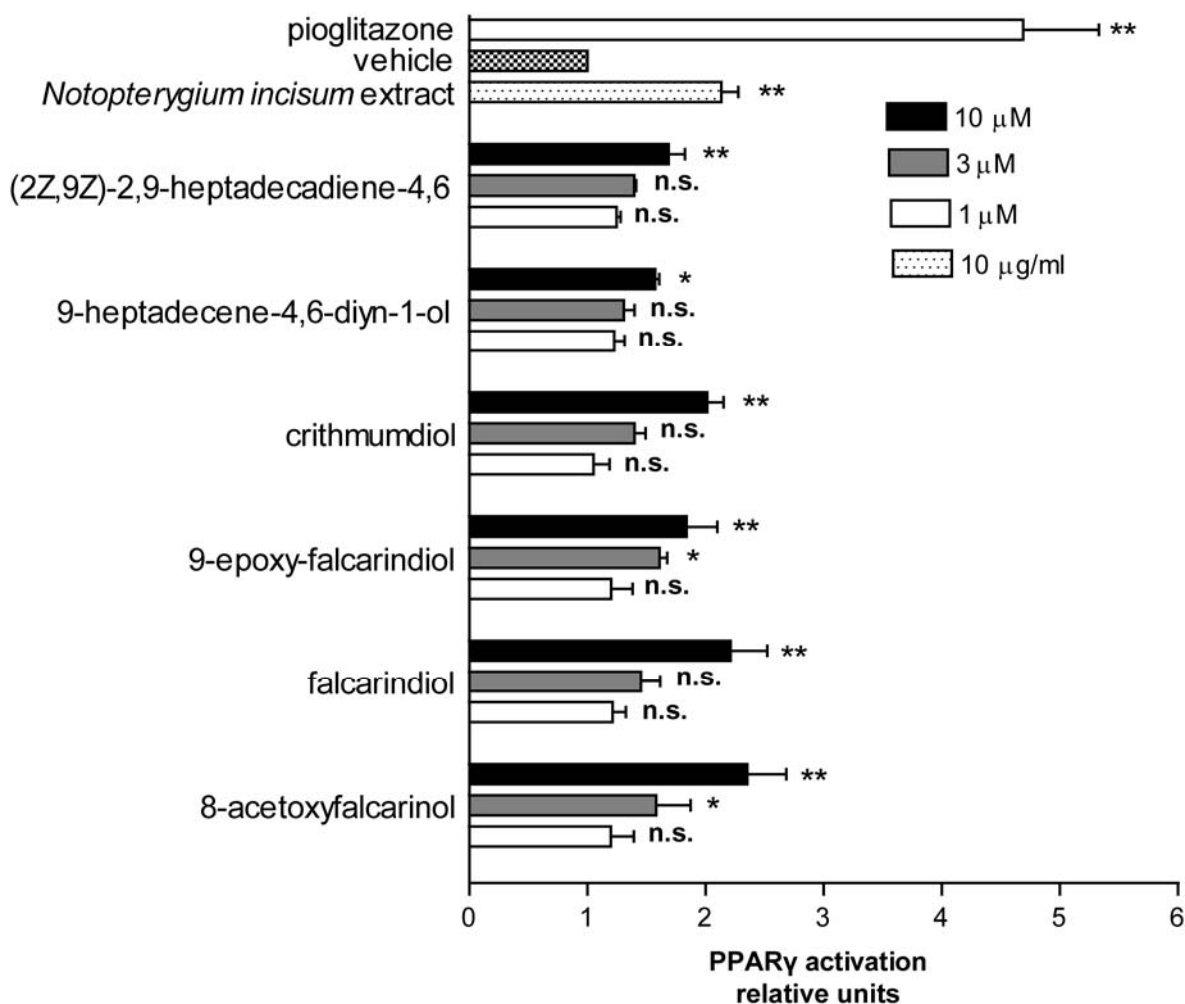


Figure 23. The activity of the polyacetylenes towards PPAR γ in the luciferase reporter transactivation assay. HEK-293 cells were transiently cotransfected with a reporter plasmid containing PPRE coupled to the luciferase reporter, a PPAR γ expression plasmid, and EGFP as internal control. Upon stimulation with the indicated concentrations of the respective compounds for 18 hours, luciferase activity was measured and normalized by the EGFP-derived fluorescence. The result is presented as fold induction compared to the vehicle (DMSO) control. The data shown are means \pm SEM, of three independent experiments performed in triplicate. *, $p < 0.05$; **, $p < 0.01$; n.s., not significant (one-way ANOVA followed by Dunnett's post-test).

Table 13. The activity of the polyacetylenes towards all subtypes of PPAR (α , β/δ , γ) in luciferase reporter transactivation assay*.

	PPAR γ		PPAR α		PPAR β/δ	
	EC ₅₀ (μ M)	maximal fold activation	EC ₅₀ (μ M)	maximal fold activation	EC ₅₀ (μ M)	maximal fold activation
GW7647	-	-	0.0021	3.08	-	-
GW0742	-	-	-	-	0.0017	20.20
Pioglitazone	0.31	7.96	-	-	-	-
8-acetoxycarinalol	3.59	2.36	n.d.	n.d.	n.d.	n.d.
Falcarindiol	4.25	2.29	n.d.	n.d.	n.d.	n.d.
9-epoxy-falcarindiol	2.03	1.88	n.d.	n.d.	n.d.	n.d.
Crithmumdiol	4.58	2.29	n.d.	n.d.	n.d.	n.d.
9-Heptadecene-4,6-diyn-1-ol	11.31	1.921	n.d.	n.d.	n.d.	n.d.
(2Z,9Z)-2,9-heptadecadiene-4,6-diyn-1-ol	4.18	1.73	n.d.	n.d.	n.d.	n.d.

* HEK-293 cells were transiently cotransfected with a reporter plasmid containing PPRE coupled to the luciferase reporter, a respective PPAR subtype expression plasmid, and EGFP as internal control. Upon stimulation with the indicated concentrations of the respective compounds for 18 hours, luciferase activity was measured and normalized by the EGFP-derived fluorescence. The result is presented as fold induction compared to the DMSO vehicle control, and n.d. denotes not detected (up to 30 μ M). To verify the specificity of the respective assays, selective agonists for PPAR α (GW7647), PPAR β/δ (GW0742), and PPAR γ (pioglitazone), were used. GraphPad Prism software version 4.03 (GraphPad Software Inc, USA) with non linear regression (sigmoidal dose response) was used to calculate the EC₅₀ and maximal fold activation. The data shown are means of three to five independent experiments performed in triplicate.

Taken together, several polyacetylene activators of PPAR γ have been identified from *Nototerigium incisum* by bioassay-guided isolation. These compounds selectively activated PPAR γ with a potency several folds lower than the clinically used selective PPAR γ agonist, pioglitazone. This finding reported for the first time that polyacetylene is a new group of compounds activating PPAR γ .

2. Discovery of NF- κ B inhibitors

2.1. Validation of the bioassay

HEK-293 cells stably transfected with a NF- κ B-driven luciferase reporter gene were used for detection of NF- κ B inhibitors in the tested samples. These cells produce luciferase upon TNF- α stimulation due to activation of NF- κ B. The presence of NF- κ B inhibitors such as parthenolide, leads to a lower level of luciferase which can be quantified in a luminometer. **Figure 24a** and **Figure 24b** demonstrate the response of the cells upon TNF- α stimulation and parthenolide treatment, respectively.

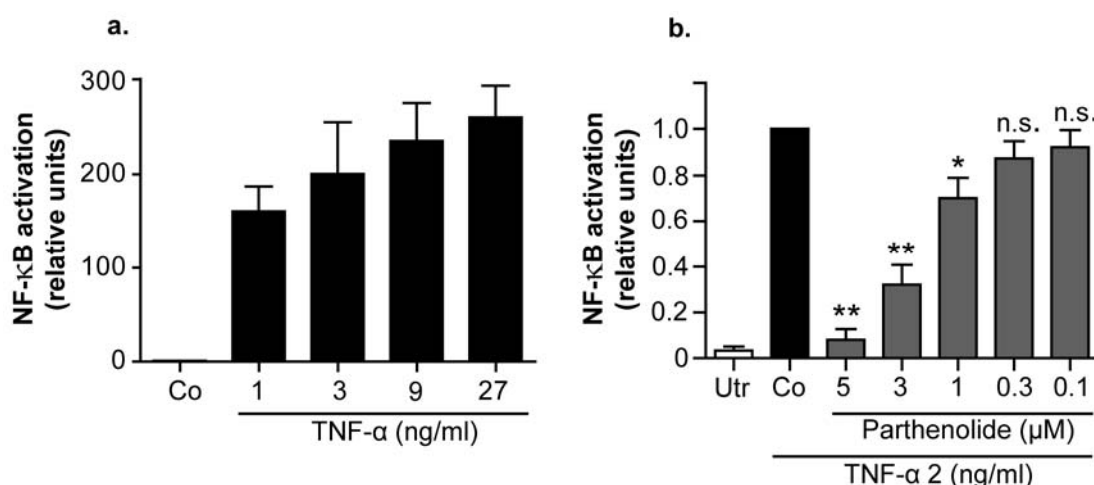


Figure 24. Validation of the NF- κ B assay in 293/NF- κ B-luc cells. (a) NF- κ B response of the cells towards TNF- α stimulation. 293/NF- κ B-luc cells were treated with various concentrations of TNF- α for 4 hours, before cell lysates were subjected to detection of luciferase activity. (b) Effect of parthenolide on TNF- α -stimulated 293/NF- κ B-luc cells. 293/NF- κ B-luc cells were pretreated with the indicated concentration of parthenolide for 30 minutes and stimulated with 2 ng/ml TNF- α for 4 hours, before cell lysates were subjected to detection of luciferase activity. Luciferase activity was normalized by the EGFP-derived fluorescence, and the result is expressed as a fold induction compared to the DMSO control (Co). Utr denotes the untreated cells. The data shown are means \pm SEM from two independent experiments each performed in quadruplet. *, $p < 0.05$; **, $p < 0.01$; n.s., not significant (one-way ANOVA followed by Dunnett's post-test).

As evident, TNF- α induces the production of luciferase in a concentration-dependent manner and pretreatment with parthenolide inhibits NF- κ B activation concentration-dependently, indicating the functionality of the test system. The

effect of DMSO was also evaluated in this system since all tested samples (extracts, fractions and compounds) were diluted in DMSO. Serial concentrations of DMSO were tested. We found that DMSO at the concentration range from 0.1 % to 1 % showed a dose-dependent inhibition of NF- κ B activation in this system (data not shown). Thus, the concentration of DMSO was kept identical in every treatment. For the initial testing of the plant extracts (screening), a final DMSO concentration of 0.1 % was always used.

2.2. Investigation of NF- κ B inhibitors from plant extracts

Extracts from plants traditionally used for the treatment of inflammation-related diseases were tested for their potency to inhibit TNF- α -induced NF- κ B activation in 293/NF- κ B-luc cells. The extracts were initially tested in at least two independent experiments at a concentration of 10 μ g/ml. The concentration was lowered to 3 μ g/ml or 1 μ g/ml if an unspecific inhibitory effect was observed, indicated by the lower value of EGFP-derived fluorescence. Parthenolide was used for every testing to confirm the functionality of the respective experiment. The tested samples showing more than 50 % inhibition were considered active, thus, marked with “+”. The detailed results are presented in the **Supplementary Table 1. Figure 25** provides a representative screening result showing the activity of the tested extracts. In this experiment, extracts number 260 and 270 were considered active.

Among the active plant extracts, several from the most promising plants were selected for further separation and identification of the active compounds (

Table 14). In this work, the discovery of compounds inhibiting NF- κ B from *Himathantus sucuuba* and *Krameria lappacea* will be described in more detail.

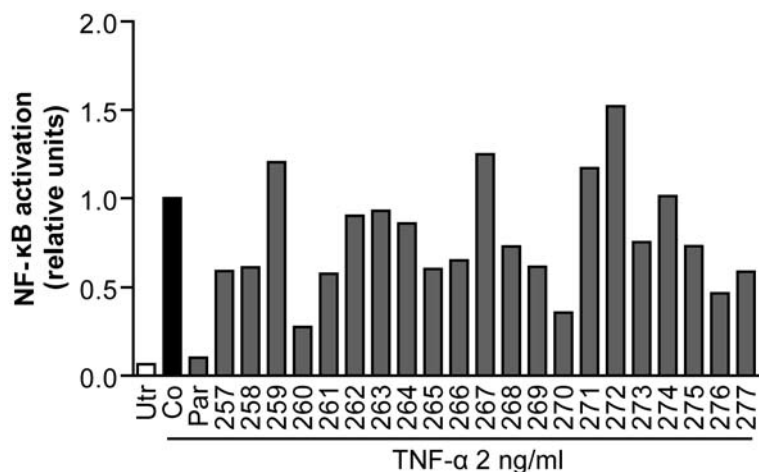


Figure 25. Representative screening results from the NF-κB-driven reporter gene assay. Samples were tested at 10 µg/ml for their inhibitory activity on TNF-α-induced NF-κB activation. Parthenolide (Par, 5 µM) was used as a positive control. The data shown are means from one representative experiment (out of two) each performed in a quadruplet. Samples exhibiting NF-κB activation less than 0.5 compared to control DMSO (Co) were considered active in each single experiment. Utr denotes the untreated cells. At least two independent experiments with similar outcome were performed before a sample was finally classified as “active” or “inactive”.

Table 14. The active plants selected for isolation and identification of NF-κB inhibitors.

Selected active plants	Current state with the identification of the bioactive compounds
<i>Melampyrum</i> sp.	Subfractions
<i>Himathantus sucuuba</i>	Plumericin
<i>Krameria lappacea</i>	Benzofurans
<i>Dryopteris filix-mas</i>	Subfractions

2.2.1. Discovery of plumericin as a NF-κB inhibitor

To find novel NF-κB inhibitors derived from medicinal plants, the *Himathantus sucuuba* methanolic extract showing NF-κB inhibitor activity was chosen for further separation and compound identification. Isolation and identification of the active compounds from this plant was done by the research group of our collaboration partner, Prof. Judith Rollinger and Prof. Hermann Stuppner resulting in the discovery of the active compound plumericin. Plumericin was isolated together with other inactive compounds: plumeridin, biochanin A, and dihydrobiochanin A (**Figure 26**).

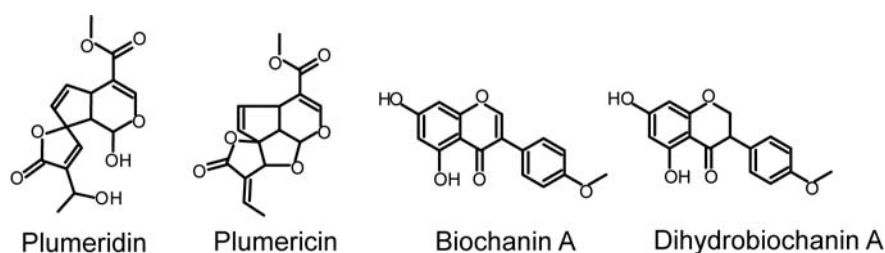


Figure 26. Chemical structure of the compounds isolated from *Himathantus sucuuba*

Among those compounds, which were derived from active subfractions, plumericin is the only active compound with a potent NF- κ B inhibitory effect in 293/NF- κ B-luc cells (EC_{50} $1.07 \pm 0.08 \mu\text{M}$, **Figure 27**). Attempts to identify additional active compounds from *Himathantus sucuuba* are still ongoing. Since plumericin exhibited promising inhibitory activity, it was further studied in additional inflammation-related models.

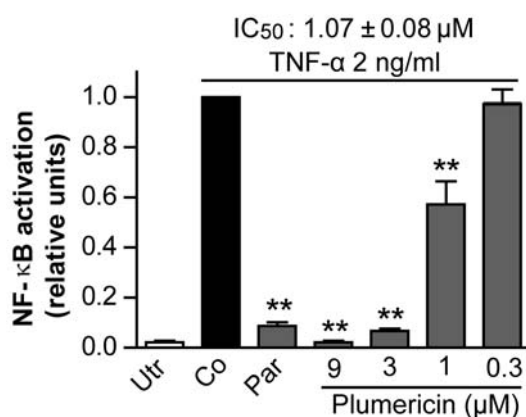


Figure 27. Effect of plumericin on TNF- α -induced NF- κ B activation. 293/NF- κ B-luc cells were pretreated with the indicated concentrations of plumericin or parthenolide (Par, $5 \mu\text{M}$) for 30 minutes prior to stimulation with 2 ng/ml TNF- α for 4 hours. The luciferase activity was determined by a luminometer and normalized to the fluorescence derived from the EGFP expression. The values are normalized to the vehicle control DMSO (Co), and Utr denotes the untransfected cells. The data shown represent means \pm SEM from three independent experiments. *, $p < 0.05$; **, $p < 0.01$; n.s., not significant (one-way ANOVA followed by Dunnett's post-test).

2.2.2.1. Effect of plumericin on endothelial cells

Endothelial dysfunction contributes to atherosclerosis by enhancing the expression of adhesion molecules that increases endothelial permeability [198]. Since the expression of these adhesion molecules is regulated by NF- κ B, we investigate the effect of plumericin on TNF- α -induced cell surface expression of adhesion molecules in endothelial cells. Immortalized human endothelial cells, HUVECtert, were used for these investigations. As shown in **Figure 28a-c**, the stimulation of cells with TNF- α led to increased expression of the adhesion molecules VCAM-1, ICAM-1, and E-selectin. Treatment with plumericin dose-dependently inhibited the cell surface expression of these adhesion molecules. Moreover, plumericin at concentration of 5 μ M suppressed the expression of these adhesion molecules to the basal level of the untreated control group. Flow cytometric analysis (**Figure 28d-f**) demonstrates that the fluorescence intensity (FL1-H) representing the binding of the respective FITC-labelled antibodies to the adhesion molecules was increased upon TNF- α stimulation, and this effect was completely reverted by plumericin treatment to the level of the unstimulated cells.

To determine the mode of action of plumericin in the NF- κ B pathway, the effect of plumericin on TNF- α -induced degradation of I κ B- α was investigated. I κ B- α was completely degraded upon stimulation with TNF- α for 10 minutes. After 30 minutes, however, the I κ B- α level started to recover (**Figure 29a**). Thus, 10 minutes stimulation was used to investigate the effect of plumericin on the degradation of I κ B- α . We found that plumericin at 5 μ M significantly inhibited the degradation of I κ B- α in HUVECtert (**Figure 29c**). The inhibitory activity of plumericin at different concentrations (1-30 μ M) is shown in **Figure 29b**.

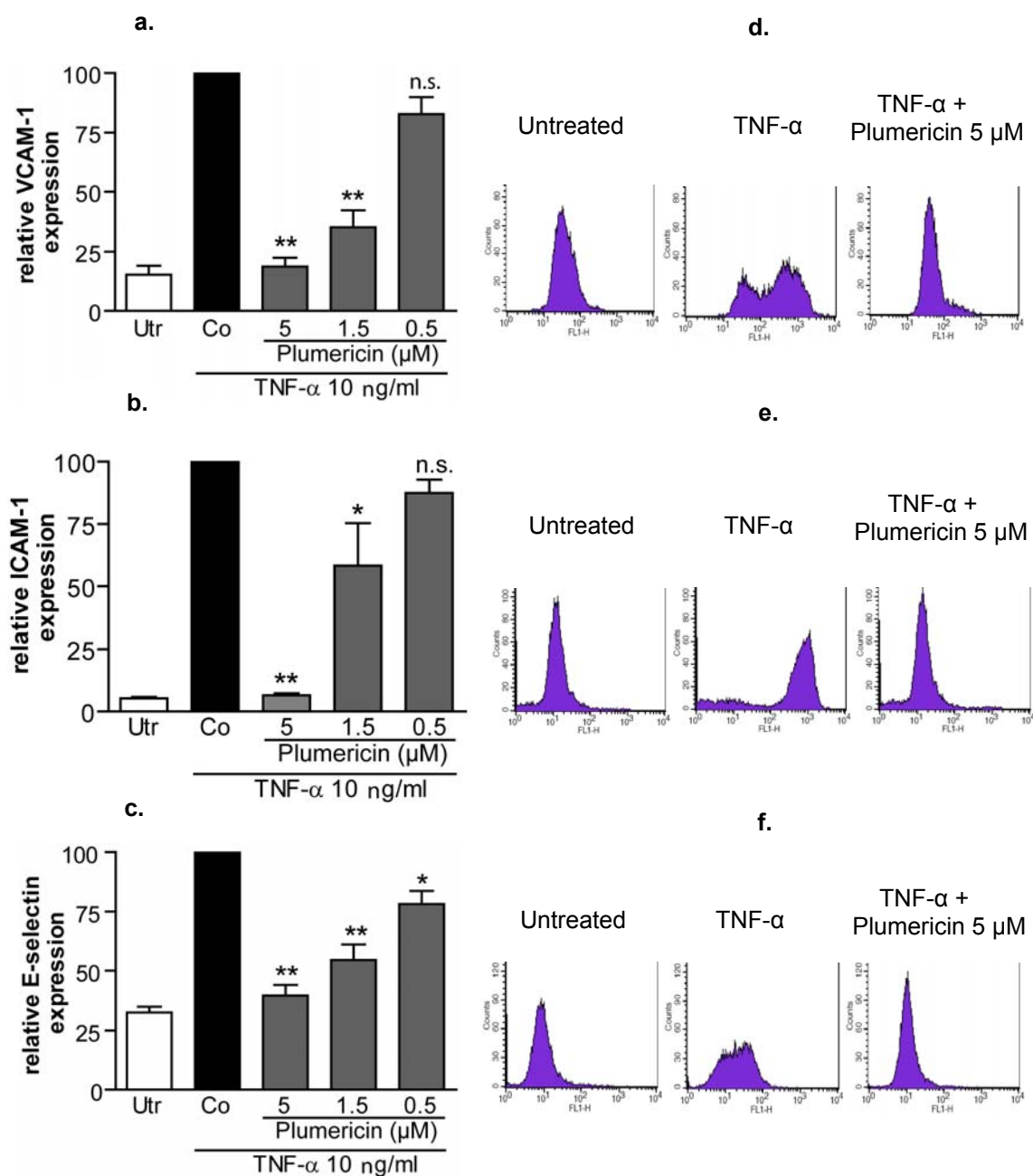


Figure 28. Influence of plumericin on cell surface expression of endothelial adhesion molecules. Plumericin inhibited TNF- α -induced VCAM-1 (a), ICAM-1 (b), and E-selectin (c) surface expression. Representative flow cytometric analyses depicting the effect of plumericin (5 μ M) are shown (d, e and f). HUVEctert were pretreated with the indicated concentrations of plumericin for 30 minutes prior to stimulation with 10 ng/ml TNF- α for 14 hours. The level of VCAM-1, ICAM-1 and E-selectin expression was determined by FACS analysis after addition of FITC-labelled respective antibody. FL1-H denotes hight of fluorescence intensity. All values were normalized to the control DMSO (Co), and Utr denotes the untreated cells. The data shown are means \pm SEM from three independent experiments. *, $p < 0.05$; **, $p < 0.01$; n.s., not significant (one-way ANOVA followed by Dunnett's post-test).

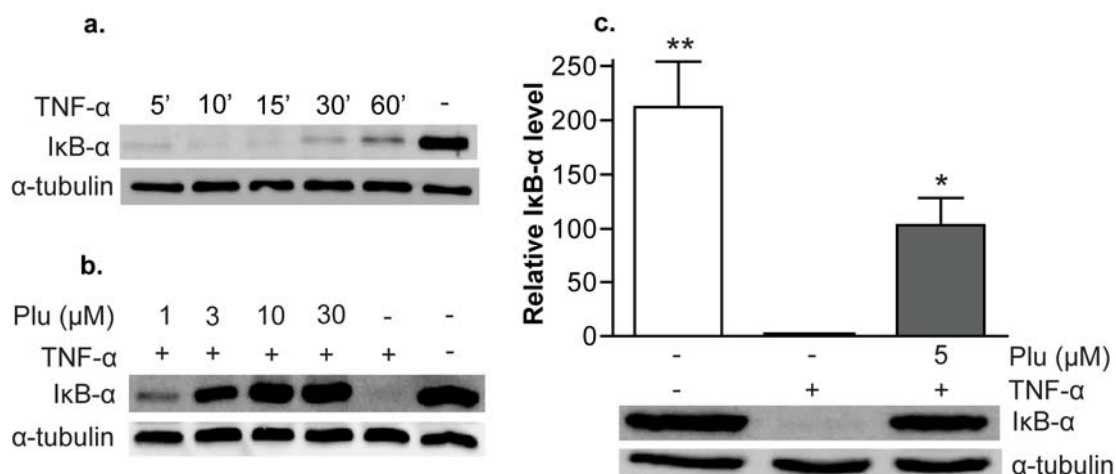


Figure 29. The inhibitory effect of plumericin on TNF- α -induced I κ B- α degradation. (a) Time course of the degradation of I κ B- α upon TNF- α treatment. (b) Concentration dependence of the inhibitory activity of plumericin on TNF- α -induced I κ B- α degradation, 10 minutes after stimulation. (c) Inhibitory activity of plumericin (5 μ M) on TNF- α -induced I κ B- α degradation for 10 minutes. HUVECTert were preincubated with the indicated concentration of plumericin for 30 minutes prior to the stimulation with TNF- α 10 ng/ml for 10 minutes. Cell lysates were subjected to western blot analysis for I κ B- α degradation and total α -tubulin. The blots shown are a representative blot from three (c) and two (a, b) independent experiments. The Graph show the band intensity calculated with densitometry as I κ B- α protein/tubulin ratios. The bars are means \pm SEM, ** $p < 0.01$; * $p < 0.05$ (one-way ANOVA followed by Dunnett's post-test).

It is known that IKK- β is an upstream kinase regulator of I κ B- α degradation [199]. Therefore, we performed IKK- β *in vitro* enzymatic assay to assess whether the effect of plumericin on the degradation of I κ B- α is due to the inhibition of IKK- β activity. Indeed, plumericin inhibited IKK- β activity in a concentration-dependent manner (**Figure 30**). However, the effective concentration to inhibit the activity of IKK- β in this *in vitro* experiment was higher compared to that in the cells-based assays. This indicates that plumericin might inhibit NF- κ B activation partly by inhibition of IKK- β .

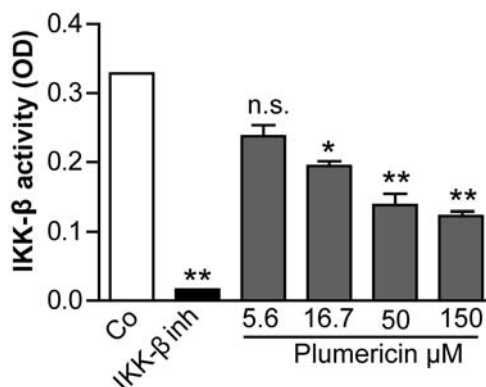


Figure 30. IKK- β inhibitory activity of plumericin in the *in vitro* enzymatic assay. IKK- β activity was determined by ELISA as described in detail in the experimental section. The enzymatic activity of human recombinant IKK- β was quantified for 30 min at 30 °C in the presence of DMSO vehicle (Co), different concentrations of plumericin, or 400 μ M 2-[(aminocarbonyl)amino]-5-(4-fluorophenyl)-3-thiophenecarboxamide (IKK- β inh). The colour development of the substrate was quantified on a GeniosPro plate reader and the IKK- β activity is presented as percentage of the activity of the vehicle treated control. The data shown are means \pm SEM from two independent experiments performed in a duplicate. The bars are means \pm SEM, ** $p < 0.01$; * $p < 0.05$ (one-way ANOVA followed by Dunnett's post-test).

2.2.2. Discovery of NF- κ B inhibitors from *Krameria lappacea*

In collaboration with the group of Prof. Judith Rollinger and Prof. Hermann Stuppner, the root extract of *Krameria lappacea* or red rhatany, a plant traditionally used in South America for the treatment of inflammatory diseases [200], was investigated for its antiinflammatory activity. The extract demonstrated inhibitory activity on TNF- α -induced NF- κ B activation in 293/NF- κ B-luc cells. Further phytochemical and pharmacological evaluation resulted in the characterization of 12 benzofurans (**Supplementary Figure 7**). Four benzofurans (KT5, KT6, KT8, and KT11, **Figure 31a**) inhibited TNF- α -induced NF- κ B activation in the low micromolar range (below 10 μ M, **Figure 31b**). Further, the activity of KT8, the most active compound among those benzofurans, was investigated for its ability to inhibit I κ B- α degradation upon TNF- α stimulation. Interestingly, it failed to inhibit the degradation of I κ B- α in HUVEctert (**Figure 31c**). In addition, KT8 did not inhibit IKK- β activity in the *in vitro* enzymatic assay (**Figure 32**), suggesting that KT8 might interfere with the NF- κ B pathway downstream of I κ B degradation.

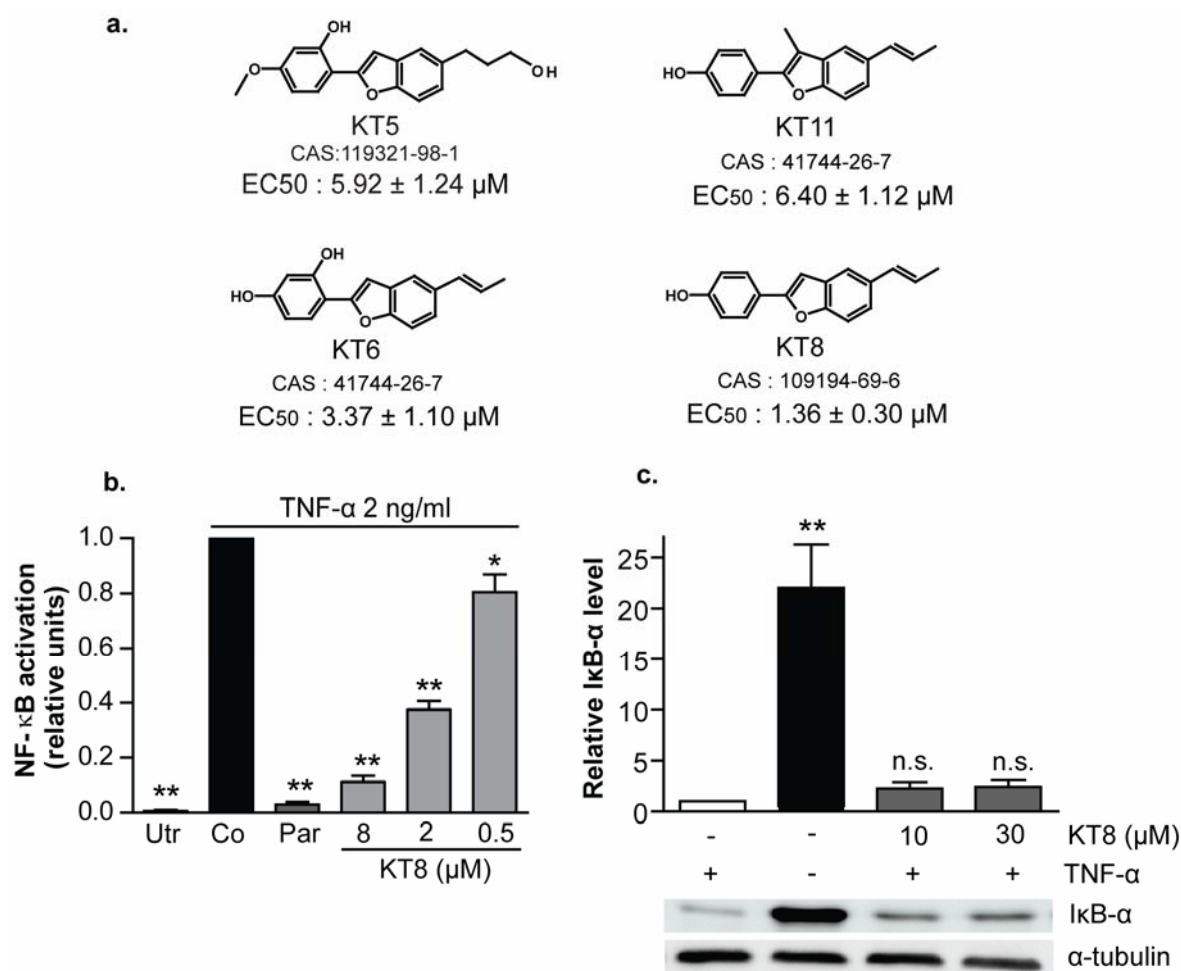


Figure 31. The activity of KT8 on TNF- α -induced NF- κ B activation in 293/NF- κ B-luc cells, and I κ B- α degradation in HUVEctert. (a) Chemical structure of the four most potent benzofuran inhibitors of NF- κ B isolated from *Krameria lappacea* and the respective IC₅₀ in TNF- α -stimulated 293/NF- κ B-luc cells. (b) The inhibitory activity of KT8 on TNF- α -stimulated 293/NF- κ B-luc cells. The 293/NF- κ B-luc cells transiently transfected with EGFP were pretreated with the compounds as indicated and further stimulated with 2 ng/ml TNF- α for 4 hours. The cell lysates were subjected to detection of luciferase activity and subsequently normalized to the fluorescence derived from EGFP. The result is expressed as fold induction compared to the DMSO control (Co), and Utr denotes the untreated cells. (c) Inhibitory activity of KT8 on I κ B- α degradation. HUVEctert were preincubated with the indicated concentration of KT8 for 30 minutes prior to stimulation with TNF- α 10 ng/ml for 10 minutes. Cell lysates were subjected to western blot analysis for I κ B- α degradation and total α -tubulin. The blot shown is a representative blot from three independent experiments. The Graph shows the band intensity calculated with densitometry as I κ B- α protein/tubulin ratios. The bars are means \pm SEM. *, $p < 0.05$; **, $p < 0.01$; n.s., not significant (one-way ANOVA followed by Dunnett's post-test).

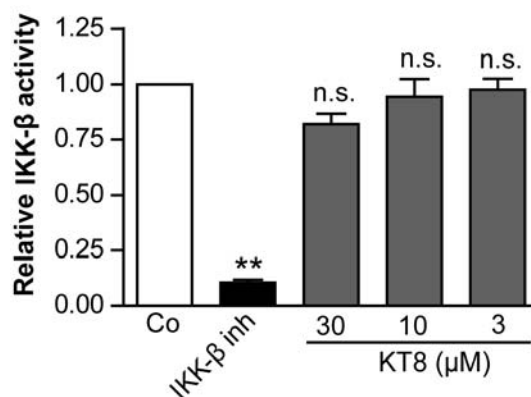


Figure 32. IKK- β inhibitory activity of KT8 in the *in vitro* enzymatic assay. IKK- β activity was determined by ELISA as described in details in the experimental section. The enzymatic activity of human recombinant IKK- β was quantified for 30 min at 30 °C in the presence of DMSO vehicle (Co), different concentrations of KT8, or 400 nM 2-[(aminocarbonyl)amino]-5-(4-fluorophenyl)-3-thiophenecarboxamide (IKK- β inh). The colour development of the substrate was quantified on a GeniosPro plate reader and the IKK- β activity is presented as percentage of the activity of the DMSO control. The data shown are means \pm SEM from two independent experiments in duplicate. *, $p < 0.05$; **, $p < 0.01$; n.s., not significant (one-way ANOVA followed by Dunnett's post-test).

In summary, four novel benzofuran inhibitors of NF- κ B were identified from the root of *Krameria lappacea* using TNF- α -stimulated 293/NF- κ B-luc cells. KT8, which represents the most active compound among them, did not inhibit I κ B- α degradation in TNF- α -stimulated HUVECtert and also failed to inhibit IKK- β activity *in vitro*. These benzofurans might target downstream events in the NF- κ B pathway.

2.3. Identification of an IKK- β inhibitor by a virtual screening approach

The ligand-based virtual screening was performed by the group of Prof. Gerhard Wolber. This virtual screening resulted in 10 top-ranked compounds predicted as IKK- β inhibitors (**Supplementary Figure 6**). From the 10 virtual hits, Compound 8, demonstrated inhibition of IKK- β in a cell-free *in vitro* assay in the low micromolar range (IC_{50} : 6.95 ± 0.55 μ M, **Figure 33a**). Compound 8 was further investigated for its ability to abolish TNF- α -induced NF- κ B activation in stably transfected HEK-293 cells having a luciferase reporter gene driven by a promoter containing multiple copies of the NF- κ B response element. In line with the effect observed in a cell-free IKK- β *in vitro* assay, it indeed significantly inhibited TNF- α -

induced NF- κ B transactivation in intact cells in a concentration-dependent manner (IC_{50} : $5.85 \pm 0.97 \mu\text{M}$, **Figure 33b**).

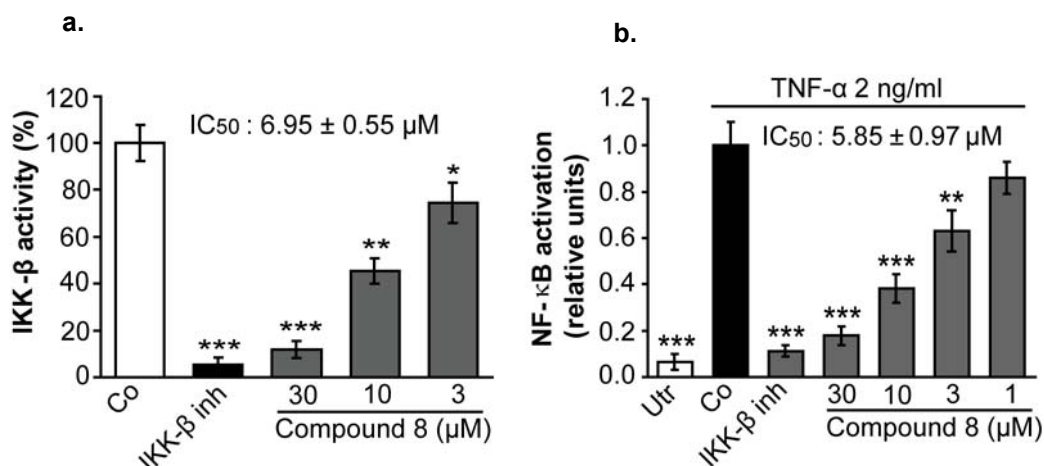


Figure 33. The activity of Compound 8 identified by the virtual screening approach on the IKK- β enzymatic activity in vitro and TNF- α -induced NF- κ B activation in 293/NF- κ B-luc cells. (a) Compound 8 inhibited IKK- β activity in vitro. The IKK- β activity was determined by ELISA as described in details in the experimental section. The enzymatic activity of human recombinant IKK- β was quantified for 30 min at 30 °C in the presence of DMSO vehicle (Co), different concentrations of the compound, or 1 μM 2-[(aminocarbonyl)amino]-5-(4-fluorophenyl)-3-thiophenecarboxamide IV (IKK- β inh). Utr denotes the untreated cells. The colour development of the substrate was quantified on a GeniosPro plate reader and the IKK- β activity is presented as percentage of the activity of the vehicle treated control. (b) The activity of Compound 8 in the NF- κ B-driven reporter gene assay. 293/NF- κ B-luc cells transiently transfected with EGFP were pretreated with the indicated concentration of compounds and stimulated with 2 ng/ml TNF- α for 4 hours. The cell lysates were subjected to detection of luciferase activity and normalized to the fluorescence derived from EGFP. Utr denotes the untreated cells. The graph represents the mean of three independent experiments \pm SD. *, $p < 0.05$; **, $p < 0.01$; and *** $p < 0.001$ (two-tailed paired t -test).

To get a deeper mechanistic understanding regarding the binding mode of Compound 8, molecular docking studies using a homology model of IKK- β were performed. This study was done by the group of Prof. Gerhard Wolber, and suggested a hydrogen bond interaction between Cys99 from the hinge region and the ester carbonyl group of Compound 8 (**Figure 34**). In addition, two other hydrogen bonds are formed between the residue Asp166 of the putative binding side with the amine in the linker chain and one phenol hydroxyl group. In this interaction, the hydrophobic pockets of the assumed binding site are occupied by the two aromatic moieties of Compound 8 [201].

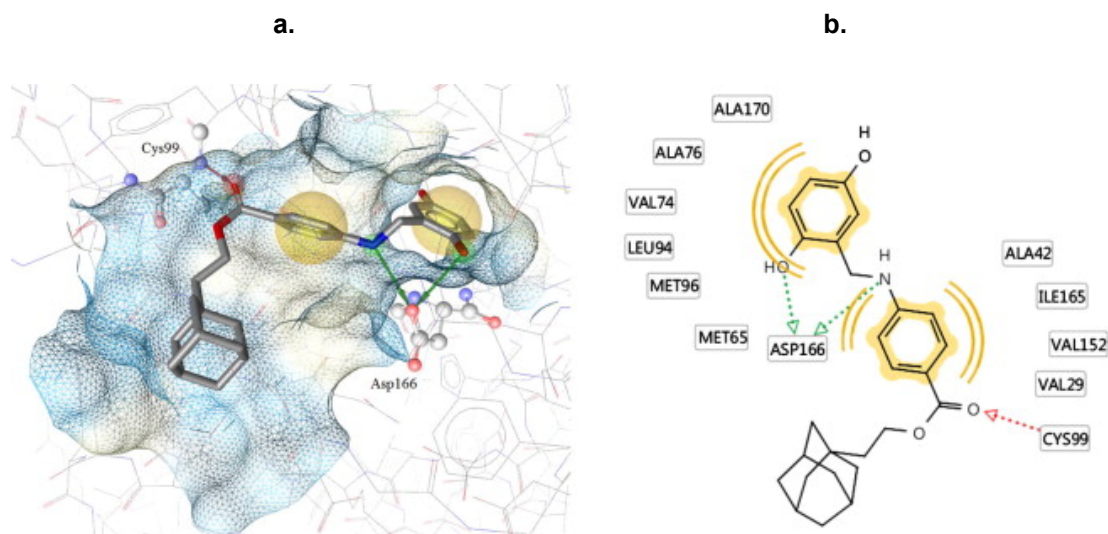


Figure 34. Docking of Compound 8 into the homology model of IKK-β [201]. (a) The predicted 3D model of the ligand binding pose is shown with the receptor binding surface (color-coded by aggregated hydrophilicity/hydrophobicity: blue/gray, respectively). (b) The predicted 2D model of protein–ligand interactions is presented. Chemical features are color-coded: red/green arrow—hydrogen-bond acceptor/donor; yellow spheres—hydrophobic interactions.

D. DISCUSSION

D. DISCUSSION

1. Assay optimization and verification

Luciferase reporter gene assays were used for the screening of plant extracts in order to identify PPAR γ agonists and NF- κ B inhibitors. The PPAR γ assay required highly transfected cells and an effective and efficient transfection method. Thus, HEK-293 cells were chosen and the transfection methods were optimized. After testing several variables including the amount and the ratio of the DNA plasmids, incubation time, and reagent composition, a highly efficient calcium phosphate-based transfection method was established. This method yielded a higher efficiency than achieved with Fugene[®] HD-based transfection. Currently this method is well established and routinely used to identify PPAR agonists and NF- κ B inhibitors either from plant extracts or synthetic compounds.

In the PPAR γ activity-driven luciferase activity, the dependency of the bioassay on PPAR γ activation was confirmed. The presence of the selective PPAR γ antagonist, GW9662, abolished the luciferase activity induced by the selective PPAR γ agonist, troglitazone. With respect to the TNF- α -induced NF- κ B activation in 293/NF- κ B-luc cells, the sensitivity of the bioassay in the presence of a NF- κ B inhibitor was also confirmed. Parthenolide, a potent known NF- κ B inhibitor, was able to inhibit TNF- α -induced luciferase activity in a dose-dependent manner. Furthermore, the effect of DMSO, the solvent mostly used in this study, was also evaluated in both bioassays. DMSO did not affect the PPAR γ activity-driven luciferase activity. In contrast, a concentration-dependent inhibition of the TNF- α -induced NF- κ B activation in 293/NF- κ B-luc by DMSO was found. The effect of DMSO on the NF- κ B pathway has been reported also in previous studies [202, 203].

2. Discovery of PPAR γ agonists and NF- κ B inhibitors from plant extracts

Using the established assays, 511 plant extracts were evaluated for their potential to activate PPAR γ and to inhibit NF- κ B. The plants were selected based on either an ethnopharmacological approach (traditional use against inflammatory diseases), or based on a computational approach. The obtained results provide a scientific basis to better understand the mechanisms of action of traditionally used medicinal herbs for combating inflammatory diseases, and represent a valuable preliminary study that could lead to further investigations aiming to identify the new interesting bioactive compounds.

Due to the promising results in these experiments, several plants were chosen for bioassay-guided isolation of compounds activating PPAR γ or inhibiting NF- κ B. Considering the measured extract activity, the known chemical constituents of each plant, and literature studies, *Notopterygium incisum* and *Magnolia officinalis*, active plants selected by the ethnopharmacological and computational approach, respectively, were chosen for further PPAR γ agonist identification. *Himatanthus sucuuba* and *Krameria lappacea* were chosen for the identification of NF- κ B inhibitors.

3. Discovery of neolignans as activators of PPAR γ

Magnolia officinalis is a Chinese medicinal plant that is suggested to be among the herbal drugs useful for combating the metabolic syndrome [204]. By using our *in silico* approach including a pharmacophore-based virtual screening of the natural product databases DIOS and CHM [205, 206], magnolol, a neolignan and major constituent in the Magnolia bark, was predicted as PPAR γ agonist. Recently, magnolol has been reported to enhance adipocyte differentiation in C3H10T1/2 cells and 3T3-L1 cells, suggesting possible PPAR γ modulation [207]. Additionally, dieugenol and tetrahydrodieugenol, two other structurally related neolignans previously reported to exert antimutagenic [208], antioxidant [209] and antiinflammatory activity [210], were also predicted to act as PPAR γ agonists.

The affinity of magnolol, dieugenol and tetrahydrodieugenol for the PPAR γ LBD was experimentally confirmed in a PPAR γ competitive ligand binding assay (**Figure 15**). As predicted from the pharmacophore model, all these neolignans strongly bind to the receptor LBD in a concentration range similar to that of the clinically approved PPAR γ agonist pioglitazone. Based on these promising *in vitro* findings, the ability of the neolignans to activate PPAR γ was further verified in a cellular model. Indeed, magnolol, dieugenol and tetrahydrodieugenol activated PPAR γ in a cell-based luciferase reporter gene transactivation model in a dose-dependent manner (**Figure 16**). The compound concentrations required to reach a saturation response were similar to that of pioglitazone indicating again a comparable affinity to the receptor binding pocket. Nevertheless, the maximal activation reached by the neolignans was several folds lower than pioglitazone, indicating partial agonism in this model.

It is known that distinct ligands of PPAR γ might induce ligand-receptor complex formation with distinct coactivator recruitment patterns, thus leading to distinct transactivation properties [192]. Hence, coactivator recruitment studies were performed by comparing the TRAP220/DRIP-2 coactivator recruitment properties of the PPAR γ -ligand complexes induced by the neolignans compared to the full PPAR γ agonist pioglitazone. Magnolol, dieugenol and tetrahydrodieugenol again demonstrated partial agonism as the maximal activation induced by these neolignans was several folds lower than that of pioglitazone (**Figure 17**). In summary, the neolignans display a similar affinity towards PPAR γ compared to pioglitazone but apparently induce PPAR γ -ligand complexes with a distinct conformation leading to partial agonism.

The development of novel partial PPAR γ agonists was suggested as a promising approach in order to evade the adverse effects of thiazolidinediones [211] [212]. Recently, metaglidasen (MBX-102), a selective partial agonist of PPAR γ with a weak transactivation activity and a distinct coactivator recruitment potential, was reported to retain antidiabetic activity without weight gain and edema side effects [66]. Therefore, the activation pattern demonstrated by magnolol, dieugenol, and tetrahydrodieugenol make them a highly promising class of PPAR γ activators. Moreover, dieugenol and tetrahydrodieugenol

selectively activated PPAR γ but not PPAR α or PPAR β/δ . As the current clinically used PPAR agonist, pioglitazone, is a subtype specific PPAR γ activator, the subtype-specific action of neolignans represents another favorable feature of action. From the other side, there are several studies indicating that PPAR pan-agonists or dual-agonists might also provide benefits [211] [213].

Dieugenol and tetrahydrodieugenol demonstrated the highest effectiveness among the tested neolignans in all systems used, followed by magnolol, whereas eugenol failed to show any activity. In order to observe the binding mode of the neolignans to the PPAR γ LBD, molecular docking was performed (**Figure 18**). The docking studies indicate that the large binding pocket of the receptor accommodates simultaneously two copies of each neolignan, and reveal that dieugenol and tetrahydrodieugenol have more interactions with the receptor binding pocket. Consequently, these two compounds demonstrated a higher bioactivity.

Since the PPAR γ luciferase reporter gene assay utilizes transient over-expression of PPAR γ and thus represents a more artificial cell-based model, the effect of all neolignans was also investigated in 3T3-L1 adipocytes, a functionally relevant cell model making use of endogenously expressed PPAR γ for differentiation. Corresponding with the results obtained from the previous models, magnolol, dieugenol, and tetrahydrodieugenol induced adipocyte differentiation and the presence of the PPAR γ antagonist BADGE abolished their effect. Again, eugenol was not active, and this confirmed the results from all previous experimental models as well as the predictions from the docking studies. Magnolol is a major bioactive compound from the traditional Chinese herbal remedy Magnolia bark. Even though this neolignan was not the most potent and specific activator of PPAR γ in this study, the activities reported here are of interest, as they are in accordance with the traditional application of Magnolia bark as a herbal medicine combating metabolic disorders [204]. Unlike dieugenol and tetrahydrodieugenol, magnolol acted as a dual agonist activating also PPAR β/δ at a higher concentration range (**Table 12**).

Taken together, several novel neolignan agonists of PPAR γ were discovered using a computational approach. In the receptor binding assays,

dieugenol and tetrahydrodieugenol demonstrated a higher affinity for PPAR γ than the clinically used agonist pioglitazone. Additionally, dieugenol and tetrahydrodieugenol acted as selective activators of PPAR γ but not PPAR α or PPAR β/δ . In comparison to pioglitazone, dieugenol and tetrahydrodieugenol exhibited a partial agonism in regard of PPAR γ luciferase reporter gene transactivation and TRAP220/DRIP-2 coactivator recruitment. Furthermore, they induced adipocytes differentiation in 3T3-L1 cells through PPAR γ activation. The activation pattern exhibited by dieugenol and tetrahydrodieugenol makes them highly promising novel PPAR γ agonists, having the potential to be further explored as leads for the development of novel pharmaceuticals or dietary supplements

4. Examination of PPAR γ agonists in further cell models relevant for atherosclerosis

Since PPAR γ is reported to play a role in the regulation of the functions of cells involved in atherosclerosis [34], we examined an influence of the identified PPAR γ agonists on NO production in macrophages and on migration of VSMC. It is known that PPAR γ is expressed in macrophages and involved in the negative regulation of inflammation. Previous studies reported an effect of PPAR γ agonists on the regulation of macrophages activation through inhibition of NO production [196] [214]. However, whether this effect is really PPAR γ -dependent remains unclear. In the experiments presented in this work, rosiglitazone inhibited NO production in RAW264.7 macrophages only a quite high concentration (30 μ M). However, the presence of PPAR γ antagonist T0070907 failed to abolish the effect of rosiglitazone, suggesting that the inhibitory effect by rosiglitazone might be PPAR γ -independent. Furthermore, another selective PPAR γ antagonist, GW9662, also failed to abolish the effect of rosiglitazone (data not shown). These findings are in line with a previous report indicating that PPAR γ is not required for the inhibition of NO production by synthetic PPAR γ agonists at concentration higher than 10 μ M [215]. The inhibitory effect seems to be mediated through the

proteasomal pathway [216]. Nevertheless, PPAR response element is present in the iNOS promoter [217].

Migration of VSMC has a significant role in atherogenesis as well as in restenosis after arterial stent. In this work, the effect of PPAR γ agonists on PDGF-induced VSMC migration was investigated. Stimulation of VSMC with 2 ng/ml PDGF-BB significantly induced cell migration. However, neither the selective full agonists of PPAR γ , troglitazone and pioglitazone, nor the neolignans exhibited a significant inhibitory effect. Although a previous study showed that the PPAR γ agonists troglitazone and 15d-PGJ2 inhibit human VSMC migration [218], this effect does not seem to occur in our experiments using rat VSMC. Additionally, the role of PPAR γ in VSMC migration remains controversial since recent studies demonstrated that PPAR β/δ but less likely PPAR γ , is responsible for the regulation of rat VSMC migration by inhibiting PDGF-induced expression of cyclin D1 and CDK4 [219]. Moreover, activation of PPAR γ by rosiglitazone tended to increase phosphorylation of Akt, a major regulator of cell proliferation and migration [220]. Therefore, further studies are needed to clarify the role of PPARs for the modulation of VSMC migration.

5. Discovery of polyacetylenes as activators of PPAR γ

Notopterygium incisum is used in Traditional Chinese Medicine (TCM) for thousands of years to treat headache, cold and rheumatism [221]. The roots and rhizomes of the plant contain Notopterol [222], phenethyl ferulate, falcarindiol and (-)-bornyl ferulate, which are responsible for the antiinflammatory activity [223, 224], as well as other compounds such as nodakenin, p-hydroxyphenethyl anisate, isoimperatorin, ferulic acid, trans-p-hydroxycinnamic acid and furocoumarins [225, 226].

Testing of *Notopterygium incisum* (radix and rhizome) dichloromethane extract on the PPAR γ -driven luciferase reporter gene, followed by bioassay-guided fractionation and isolation resulted in the discovery of six polyacetylenes as novel activators of PPAR γ . Although a previous study reported an *in vivo* antidiabetic

activity of polyacetylenes isolated from *Bidens pilosa* [227], activation of PPAR γ by polyacetylenes was never described before. The polyacetylenes exhibited activation patterns similar to the neolignans, with maximal activation several folds lower than the full PPAR γ agonist pioglitazone, suggesting again a partial agonism. Interestingly, the polyacetylenes selectively activated PPAR γ without affecting PPAR α or PPAR β activation. The maximal activation achieved by the polyacetylenes was equal to that of the initial extract which exhibits around 2-fold activation compared to the DMSO control. Further experiments are necessary to confirm their direct binding affinity to the receptor and functionality in relevant cell models endogenously expressing PPAR γ , such as adipocytes.

6. Discovery of plumericin as a NF- κ B inhibitor

Himatanthus sucuuba is an Amazonian plant that traditionally has been used in South America as painkiller, anaesthetic, antitumor agent, analgesic, antitussive agent, aphrodisiac, antiarthritis and antiulcer agent [228-230]. Fractionation of the extract and further isolation of active compounds led to the discovery of the spirolactone iridoid plumericin. This compound has been previously reported to exhibit weak cytotoxic activity [231], as well as antimicrobial [232], antifungal [233], and antileishmanial activity [234]. In this study, we demonstrate that plumericin inhibits TNF- α -induced NF- κ B activation in 293/NF- κ B-luc cells (EC_{50} 1.07 ± 0.08 μ M) with the potency equal to the positive control, parthenolide (**Figure 27**). In TNF- α -stimulated HUVEctert, plumericin inhibited cell surface expression of the adhesion molecules E-selectin, VCAM-1, and ECAM-1 in a dose-dependent manner. At a concentration of 5 μ M, this iridoid dampened the expression of adhesions molecules to the basal level. Moreover, the activity of plumericin on adhesion molecules was also confirmed at the level of mRNA (data not shown, these experiments were done by the group of Prof. Bernd Binder, Department of Vascular Biology and Thrombosis Research, Medical University of Vienna).

Plumericin might act by interfering with upstream proteins of the NF- κ B pathway, as it inhibited the degradation of I κ B- α in TNF- α -stimulated HUVECtert (**Figure 29**). Inhibition of I κ B degradation by NF- κ B inhibitors can occur through several possible mechanisms. It might be explained by inhibition of IKK activity (I κ B phosphorylation), proteasomal degradation, ubiquitination or even interaction with proteins upstream of IKK [235]. Considering the presence of an α,β -unsaturated carbonyl in plumericin, this iridoid might potentially interact with proteins from the NF- κ B signalling cascade through Michael's addition to the sulfhydryl groups of cystein residues [139]. Interestingly, plumeridin, an iridoid with a highly similar structure and having an endocyclic α, β -unsaturated carbonyl did not inhibit TNF- α -induced NF- κ B activation in 293/NF- κ B-luc cells up to 10 μ M. This indicates that the exocyclic α, β -unsaturated carbonyl in plumericin might be crucial for the activity.

Apart from the NF- κ B inhibition activity, plumericin strongly activated Nrf2 (**Supplementary Figure 4**), a transcription factor regulating broad range of genes involved in the antioxidant response to extrinsic and intrinsic cellular stress [236]. This transcription factor is also involved in the prevention of cancer, cardiovascular disease and inflammation [237]. Plumericin significantly activated Nrf2 with a potency stronger than parthenolide and lower than 2-cyano- 3,12-dioxooleana-1,9-dien-28-oic imidazole (CDDO-IM), a known synthetic activator of Nrf2. Since Nrf2 is able to block the NF- κ B-dependent transcription machinery and dampen NF- κ B-controlled responses to pro-inflammatory stimuli [238], further investigation on this effect is of great interest.

In summary, we discovered plumericin as a novel NF- κ B inhibitor targeting the signalling cascade upstream of I κ B degradation, and inhibiting the surface expression of adhesion molecules in HUVECtert. However, further investigation to identify the specific protein targets is required to get deeper insight into the mode of action of this compound. These findings might contribute to the development of promising leads for an anti-inflammatory therapy, and provide scientific evidence regarding the traditional use of *Himathantus sucuuba* as an herbal medicine for the treatment of inflammatory diseases.

7. Discovery of benzofurans as NF- κ B inhibitors

Another Amazonian plant that demonstrated inhibition of TNF- α -induced NF- κ B activation in 293/NF- κ B-luc cells is *Krameria lappacea*. The root of this plant has been used as a folk medicine in South America for the treatment of inflammatory diseases, diarrhea and stomach cancer [200]. However, there is a lack of scientific evidence clarifying these activities. By utilizing 293/NF- κ B-luc cells, four benzofurans with a high structural similarity were found to inhibit NF- κ B activation in the low micromolar range. Among them, KT8 is the most potent compound with EC_{50} 1.36 ± 0.30 μ M, exhibiting activity similar to that of plumericin. In contrast to plumericin, KT8 failed to inhibit I κ B- α degradation in TNF- α -induced HUVEctert and IKK- β *in vitro*, suggesting that KT8 might inhibit NF- κ B signalling by targeting proteins downstream of I κ B- α degradation. However, further experiments clarifying the effect of KT8 and the other active benzofurans on NF- κ B-related signalling is needed. Apart from these results, the experiments performed by our collaboration partner Dr. Aurelia Tubaro (Dipartimento dei Materiali e delle Risorse Naturali, University of Trieste, Italy) showed that these benzofurans exhibited *in vivo* antiinflammatory activity in a croton oil-induced mouse ear dermatitis with effectiveness comparable to the positive control indomethacin (data not shown).

In summary, this work describes the identification of several benzofuran inhibitors of NF- κ B from the Amazonian plant *Krameria lappacea*. These compounds inhibit NF- κ B activation probably by interfering with signalling proteins downstream of I κ B- α degradation, having the potential as antiinflammatory lead compounds.

8. Discovery of a novel IKK- β inhibitor by ligand-based virtual screening

Recently, Nagarajan et al. established an IKK- β homology model using a biological screening of predicted inhibitors to validate the model [239]. In our collaborative work with the group of Prof. Gerhard Wolber, a 3D pharmacophore

model based on the reported IKK- β inhibitors was developed and pharmacophore-based virtual screening of compounds from the database of the National Cancer Institute was performed. Furthermore, the pharmacophore-based hitlist were ranked by 3D shape-based scoring [201]. The biological evaluation of the 10 top-ranked virtual screening hits was performed on a TNF- α -induced NF- κ B transactivation in 293/NF- κ B-luc cells and on IKK- β *in vitro* activity.

Among the virtual hits, Compound 8 was the most potent and inhibited NF- κ B activation in the low micromolar range with a comparable potency in 293/NF- κ B-luc cells, as well as IKK- β activity in a cell-free *in vitro* assay. This verified the effectiveness of Compound 8 in intact cells, and thus it could represent an interesting lead for further medicinal chemistry optimization to obtain novel agents to combat inflammatory diseases. Molecular docking study using the homology model of IKK- β demonstrated that the two aromatic moieties of Compound 8 were situated at the hydrophobic pockets of the assumed binding site and several hydrogen bonds were formed [201]. Apart from that, the unprecedented development of a ligand-based pharmacophore model for IKK- β inhibitors and the application of pharmacophore-based virtual screening techniques combined with 3D shape-based re-scoring might contribute to the development of tools for identification inhibitors of IKK- β .

E. SUMMARY

E. SUMMARY

It is known that inflammation contributes to the development of atherosclerosis. PPAR γ and NF- κ B are transcription factors that are involved in the regulation of the inflammatory response. Thus, the discovery of compounds targeting the activity of both transcription factors is of great interest. The aim of this study was to discover natural compounds activating PPAR γ or inhibiting NF- κ B and to characterize their mechanism of action in the cellular context. Plants traditionally used for the treatment of inflammatory diseases were tested for PPAR γ activation and NF- κ B inhibition using the established luciferase reporter gene assays. Several active plants were selected for further isolation and identification of the bioactive compounds.

Magnolol, a neolignan isolated from *Magnolia officinalis*, together with two other neolignans with high structural similarity, dieugenol and tetrahydrodieugenol, were discovered as PPAR γ agonist guided by a computational model. Their activation profile in the luciferase reporter gene- and coactivator recruitment-assays indicated that these neolignans act as PPAR γ partial agonists. Interestingly, dieugenol and tetrahydrodieugenol selectively activated PPAR γ with a binding affinity higher than pioglitazone, a clinically used PPAR γ full agonist, whereas magnolol was binding to the PPAR γ LBD with a slightly lower affinity. Docking studies suggested that two copies of the neolignans simultaneously bind to the binding site of PPAR γ . The functionality of the neolignans was also confirmed by induction of adipogenesis of 3T3-L1 preadipocytes, a functionally relevant cell model with endogenous expression of PPAR γ . Apart from that, several polyacetylenes isolated from *Notopterygium incisum* were also discovered as PPAR γ agonists utilizing bioassay-guided isolation. These compounds selectively activated PPAR γ with an activation profile suggesting a partial agonism.

In respect of identification of the NF- κ B inhibitors from plants, plumericin, an iridoid isolated from *Himatanthus sucuuba*, was found as a novel NF- κ B inhibitor.

It exhibited potency comparable to the positive control parthenolide in TNF- α -induced 293/NF- κ B-luc cells. Plumericin also inhibited the cell surface expression of adhesion molecules and I κ B degradation in TNF- α -stimulated HUVECTert, suggesting that it targets signaling events upstream of I κ B degradation. In addition, four benzofurans isolated from *Krameria lappacea* were also found to inhibit NF- κ B activation in TNF- α -induced 293/NF- κ B-luc cells. Unlike plumericin, the benzofurans failed to inhibit the enzymatic *in vitro* IKK- β activity and the I κ B- α degradation in TNF- α -stimulated HUVECTert. We further identified Compound 8 as novel IKK- β inhibitor by ligand-based virtual screening techniques. It showed a comparable potency in the *in vitro* assay with purified IKK- β enzyme as well as in intact cells. This synthetic compound represents a new chemical class of IKK- β inhibitor, and the finding demonstrated the validity of the method for identification and development of IKK- β inhibitors.

In this study, we present the discovery of several PPAR γ agonists and NF- κ B inhibitors from medicinal plants and provide scientific evidence regarding the traditional usage of medicinal herbs for combating inflammatory diseases. These findings might contribute to the development of highly promising novel PPAR γ agonists and NF- κ B inhibitors having the potential to be further explored as leads for the development of novel pharmaceuticals or dietary supplements.

F. REFERENCES

F. REFERENCES

- 1 Libby P, Ridker PM, Maseri A. Inflammation and Atherosclerosis. *Circulation*. 2002; **105**: 1135-43.
- 2 Dzau VJ, Braun-Dullaeus RC, Sedding DG. Vascular proliferation and atherosclerosis: new perspectives and therapeutic strategies. *Nat Med*. 2002; **8**: 1249-56.
- 3 Webb NR. Getting to the core of atherosclerosis. *Nat Med*. 2008; **14**: 1015-6.
- 4 Steinberg D. Atherogenesis in perspective: hypercholesterolemia and inflammation as partners in crime. *Nat Med*. 2002; **8**: 1211-7.
- 5 Tabas I, Williams KJ, Boren J. Subendothelial lipoprotein retention as the initiating process in atherosclerosis: update and therapeutic implications. *Circulation*. 2007; **116**: 1832-44.
- 6 Lusis AJ. Atherosclerosis. *Nature*. 2000; **407**: 233-41.
- 7 Hansson GK, Robertson AK, Soderberg-Naucler C. Inflammation and atherosclerosis. *Annu Rev Pathol*. 2006; **1**: 297-329.
- 8 Klingenberg R, Hansson GrK. Treating inflammation in atherosclerotic cardiovascular disease: emerging therapies. *European Heart Journal*. 2009; **30**: 2838-44.
- 9 Libby P, Okamoto Y, Rocha VZ, Folco E. Inflammation in Atherosclerosis Transition From Theory to Practice. *Circulation Journal*. 2010; **74**: 213-20.
- 10 Tergaonkar V. NF- κ B pathway: a good signaling paradigm and therapeutic target. *Int J Biochem Cell Biol*. 2006; **38**: 1647-53.
- 11 de Winther MP, Kanters E, Kraal G, Hofker MH. Nuclear factor- κ B signaling in atherogenesis. *Arterioscler Thromb Vasc Biol*. 2005; **25**: 904-14.
- 12 Pahl HL. Activators and target genes of Rel/NF- κ B transcription factors. *Oncogene*. 1999; **18**: 6853-66.

- 13 Lehrke M, Lazar MA. The many faces of PPARgamma. *Cell*. 2005; **123**: 993-9.
- 14 Desvergne B, Wahli W. Peroxisome proliferator-activated receptors: nuclear control of metabolism. *Endocr Rev*. 1999; **20**: 649-88.
- 15 Fajas L, Auboeuf D, Raspe E, Schoonjans K, Lefebvre AM, Saladin R, *et al*. The organization, promoter analysis, and expression of the human PPARgamma gene. *J Biol Chem*. 1997; **272**: 18779-89.
- 16 Abbott BD. Review of the expression of peroxisome proliferator-activated receptors alpha (PPAR alpha), beta (PPAR beta), and gamma (PPAR gamma) in rodent and human development. *Reprod Toxicol*. 2009; **27**: 246-57.
- 17 Benson S, Wu J, Padmanabhan S, Kurtz TW, Pershadsingh HA. Peroxisome proliferator-activated receptor (PPAR)-gamma expression in human vascular smooth muscle cells: inhibition of growth, migration, and c-fos expression by the peroxisome proliferator-activated receptor (PPAR)-gamma activator troglitazone. *Am J Hypertens*. 2000; **13**: 74-82.
- 18 Martin H. Role of PPAR-gamma in inflammation. Prospects for therapeutic intervention by food components. *Mutat Res*. 2009; **669**: 1-7.
- 19 Subramanian V, Golledge J, Ijaz T, Bruemmer D, Daugherty A. Pioglitazone-induced reductions in atherosclerosis occur via smooth muscle cell-specific interaction with PPARgamma. *Circ Res*. 2010; **107**: 953-8.
- 20 Wahli W. A gut feeling of the PXR, PPAR and NF- κ B connection. *J Intern Med*. 2008; **263**: 613-9.
- 21 Enmark E, Gustafsson JA. Orphan nuclear receptors--the first eight years. *Mol Endocrinol*. 1996; **10**: 1293-307.
- 22 Miller RT, Willson TM. Regulation of xenobiotic metabolism by orphan nuclear receptors. *Toxicol Pathol*. 2001; **29**: 3-5.
- 23 Shi Y. Orphan nuclear receptors in drug discovery. *Drug Discov Today*. 2007; **12**: 440-5.
- 24 Giguere V. Orphan Nuclear Receptors: From Gene to Function. *Endocr Rev*. 1999; **20**: 689-725.
- 25 Nagy L, Schwabe JW. Mechanism of the nuclear receptor molecular switch. *Trends Biochem Sci*. 2004; **29**: 317-24.

- 26 Reddy JK, Lalwai ND. Carcinogenesis by hepatic peroxisome proliferators: evaluation of the risk of hypolipidemic drugs and industrial plasticizers to humans. *Crit Rev Toxicol*. 1983; **12**: 1-58.
- 27 Issemann I, Green S. Activation of a member of the steroid hormone receptor superfamily by peroxisome proliferators. *Nature*. 1990; **347**: 645-50.
- 28 Sher T, Yi HF, McBride OW, Gonzalez FJ. cDNA cloning, chromosomal mapping, and functional characterization of the human peroxisome proliferator activated receptor. *Biochemistry*. 1993; **32**: 5598-604.
- 29 Zhou J, Wilson KM, Medh JD. Genetic analysis of four novel peroxisome proliferator activated receptor-gamma splice variants in monkey macrophages. *Biochem Biophys Res Commun*. 2002; **293**: 274-83.
- 30 Kliewer SA, Forman BM, Blumberg B, Ong ES, Borgmeyer U, Mangelsdorf DJ, *et al*. Differential expression and activation of a family of murine peroxisome proliferator-activated receptors. *Proc Natl Acad Sci U S A*. 1994; **91**: 7355-9.
- 31 Kondo H, Misaki R, Gelman L, Watabe S. Ligand-dependent transcriptional activities of four torafugu pufferfish *Takifugu rubripes* peroxisome proliferator-activated receptors. *Gen Comp Endocrinol*. 2007; **154**: 120-7.
- 32 Yoshikawa T, Brkanac Z, Dupont BR, Xing GQ, Leach RJ, Detera-Wadleigh SD. Assignment of the human nuclear hormone receptor, NUC1 (PPARD), to chromosome 6p21.1-p21.2. *Genomics*. 1996; **35**: 637-8.
- 33 Greene ME, Blumberg B, McBride OW, Yi HF, Kronquist K, Kwan K, *et al*. Isolation of the human peroxisome proliferator activated receptor gamma cDNA: expression in hematopoietic cells and chromosomal mapping. *Gene Expr*. 1995; **4**: 281-99.
- 34 Marx N, Duez H, Fruchart JC, Staels B. Peroxisome proliferator-activated receptors and atherogenesis: regulators of gene expression in vascular cells. *Circ Res*. 2004; **94**: 1168-78.
- 35 Ziouzenkova O, Plutzky J. Lipolytic PPAR activation: new insights into the intersection of triglycerides and inflammation? *Curr Opin Clin Nutr Metab Care*. 2004; **7**: 369-75.
- 36 Auwerx J. PPARgamma, the ultimate thrifty gene. *Diabetologia*. 1999; **42**: 1033-49.

- 37 Fredenrich A, Grimaldi PA. PPAR delta: an uncompletely known nuclear receptor. *Diabetes Metab.* 2005; **31**: 23-7.
- 38 Escher P, Wahli W. Peroxisome proliferator-activated receptors: insight into multiple cellular functions. *Mutat Res.* 2000; **448**: 121-38.
- 39 Mangelsdorf DJ, Thummel C, Beato M, Herrlich P, Schutz G, Umesono K, *et al.* The nuclear receptor superfamily: the second decade. *Cell.* 1995; **83**: 835-9.
- 40 Bardot O, Aldridge TC, Latruffe N, Green S. PPAR-RXR heterodimer activates a peroxisome proliferator response element upstream of the bifunctional enzyme gene. *Biochem Biophys Res Commun.* 1993; **192**: 37-45.
- 41 Kliewer SA, Umesono K, Noonan DJ, Heyman RA, Evans RM. Convergence of 9-cis retinoic acid and peroxisome proliferator signalling pathways through heterodimer formation of their receptors. *Nature.* 1992; **358**: 771-74.
- 42 Ge K, Guermah M, Yuan CX, Ito M, Wallberg AE, Spiegelman BM, *et al.* Transcription coactivator TRAP220 is required for PPAR gamma 2-stimulated adipogenesis. *Nature.* 2002; **417**: 563-7.
- 43 Yao TP, Ku G, Zhou N, Scully R, Livingston DM. The nuclear hormone receptor coactivator SRC-1 is a specific target of p300. *Proc Natl Acad Sci U S A.* 1996; **93**: 10626-31.
- 44 Kota BP, Huang TH, Roufogalis BD. An overview on biological mechanisms of PPARs. *Pharmacol Res.* 2005; **51**: 85-94.
- 45 Ricote M, Glass CK. PPARs and molecular mechanisms of transrepression. *Biochim Biophys Acta.* 2007; **1771**: 926-35.
- 46 Mangelsdorf DJ, Evans RM. The RXR heterodimers and orphan receptors. *Cell.* 1995; **83**: 841-50.
- 47 Krey G, Braissant O, L'Horsset F, Kalkhoven E, Perroud M, Parker MG, *et al.* Fatty acids, eicosanoids, and hypolipidemic agents identified as ligands of peroxisome proliferator-activated receptors by coactivator-dependent receptor ligand assay. *Mol Endocrinol.* 1997; **11**: 779-91.
- 48 Moraes LA, Piqueras L, Bishop-Bailey D. Peroxisome proliferator-activated receptors and inflammation. *Pharmacology & Therapeutics.* 2006; **110**: 371-85.

- 49 Gervois P, Chopin-Delannoy S, Fadel A, Dubois G, Kosykh V, Fruchart JC, *et al.* Fibrates increase human REV-ERB α expression in liver via a novel peroxisome proliferator-activated receptor response element. *Mol Endocrinol.* 1999; **13**: 400-9.
- 50 Oliver WR, Shenk JL, Snaith MR, Russell CS, Plunket KD, Bodkin NL, *et al.* A selective peroxisome proliferator-activated receptor δ agonist promotes reverse cholesterol transport. *Proceedings of the National Academy of Sciences of the United States of America.* 2001; **98**: 5306-11.
- 51 Sznajdman ML, Haffner CD, Maloney PR, Fivush A, Chao E, Goreham D, *et al.* Novel selective small molecule agonists for peroxisome proliferator-activated receptor delta (PPAR δ)-synthesis and biological activity. *Bioorg Med Chem Lett.* 2003; **13**: 1517-21.
- 52 FDA. Safety Review of Avandia (Rosiglitazone). Vol. 2011. Madison: U.S. Food and Drug Administration 2010. Available from: <http://www.fda.gov/ForConsumers/ConsumerUpdates/ucm201509.htm>.
- 53 Cavender MA, Nicholls SJ, Lincoff AM. Strategies for the development of new PPAR agonists in diabetes. *Eur J Cardiovasc Prev Rehabil.* 2010; **17 Suppl 1**: S32-7.
- 54 EMA. European Medicines Agency recommends suspension of Avandia, Avandamet and Avaglim. London: European Medicines Agency 2010; Press release. Available from: http://www.ema.europa.eu/docs/en_GB/document_library/Press_release/2010/09/WC500096996.pdf.
- 55 Javiya V, Patel J. The role of peroxisome proliferator-activated receptors in human disease. *Indian journal of pharmacology.* 2006; **38**: 243-53.
- 56 Brun RP, Spiegelman BM. PPAR gamma and the molecular control of adipogenesis. *J Endocrinol.* 1997; **155**: 217-8.
- 57 Chawla A, Schwarz EJ, Dimaculangan DD, Lazar MA. Peroxisome proliferator-activated receptor (PPAR) gamma: adipose-predominant expression and induction early in adipocyte differentiation. *Endocrinology.* 1994; **135**: 798-800.
- 58 Hamm JK, el Jack AK, Pilch PF, Farmer SR. Role of PPAR gamma in regulating adipocyte differentiation and insulin-responsive glucose uptake. *Ann N Y Acad Sci.* 1999; **892**: 134-45.

- 59 Liao W, Nguyen MT, Yoshizaki T, Favelyukis S, Patsouris D, Imamura T, *et al.* Suppression of PPAR-gamma attenuates insulin-stimulated glucose uptake by affecting both GLUT1 and GLUT4 in 3T3-L1 adipocytes. *Am J Physiol Endocrinol Metab.* 2007; **293**: E219-27.
- 60 Armoni M, Harel C, Karnieli E. Transcriptional regulation of the GLUT4 gene: from PPAR-[gamma] and FOXO1 to FFA and inflammation. *Trends in Endocrinology & Metabolism.* 2007; **18**: 100-07.
- 61 Hontecillas R, O'Shea M, Einerhand A, Diguardo M, Bassaganya-Riera J. Activation of PPAR gamma and alpha by puniceic acid ameliorates glucose tolerance and suppresses obesity-related inflammation. *J Am Coll Nutr.* 2009; **28**: 184-95.
- 62 Fernandez-Boyanapalli R, Frasc SC, Riches DW, Vandivier RW, Henson PM, Bratton DL. PPARgamma activation normalizes resolution of acute sterile inflammation in murine chronic granulomatous disease. *Blood.* 2010; **116**: 4512-22.
- 63 Glass CK, Saijo K. Nuclear receptor transrepression pathways that regulate inflammation in macrophages and T cells. *Nat Rev Immunol.* 2010; **10**: 365-76.
- 64 Nolte RT, Wisely GB, Westin S, Cobb JE, Lambert MH, Kurokawa R, *et al.* Ligand binding and co-activator assembly of the peroxisome proliferator-activated receptor-[gamma]. *Nature.* 1998; **395**: 137-43.
- 65 Chandra V, Huang P, Hamuro Y, Raghuram S, Wang Y, Burris TP, *et al.* Structure of the intact PPAR-gamma-RXR-alpha nuclear receptor complex on DNA. *Nature.* 2008: 350-56.
- 66 Gregoire FM, Zhang F, Clarke HJ, Gustafson TA, Sears DD, Favelyukis S, *et al.* MBX-102/JNJ39659100, a Novel Peroxisome Proliferator Activated Receptor-gamma Ligand with Weak Transactivation Activity Retains Full Anti-Diabetic Properties in the Absence of Side Effects. *Mol Endocrinol.* 2009; **23**: 975-88.
- 67 Jin L, Li Y. Structural and functional insights into nuclear receptor signaling. *Advanced Drug Delivery Reviews.* 2010; **62**: 1218-26.
- 68 Waku T, Shiraki T, Oyama T, Fujimoto Y, Maebara K, Kamiya N, *et al.* Structural Insight into PPARgamma Activation Through Covalent Modification with Endogenous Fatty Acids. *Journal of Molecular Biology.* 2009; **385**: 188-99.

- 69 Huang TH, Teoh AW, Lin BL, Lin DS, Roufogalis B. The role of herbal PPAR modulators in the treatment of cardiometabolic syndrome. *Pharmacol Res.* 2009; **60**: 195-206.
- 70 Pascual G, Glass CK. Nuclear receptors versus inflammation: mechanisms of transrepression. *Trends Endocrinol Metab.* 2006; **17**: 321-7.
- 71 Pascual G, Fong AL, Ogawa S, Gamliel A, Li AC, Perissi V, *et al.* A SUMOylation-dependent pathway mediates transrepression of inflammatory response genes by PPAR-gamma. *Nature.* 2005; **437**: 759-63.
- 72 Wang N, Verna L, Chen NG, Chen J, Li H, Forman BM, *et al.* Constitutive activation of peroxisome proliferator-activated receptor-gamma suppresses pro-inflammatory adhesion molecules in human vascular endothelial cells. *J Biol Chem.* 2002; **277**: 34176-81.
- 73 Jung Y, Song S, Choi C. Peroxisome proliferator activated receptor gamma agonists suppress TNFalpha-induced ICAM-1 expression by endothelial cells in a manner potentially dependent on inhibition of reactive oxygen species. *Immunol Lett.* 2008; **117**: 63-9.
- 74 Dushkin MI, Khoshchenko OM, Posokhova EN, Schvarts Y. Agonists of PPAR-alpha, PPAR-gamma, and RXR inhibit the formation of foam cells from macrophages in mice with inflammation. *Bull Exp Biol Med.* 2007; **144**: 713-6.
- 75 Ricote M, Huang J, Fajas L, Li A, Welch J, Najib J, *et al.* Expression of the peroxisome proliferator-activated receptor gamma (PPARgamma) in human atherosclerosis and regulation in macrophages by colony stimulating factors and oxidized low density lipoprotein. *Proc Natl Acad Sci U S A.* 1998; **95**: 7614-9.
- 76 Remick J, Weintraub H, Setton R, Offenbacher J, Fisher E, Schwartzbard A. Fibrate therapy: an update. *Cardiol Rev.* 2008; **16**: 129-41.
- 77 Lehmann JM, Moore LB, Smith-Oliver TA, Wilkison WO, Willson TM, Kliewer SA. An antidiabetic thiazolidinedione is a high affinity ligand for peroxisome proliferator-activated receptor gamma (PPAR gamma). *J Biol Chem.* 1995; **270**: 12953-6.
- 78 Rizos CV, Elisaf MS, Mikhailidis DP, Liberopoulos EN. How safe is the use of thiazolidinediones in clinical practice? *Expert Opin Drug Saf.* 2009; **8**: 15-32.

- 79 Doshi LS, Brahma MK, Bahirat UA, Dixit AV, Nemmani KVS. Discovery and development of selective PPAR γ modulators as safe and effective antidiabetic agents. *Expert Opinion on Investigational Drugs*. 2010; **19**: 489-512.
- 80 Furukawa A, Arita T, Satoh S, Wakabayashi K, Hayashi S, Matsui Y, *et al.* Discovery of a novel selective PPAR γ modulator from (-)-Cercosporamide derivatives. *Bioorganic & Medicinal Chemistry Letters*. 2010; **20**: 2095-98.
- 81 Christensen KB, Minet A, Svenstrup H, Grevsen K, Zhang H, Schrader E, *et al.* Identification of plant extracts with potential antidiabetic properties: effect on human peroxisome proliferator-activated receptor (PPAR), adipocyte differentiation and insulin-stimulated glucose uptake. *Phytother Res*. 2009; **23**: 1316-25.
- 82 Dat NT, Lee K, Hong YS, Kim YH, Minh CV, Lee JJ. A peroxisome proliferator-activated receptor-gamma agonist and other constituents from *Chromolaena odorata*. *Planta Med*. 2009; **75**: 803-7.
- 83 Poeckel D, Greiner C, Verhoff M, Rau O, Tausch L, Hornig C, *et al.* Carnosic acid and carnosol potently inhibit human 5-lipoxygenase and suppress pro-inflammatory responses of stimulated human polymorphonuclear leukocytes. *Biochem Pharmacol*. 2008; **76**: 91-7.
- 84 Ulrich S, Loitsch SM, Rau O, von Knethen A, Brune B, Schubert-Zsilavecz M, *et al.* Peroxisome proliferator-activated receptor gamma as a molecular target of resveratrol-induced modulation of polyamine metabolism. *Cancer Res*. 2006; **66**: 7348-54.
- 85 Fang XK, Gao J, Zhu DN. Kaempferol and quercetin isolated from *Euonymus alatus* improve glucose uptake of 3T3-L1 cells without adipogenesis activity. *Life Sci*. 2008; **82**: 615-22.
- 86 Kuroda M, Mimaki Y, Honda S, Tanaka H, Yokota S, Mae T. Phenolics from *Glycyrrhiza glabra* roots and their PPAR-gamma ligand-binding activity. *Bioorg Med Chem*. 2010; **18**: 962-70.
- 87 Mueller M, Jungbauer A. Red clover extract: a putative source for simultaneous treatment of menopausal disorders and the metabolic syndrome. *Menopause*. 2008; **15**: 1120-31.
- 88 Christensen KB, Petersen RK, Kristiansen K, Christensen LP. Identification of bioactive compounds from flowers of black elder (*Sambucus nigra* L.) that activate the human peroxisome proliferator-activated receptor (PPAR) γ . *Phytotherapy Research*. 2010; **24**: S129-S32.

- 89 Yokoi H, Mizukami H, Nagatsu A, Ohno T, Tanabe H, Inoue M. Peroxisome proliferator-activated receptor gamma ligands isolated from adlay seed (*Coix lacryma-jobi* L. var. *ma-yuen* STAPF.). *Biol Pharm Bull.* 2009; **32**: 735-40.
- 90 Christensen KB, Jørgensen M, Kotowska D, Petersen RK, Kristiansen K, Christensen LP. Activation of the nuclear receptor PPARgamma by metabolites isolated from sage (*Salvia officinalis* L.). *Journal of Ethnopharmacology.* 2010; **132**: 127-33.
- 91 Hotta M, Nakata R, Katsukawa M, Hori K, Takahashi S, Inoue H. Carvacrol, a component of thyme oil, activates PPARalpha and gamma and suppresses COX-2 expression. *J Lipid Res.* 2010; **51**: 132-9.
- 92 Kuroyanagi K, Kang MS, Goto T, Hirai S, Ohyama K, Kusudo T, *et al.* Citrus auraptene acts as an agonist for PPARs and enhances adiponectin production and MCP-1 reduction in 3T3-L1 adipocytes. *Biochem Biophys Res Commun.* 2008; **366**: 219-25.
- 93 Katsukawa M, Nakata R, Takizawa Y, Hori K, Takahashi S, Inoue H. Citral, a component of lemongrass oil, activates PPARalpha and gamma and suppresses COX-2 expression. *Biochimica et Biophysica Acta (BBA) - Molecular and Cell Biology of Lipids.* 2010; **1801**: 1214-20.
- 94 Cornick CL, Strongitharm BH, Sassano G, Rawlins C, Mayes AE, Joseph AN, *et al.* Identification of a novel agonist of peroxisome proliferator-activated receptors alpha and gamma that may contribute to the anti-diabetic activity of guggulipid in Lep(ob)/Lep(ob) mice. *J Nutr Biochem.* 2009; **20**: 806-15.
- 95 Monden T, Hosoya T, Nakajima Y, Kishi M, Satoh T, Hashimoto K, *et al.* Herbal medicine, Hachimi-jio-gan, and its component cinnamomi cortex activate the peroxisome proliferator-activated receptor alpha in renal cells. *Endocr J.* 2008; **55**: 529-33.
- 96 Huang TH, Kota BP, Razmovski V, Roufogalis BD. Herbal or natural medicines as modulators of peroxisome proliferator-activated receptors and related nuclear receptors for therapy of metabolic syndrome. *Basic Clin Pharmacol Toxicol.* 2005; **96**: 3-14.
- 97 Sen R, Baltimore D. Multiple nuclear factors interact with the immunoglobulin enhancer sequences. *Cell.* 1986; **46**: 705-16.
- 98 Perkins ND. Integrating cell-signalling pathways with NF-κB and IKK function. *Nat Rev Mol Cell Biol.* 2007; **8**: 49-62.

- 99 Hayden MS, Ghosh S. Shared Principles in NF- κ B Signaling. *Cell*. 2008; **132**: 344-62.
- 100 Gilmore TD. Introduction to NF- κ B: players, pathways, perspectives. *Oncogene*. 2006; **25**: 6680-84.
- 101 Li Q, Verma IM. NF- κ B regulation in the immune system. *Nat Rev Immunol*. 2002; **2**: 725-34.
- 102 Hayden MS, Ghosh S. Signaling to NF- κ B. *Genes Dev*. 2004; **18**: 2195-224.
- 103 Karin M, Yamamoto Y, Wang QM. The IKK NF- κ B system: a treasure trove for drug development. *Nat Rev Drug Discov*. 2004; **3**: 17-26.
- 104 May MJ, Ghosh S. Signal transduction through NF- κ B. *Immunology Today*. 1998; **19**: 80-88.
- 105 Karin M, Greten FR. NF- κ B: linking inflammation and immunity to cancer development and progression. *Nat Rev Immunol*. 2005; **5**: 749-59.
- 106 Bonizzi G, Karin M. The two NF- κ B activation pathways and their role in innate and adaptive immunity. *Trends Immunol*. 2004; **25**: 280-8.
- 107 Ghosh S, Hayden MS. New regulators of NF- κ B in inflammation. *Nat Rev Immunol*. 2008; **8**: 837-48.
- 108 Karin M, Delhase M. The I κ B kinase (IKK) and NF- κ B: key elements of proinflammatory signalling. *Semin Immunol*. 2000; **12**: 85-98.
- 109 Palombella VJ, Rando OJ, Goldberg AL, Maniatis T. The ubiquitin-proteasome pathway is required for processing the NF- κ B1 precursor protein and the activation of NF- κ B. *Cell*. 1994; **78**: 773-85.
- 110 Yaron A, Gonen H, Alkalay I, Hatzubai A, Jung S, Beyth S, *et al*. Inhibition of NF- κ B cellular function via specific targeting of the I κ B-ubiquitin ligase. *EMBO J*. 1997; **16**: 6486-94.
- 111 Voges D, Zwickl P, Baumeister W. The 26S proteasome: a molecular machine designed for controlled proteolysis. *Annu Rev Biochem*. 1999; **68**: 1015-68.
- 112 Glickman MH, Ciechanover A. The Ubiquitin-Proteasome Proteolytic Pathway: Destruction for the Sake of Construction. *Physiol Rev*. 2002; **82**: 373-428.

- 113 Rothwarf DM, Zandi E, Natoli G, Karin M. IKK-gamma is an essential regulatory subunit of the I κ B kinase complex. *Nature*. 1998; **395**: 297-300.
- 114 Schmid JA, Birbach A. I κ B kinase beta (IKKbeta/IKK2/I κ BKB)--A key molecule in signaling to the transcription factor NF- κ B. *Cytokine & Growth Factor Reviews*. 2008; **19**: 157-65.
- 115 Hacker H, Karin M. Regulation and function of IKK and IKK-related kinases. *Sci STKE*. 2006; **2006**: re13.
- 116 Li ZW, Chu W, Hu Y, Delhase M, Deerinck T, Ellisman M, *et al.* The IKKbeta subunit of I κ B kinase (IKK) is essential for nuclear factor κ B activation and prevention of apoptosis. *J Exp Med*. 1999; **189**: 1839-45.
- 117 Chen LW, Egan L, Li ZW, Greten FR, Kagnoff MF, Karin M. The two faces of IKK and NF- κ B inhibition: prevention of systemic inflammation but increased local injury following intestinal ischemia-reperfusion. *Nat Med*. 2003; **9**: 575-81.
- 118 Prajapati S, Gaynor RB. Regulation of I κ B kinase (IKK)gamma /NEMO function by IKKbeta -mediated phosphorylation. *J Biol Chem*. 2002; **277**: 24331-9.
- 119 Solt LA, Madge LA, May MJ. NEMO-binding Domains of Both IKK α and IKK β Regulate I κ B Kinase Complex Assembly and Classical NF- κ B Activation. *Journal of Biological Chemistry*. 2009; **284**: 27596-608.
- 120 Chen RAJ, Ryzhakov G, Cooray S, Randow F, Smith GL. Inhibition of I κ B Kinase by Vaccinia Virus Virulence Factor B14. *PLoS Pathog*. 2008; **4**: e22.
- 121 Hu Y, Baud V, eacute, ronique, Delhase M, Zhang P, *et al.* Abnormal Morphogenesis But Intact IKK Activation in Mice Lacking the IKK Subunit of I κ B Kinase. *Science*. 1999; **284**: 316-20.
- 122 Senftleben U, Cao Y, Xiao G, Greten FR, Krahn G, Bonizzi G, *et al.* Activation by IKKalpha of a second, evolutionary conserved, NF- κ B signaling pathway. *Science*. 2001; **293**: 1495-9.
- 123 Derudder E, Dejardin E, Pritchard LL, Green DR, KÄ¶rner M, Baud Vr. RelB/p50 Dimers Are Differentially Regulated by Tumor Necrosis Factor- α and Lymphotoxin- β Receptor Activation. *Journal of Biological Chemistry*. 2003; **278**: 23278-84.

- 124 Coope HJ, Atkinson PG, Huhse B, Belich M, Janzen J, Holman MJ, *et al.* CD40 regulates the processing of NF- κ B2 p100 to p52. *EMBO J.* 2002; **21**: 5375-85.
- 125 Vallabhapurapu S, Karin M. Regulation and function of NF- κ B transcription factors in the immune system. *Annu Rev Immunol.* 2009; **27**: 693-733.
- 126 Yang F, Tang E, Guan K, Wang CY. IKK beta plays an essential role in the phosphorylation of RelA/p65 on serine 536 induced by lipopolysaccharide. *J Immunol.* 2003; **170**: 5630-5.
- 127 Beinke S, Robinson MJ, Hugunin M, Ley SC. Lipopolysaccharide activation of the TPL-2/MEK/extracellular signal-regulated kinase mitogen-activated protein kinase cascade is regulated by I κ B kinase-induced proteolysis of NF- κ B1 p105. *Mol Cell Biol.* 2004; **24**: 9658-67.
- 128 Hu MC, Lee DF, Xia W, Golfman LS, Ou-Yang F, Yang JY, *et al.* I κ B kinase promotes tumorigenesis through inhibition of forkhead FOXO3a. *Cell.* 2004; **117**: 225-37.
- 129 Libby P. Inflammation in atherosclerosis. *Nature.* 2002; **420**: 868-74.
- 130 Aparicio CL, Berthiaume F, Chang CC, Yarmush ML. Tumor necrosis factor-alpha (TNF-alpha) induces a reversible, time- and dose-dependent adhesion of progenitor T cells to endothelial cells. *Mol Immunol.* 1996; **33**: 671-80.
- 131 Burleigh ME, Babaev VR, Oates JA, Harris RC, Gautam S, Riendeau D, *et al.* Cyclooxygenase-2 promotes early atherosclerotic lesion formation in LDL receptor-deficient mice. *Circulation.* 2002; **105**: 1816-23.
- 132 Ivandic B, Castellani LW, Wang XP, Qiao JH, Mehrabian M, Navab M, *et al.* Role of group II secretory phospholipase A2 in atherosclerosis: 1. Increased atherogenesis and altered lipoproteins in transgenic mice expressing group IIa phospholipase A2. *Arterioscler Thromb Vasc Biol.* 1999; **19**: 1284-90.
- 133 Zhao L, Funk CD. Lipoxygenase pathways in atherogenesis. *Trends Cardiovasc Med.* 2004; **14**: 191-5.
- 134 Aiello RJ, Bourassa PA, Lindsey S, Weng W, Natoli E, Rollins BJ, *et al.* Monocyte chemoattractant protein-1 accelerates atherosclerosis in apolipoprotein E-deficient mice. *Arterioscler Thromb Vasc Biol.* 1999; **19**: 1518-25.
- 135 Wolle J, Ferguson E, Keshava C, Devall LJ, Boschelli DH, Newton RS, *et al.* Inhibition of tumor necrosis factor induced human aortic endothelial cell

- adhesion molecule gene expression by an alkoxybenzo[b]thiophene-2-carboxamide. *Biochem Biophys Res Commun*. 1995; **214**: 6-10.
- 136 Zahradka P, Werner JP, Buhay S, Litchie B, Helwer G, Thomas S. NF- κ B Activation is Essential for Angiotensin II-dependent Proliferation and Migration of Vascular Smooth Muscle Cells. *Journal of Molecular and Cellular Cardiology*. 2002; **34**: 1609-21.
- 137 Yang J, Jiang H, Chen S-s, Chen J, Xu S-k, Li W-q, *et al*. CBP knockdown inhibits angiotensin II-induced vascular smooth muscle cells proliferation through downregulating NF- κ B transcriptional activity. *Molecular and Cellular Biochemistry*. 2010; **340**: 55-62.
- 138 Gilmore TD, Herscovitch M. Inhibitors of NF- κ B signaling: 785 and counting. *Oncogene*. 2006; **25**: 6887-99.
- 139 Folmer F, Jaspars M, Dicato M, Diederich M. Marine natural products as targeted modulators of the transcription factor NF- κ B. *Biochemical Pharmacology*. 2008; **75**: 603-17.
- 140 Hehner SP, Hofmann TG, Droge W, Schmitz ML. The antiinflammatory sesquiterpene lactone parthenolide inhibits NF- κ B by targeting the I κ B kinase complex. *J Immunol*. 1999; **163**: 5617-23.
- 141 Kwok BHB, Koh B, Ndubuisi MI, Elofsson M, Crews CM. The anti-inflammatory natural product parthenolide from the medicinal herb Feverfew directly binds to and inhibits I κ B kinase. *Chemistry & Biology*. 2001; **8**: 759-66.
- 142 Pandey MK, Sandur SK, Sung B, Sethi G, Kunnumakkara AB, Aggarwal BB. Butein, a Tetrahydroxychalcone, Inhibits Nuclear Factor (NF)- κ B and NF- κ B-regulated Gene Expression through Direct Inhibition of I κ B α Kinase β on Cysteine 179 Residue. *Journal of Biological Chemistry*. 2007; **282**: 17340-50.
- 143 Lyss G, Knorre A, Schmidt TJ, Pahl HL, Merfort I. The anti-inflammatory sesquiterpene lactone helenalin inhibits the transcription factor NF- κ B by directly targeting p65. *J Biol Chem*. 1998; **273**: 33508-16.
- 144 Leung CH, Grill SP, Lam W, Han QB, Sun HD, Cheng YC. Novel mechanism of inhibition of nuclear factor- κ B DNA-binding activity by diterpenoids isolated from *Isodon rubescens*. *Mol Pharmacol*. 2005; **68**: 286-97.

- 145 de las Heras B, Hortelano S. Molecular basis of the anti-inflammatory effects of terpenoids. *Inflamm Allergy Drug Targets*. 2009; **8**: 28-39.
- 146 Matsumoto N, Ariga A, To-e S, Nakamura H, Agata N, Hirano S-i, *et al.* Synthesis of NF- κ B activation inhibitors derived from epoxyquinomicin C. *Bioorganic & Medicinal Chemistry Letters*. 2000; **10**: 865-69.
- 147 Srinivasan B, Johnson TE, Lad R, Xing C. Structure-Activity Relationship Studies of Chalcone Leading to 3-Hydroxy-4,3',4',5'-tetramethoxychalcone and Its Analogues as Potent Nuclear Factor κ B Inhibitors and Their Anticancer Activities. *Journal of Medicinal Chemistry*. 2009; **52**: 7228-35.
- 148 Matsumoto N, Iinuma H, Sawa T, Takeuchi T, Hirano S, Yoshioka T, *et al.* Epoxyquinomicins A, B, C and D, new antibiotics from *Amycolatopsis*. II. Effect on type II collagen-induced arthritis in mice. *J Antibiot (Tokyo)*. 1997; **50**: 906-11.
- 149 Ariga A, Namekawa J-i, Matsumoto N, Inoue J-i, Umezawa K. Inhibition of Tumor Necrosis Factor- α -induced Nuclear Translocation and Activation of NF- κ B by Dehydroxymethylepoxyquinomicin. *Journal of Biological Chemistry*. 2002; **277**: 24625-30.
- 150 Yamamoto M, Horie R, Takeiri M, Kozawa I, Umezawa K. Inactivation of NF- κ B Components by Covalent Binding of (-)-Dehydroxymethylepoxyquinomicin to Specific Cysteine Residues. *Journal of Medicinal Chemistry*. 2008; **51**: 5780-88.
- 151 Saitoh T, Suzuki E, Takasugi A, Obata R, Ishikawa Y, Umezawa K, *et al.* Efficient synthesis of (\pm)-parasitenone, a novel inhibitor of NF- κ B. *Bioorganic & Medicinal Chemistry Letters*. 2009; **19**: 5383-86.
- 152 Manna SK, Bueso-Ramos C, Alvarado F, Aggarwal BB. Calagualine inhibits nuclear transcription factors- κ B activated by various inflammatory and tumor promoting agents. *Cancer Letters* 2003; **190**:171-182.
- 153 Go EK, Jung KJ, Kim JY, Yu BP, Chung HY. Betaine suppresses proinflammatory signaling during aging: the involvement of nuclear factor- κ B via nuclear factor-inducing kinase/I κ B kinase and mitogen-activated protein kinases. *J Gerontol A Biol Sci Med Sci*. 2005; **60**: 1252-64.
- 154 Morwick T, Berry A, Brickwood J, Cardozo M, Catron K, DeTuri M, *et al.* Evolution of the Thienopyridine Class of Inhibitors of I κ B Kinase- β : Part I: Hit-to-Lead Strategies. *Journal of Medicinal Chemistry*. 2006; **49**: 2898-908.

- 155 Burke JR, Pattoli MA, Gregor KR, Brassil PJ, MacMaster JF, McIntyre KW, *et al.* BMS-345541 Is a Highly Selective Inhibitor of I κ B Kinase That Binds at an Allosteric Site of the Enzyme and Blocks NF- κ B-dependent Transcription in Mice. *Journal of Biological Chemistry*. 2003; **278**: 1450-56.
- 156 Singh S, Natarajan K, Aggarwal BB. Capsaicin (8-methyl-N-vanillyl-6-nonenamide) is a potent inhibitor of nuclear transcription factor- κ B activation by diverse agents. *The Journal of Immunology*. 1996; **157**: 4412-20.
- 157 Mori A, Lehmann Sr, O'Kelly J, Kumagai T, Desmond JC, Pervan M, *et al.* Capsaicin, a Component of Red Peppers, Inhibits the Growth of Androgen-Independent, p53 Mutant Prostate Cancer Cells. *Cancer Research*. 2006; **66**: 3222-29.
- 158 Yoshida Y, Liu JQ, Nakano Y, Ueno S, Ohmori S, Fueta Y, *et al.* 1-BP inhibits NF- κ B activity and Bcl-xL expression in astrocytes in vitro and reduces Bcl-xL expression in the brains of rats in vivo. *NeuroToxicology*. 2007; **28**: 381-86.
- 159 Meyer S, Kohler NG, Joly A. Cyclosporine A is an uncompetitive inhibitor of proteasome activity and prevents NF- κ B activation. *FEBS Letters*. 1997; **413**: 354-58.
- 160 Frantz B, Nordby EC, Bren G, Steffan N, Paya CV, Kincaid RL, *et al.* Calcineurin acts in synergy with PMA to inactivate I κ B/MAD3, an inhibitor of NF- κ B. *EMBO J*. 1994; **13**: 861-70.
- 161 Lövborg H, Öberg F, Rickardson L, Gullbo J, Nygren P, Larsson R. Inhibition of proteasome activity, nuclear factor- κ B translocation and cell survival by the antialcoholism drug disulfiram. *International Journal of Cancer*. 2006; **118**: 1577-80.
- 162 Jeong HJ, Lee SA, Moon PD, Na HJ, Park RK, Um JY, *et al.* Alginic acid has anti-anaphylactic effects and inhibits inflammatory cytokine expression via suppression of nuclear factor- κ B activation. *Clinical & Experimental Allergy*. 2006; **36**: 785-94.
- 163 Sánchez AJ, Puerta C, Ballester S, González P, Arriaga A, Garcí'a-Merino A. Rolipram impairs NF- κ B activity and MMP-9 expression in experimental autoimmune encephalomyelitis. *Journal of Neuroimmunology*. 2005; **168**: 13-20.
- 164 Aldieri E, Atragene D, Bergandi L, Riganti C, Costamagna C, Bosia A, *et al.* Artemisinin inhibits inducible nitric oxide synthase and nuclear factor NF- κ B activation. *FEBS Letters*. 2003; **552**: 141-44.

- 165 Olivier S, Close P, Castermans E, de Leval L, Tabruyn S, Chariot A, *et al.* Raloxifene-Induced Myeloma Cell Apoptosis: A Study of Nuclear Factor- κ B Inhibition and Gene Expression Signature. *Molecular Pharmacology*. 2006; **69**: 1615-23.
- 166 Huang T, Li Y, Razmovski-Naumovski V, Tran V, Li G, Duke C, *et al.* Gypenoside XLIX isolated from *Gynostemma pentaphyllum* inhibits nuclear factor- κ B activation via a PPAR- α -dependent pathway *Journal of Biomedical Science*. 2006; **13**: 535-48.
- 167 Cheng J-F, Ishikawa A, Ono Y, Arrhenius T, Nadzan A. Novel chromene derivatives as TNF- α inhibitors. *Bioorganic & Medicinal Chemistry Letters*. 2003; **13**: 3647-50.
- 168 Singh S, Aggarwal BB. Activation of Transcription Factor NF- κ B Is Suppressed by Curcumin (Diferuloylmethane). *Journal of Biological Chemistry*. 1995; **270**: 24995-5000.
- 169 Zhang D-L, Zhang Y-T, Yin J-J, Zhao B-L. Oral administration of Crataegus flavonoids protects against ischemia/reperfusion brain damage in gerbils. *Journal of Neurochemistry*. 2004; **90**: 211-19.
- 170 Colgate EC, Miranda CL, Stevens JF, Bray TM, Ho E. Xanthohumol, a prenylflavonoid derived from hops induces apoptosis and inhibits NF- κ B activation in prostate epithelial cells. *Cancer Letters*. 2007; **246**: 201-09.
- 171 Schreck R, Meier B, Mannel DN, Droge W, Baeuerle PA. Dithiocarbamates as potent inhibitors of nuclear factor κ B activation in intact cells. *J Exp Med*. 1992; **175**: 1181-94.
- 172 Saukel J., W. K. Pflanzen in der österreichischen Volksmedizin. Die "Volkmed Datenbank" *Sci Pharm*. 1993; **62**: 100.
- 173 Graham FL, Smiley J, Russell WC, Nairn R. Characteristics of a Human Cell Line Transformed by DNA from Human Adenovirus Type 5. *J Gen Virol*. 1977; **36**: 59-72.
- 174 Louis N, Eveleigh C, Graham FL. Cloning and Sequencing of the Cellular-Viral Junctions from the Human Adenovirus Type 5 Transformed 293 Cell Line. *Virology*. 1997; **233**: 423-29.
- 175 Hibberts NA, Howell AE, Randall VA. Balding hair follicle dermal papilla cells contain higher levels of androgen receptors than those from non-balding scalp. *J Endocrinol*. 1998; **156**: 59-65.

- 176 Rachez C, Gamble M, Chang CP, Atkins GB, Lazar MA, Freedman LP. The DRIP complex and SRC-1/p160 coactivators share similar nuclear receptor binding determinants but constitute functionally distinct complexes. *Mol Cell Biol*. 2000; **20**: 2718-26.
- 177 Fakhrudin N, Ladurner A, Atanasov AG, Heiss EH, Baumgartner L, Markt P, *et al*. Computer-Aided Discovery, Validation, and Mechanistic Characterization of Novel Neolignan Activators of Peroxisome Proliferator-Activated Receptor γ *Molecular Pharmacology*. 2010; **77**: 559-66.
- 178 Schiller HB, Szekeres A, Binder BR, Stockinger H, Leksa V. Mannose 6-phosphate/insulin-like growth factor 2 receptor limits cell invasion by controlling α V β 3 integrin expression and proteolytic processing of urokinase-type plasminogen activator receptor. *Mol Biol Cell*. 2009; **20**: 745-56.
- 179 Yang J, Chang E, Cherry AM, Bangs CD, Oei Y, Bodnar A, *et al*. Human Endothelial Cell Life Extension by Telomerase Expression. *Journal of Biological Chemistry*. 1999; **274**: 26141-48.
- 180 Anno K, Hayashi A, Takahashi T, Mitsui Y, Ide T, Tahara H. Telomerase activation induces elongation of the telomeric single-stranded overhang, but does not prevent chromosome aberrations in human vascular endothelial cells. *Biochemical and Biophysical Research Communications*. 2007; **353**: 926-32.
- 181 Bradford MM. A rapid and sensitive method for the quantitation of microgram quantities of protein utilizing the principle of protein-dye binding. *Anal Biochem*. 1976; **72**: 248-54.
- 182 Schreiner C. Mechanistic studies on resveratrol and its influence on angiotensin II- and epidermal growth factor-induced signaling pathways in vascular smooth muscle cells. *Dissertation, University of Vienna*,. 2009.
- 183 Raschke WC, Baird S, Ralph P, Nakoinz I. Functional macrophage cell lines transformed by abelson leukemia virus. *Cell*. 1978; **15**: 261-67.
- 184 Griess P. Bemerkungen zu der Abhandlung der HH. Weselsky und Benedikt „Ueber einige Azoverbindungen“ *Berichte der deutschen chemischen Gesellschaft*. 1879; **12**: 426-28.
- 185 Hensley k, Mou S, Pye QN. Nitrite Determination by Colorimetric and Fluorometric Griess Diazotization Assays. *Methods in Pharmacology and Toxicology*. 2003; **III**: 185-93.

- 186 Mariscal A, Lopez-Gigosos RM, Carnero-Varo M, Fernandez-Crehuet J. Fluorescent assay based on resazurin for detection of activity of disinfectants against bacterial biofilm. *Appl Microbiol Biotechnol.* 2009; **82**: 773-83.
- 187 O'Brien J, Wilson I, Orton T, Pognan F. Investigation of the Alamar Blue (resazurin) fluorescent dye for the assessment of mammalian cell cytotoxicity. *Eur J Biochem.* 2000; **267**: 5421-6.
- 188 Markt P, Schuster D, Kirchmair J, Laggner C, Langer T. Pharmacophore modeling and parallel screening for PPAR ligands. *J Comput Aided Mol Des.* 2007; **21**: 575-90.
- 189 Markt P, Petersen RK, Flindt EN, Kristiansen K, Kirchmair J, Spitzer G, *et al.* Discovery of novel PPAR ligands by a virtual screening approach based on pharmacophore modeling, 3D shape, and electrostatic similarity screening. *J Med Chem.* 2008; **51**: 6303-17.
- 190 Lu I-L, Huang C-F, Peng Y-H, Lin Y-T, Hsieh H-P, Chen C-T, *et al.* Structure-based drug design of a novel family of PPAR α partial agonists: Virtual screening, x-ray crystallography, and in vitro/in vivo biological activities. *J Med Chem.* 2006; **49**: 2703-12.
- 191 Wang X, Wang Y, Geng Y, Li F, Zheng C. Isolation and purification of honokiol and magnolol from cortex *Magnoliae officinalis* by high-speed counter-current chromatography. *J Chromatogr A.* 2004; **1036**: 171-5.
- 192 Yu S, Reddy JK. Transcription coactivators for peroxisome proliferator-activated receptors. *Biochimica et Biophysica Acta (BBA) - Molecular and Cell Biology of Lipids.* 2007; **1771**: 936-51.
- 193 Itoh T, Fairall L, Amin K, Inaba Y, Szanto A, Balint Balint L, *et al.* Structural basis for the activation of PPAR γ by oxidized fatty acids. *Nat Struct Mol Biol.* 2008; **15**: 924-31.
- 194 Rosen ED, Sarraf P, Troy AE, Bradwin G, Moore K, Milstone DS, *et al.* PPAR gamma is required for the differentiation of adipose tissue in vivo and in vitro. *Mol Cell.* 1999; **4**: 611-7.
- 195 Wright HM, Clish CB, Mikami T, Hauser S, Yanagi K, Hiramatsu R, *et al.* A synthetic antagonist for the peroxisome proliferator-activated receptor gamma inhibits adipocyte differentiation. *J Biol Chem.* 2000; **275**: 1873-7.
- 196 Alleva DG, Johnson EB, Lio FM, Boehme SA, Conlon PJ, Crowe PD. Regulation of murine macrophage proinflammatory and anti-inflammatory

- cytokines by ligands for peroxisome proliferator-activated receptor-gamma: counter-regulatory activity by IFN-gamma. *J Leukoc Biol.* 2002; **71**: 677-85.
- 197 Goetze S, Xi XP, Kawano Y, Kawano H, Fleck E, Hsueh WA, *et al.* TNF-alpha-induced migration of vascular smooth muscle cells is MAPK dependent. *Hypertension.* 1999; **33**: 183-9.
- 198 Bevilacqua PM, Nelson MD, Mannori G, Cecconi O. Endothelial-leukocyte adhesion molecules in human diseases. *Annual Review of Medicine.* 1994; **45**: 361-78.
- 199 Viatour P, Merville MP, Bours V, Chariot A. Phosphorylation of NF- κ B and I κ B proteins: implications in cancer and inflammation. *Trends Biochem Sci.* 2005; **30**: 43-52.
- 200 Hammond GB, Fernandez ID, Villegas LF, Vaisberg AJ. A survey of traditional medicinal plants from the Callejon de Huaylas, Department of Ancash, Peru. *J Ethnopharmacol.* 1998; **61**: 17-30.
- 201 Noha SM, Atanasov AG, Schuster D, Markt P, Fakhrudin N, Heiss EH, *et al.* Discovery of a novel IKK-beta inhibitor by ligand-based virtual screening techniques. *Bioorganic & Medicinal Chemistry Letters.* 2011; **21**: 577-83.
- 202 Kelly KA, Hill MR, Youkhana K, Wanker F, Gimble JM. Dimethyl sulfoxide modulates NF- κ B and cytokine activation in lipopolysaccharide-treated murine macrophages. *Infect Immun.* 1994; **62**: 3122-8.
- 203 Essani NA, Fisher MA, Jaeschke H. Inhibition of NF- κ B activation by dimethyl sulfoxide correlates with suppression of TNF-alpha formation, reduced ICAM-1 gene transcription, and protection against endotoxin-induced liver injury. *Shock.* 1997; **7**: 90-96.
- 204 Banos G, Perez-Torres I, El Hafidi M. Medicinal agents in the metabolic syndrome. *Cardiovasc Hematol Agents Med Chem.* 2008; **6**: 237-52.
- 205 Rollinger JM, Haupt S, Stuppner H, Langer T. Combining Ethnopharmacology and Virtual Screening for Lead Structure Discovery: COX-Inhibitors as Application Example. *Journal of Chemical Information and Computer Sciences.* 2004; **44**: 480-88.
- 206 Rollinger JM, Steindl TM, Schuster D, Kirchmair J, Anrain K, Ellmerer EP, *et al.* Structure-based virtual screening for the discovery of natural inhibitors for human rhinovirus coat protein. *J Med Chem.* 2008; **51**: 842-51.

- 207 Choi SS, Cha BY, Lee YS, Yonezawa T, Teruya T, Nagai K, *et al.* Magnolol enhances adipocyte differentiation and glucose uptake in 3T3-L1 cells. *Life Sci.* 2009; **84**: 908-14
- 208 Miyazawa M, Hisama M. Antimutagenic Activity of Phenylpropanoids from Clove (*Syzygium aromaticum*). *Journal of Agricultural and Food Chemistry.* 2003; **51**: 6413-22.
- 209 Ogata M, Hoshi M, Urano S, Endo T. Antioxidant activity of eugenol and related monomeric and dimeric compounds. *Chem Pharm Bull.* 2000; **48**: 1467-69.
- 210 Murakami Y, Shoji M, Hanazawa S, Tanaka S, Fujisawa S. Preventive effect of bis-eugenol, a eugenol ortho dimer, on lipopolysaccharide-stimulated nuclear factor κ B activation and inflammatory cytokine expression in macrophages. *Biochemical Pharmacology.* 2003; **66**: 1061-66.
- 211 Chang F, Jaber LA, Berlie HD, O'Connell MB. Evolution of peroxisome proliferator-activated receptor agonists. *Ann Pharmacother.* 2007; **41**: 973-83.
- 212 Yumuk VD. Targeting Components of the Stress System as Potential Therapies for the Metabolic Syndrome. *Annals of the New York Academy of Sciences.* 2006; **1083**: 306-18.
- 213 Cho N, Momose Y. Peroxisome proliferator-activated receptor gamma agonists as insulin sensitizers: from the discovery to recent progress. *Curr Top Med Chem.* 2008; **8**: 1483-507.
- 214 Ricote M, Li AC, Willson TM, Kelly CJ, Glass CK. The peroxisome proliferator-activated receptor-gamma is a negative regulator of macrophage activation. *Nature.* 1998; **391**: 79-82.
- 215 Crosby MB, Svenson JL, Zhang J, Nicol CJ, Gonzalez FJ, Gilkeson GS. Peroxisome proliferation-activated receptor (PPAR)gamma is not necessary for synthetic PPARgamma agonist inhibition of inducible nitric-oxide synthase and nitric oxide. *J Pharmacol Exp Ther.* 2005; **312**: 69-76.
- 216 Paukkeri EL, Leppanen T, Sareila O, Vuolteenaho K, Kankaanranta H, Moilanen E. PPARalpha agonists inhibit nitric oxide production by enhancing iNOS degradation in LPS-treated macrophages. *Br J Pharmacol.* 2007; **152**: 1081-91.
- 217 Crosby MB, Svenson J, Gilkeson GS, Nowling TK. A novel PPAR response element in the murine iNOS promoter. *Mol Immunol.* 2005; **42**: 1303-10.

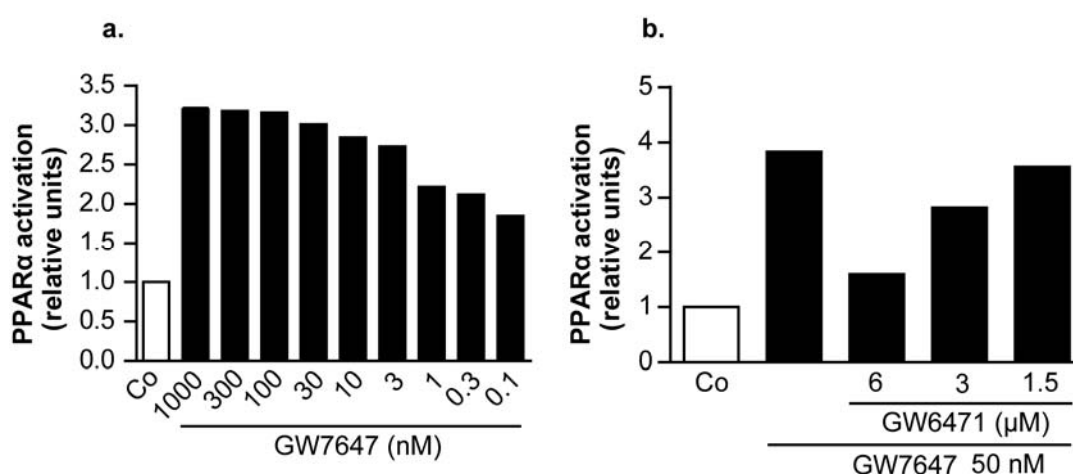
- 218 Marx N, Schonbeck U, Lazar MA, Libby P, Plutzky J. Peroxisome Proliferator-Activated Receptor Gamma Activators Inhibit Gene Expression and Migration in Human Vascular Smooth Muscle Cells. *Circ Res*. 1998; **83**: 1097-103.
- 219 Lim HJ, Lee S, Park JH, Lee KS, Choi HE, Chung KS, *et al*. PPAR delta agonist L-165041 inhibits rat vascular smooth muscle cell proliferation and migration via inhibition of cell cycle. *Atherosclerosis*. 2009; **202**: 446-54.
- 220 Pandey NR, Benkirane K, Amiri F, Schiffrin EL. Effects of PPAR-gamma knock-down and hyperglycemia on insulin signaling in vascular smooth muscle cells from hypertensive rats. *J Cardiovasc Pharmacol*. 2007; **49**: 346-54.
- 221 Jiang F, Tao Y, Shao Y. Fingerprinting quality control of Qianghuo by high-performance liquid chromatography-photodiode array detection. *Journal of Ethnopharmacology*. 2007; **111**: 265-70.
- 222 Okuyama E, Nishimura S, Ohmori S, Ozaki Y, Satake M, Yamazaki M. Analgesic component of *Notopterygium incisum* Ting. *Chem Pharm Bull (Tokyo)*. 1993; **41**: 926-9.
- 223 Yang XW, Gu ZM, Wang BX, Hattori M, Namba T. Comparison of anti-lipid peroxidative effects of the underground parts of *Notopterygium incisum* and *N. forbesii* in mice. *Planta Med*. 1991; **57**: 399-402.
- 224 Zschocke S, Lehner M, Bauer R. 5-Lipoxygenase and cyclooxygenase inhibitory active constituents from Qianghuo (*Notopterygium incisum*). *Planta Med*. 1997; **63**: 203-6.
- 225 Liu X, Jiang S, Xu K, Sun H, Zhou Y, Xu X, *et al*. Quantitative analysis of chemical constituents in different commercial parts of *Notopterygium incisum* by HPLC-DAD-MS. *Journal of Ethnopharmacology*. 2009; **126**: 474-79.
- 226 Wu SB, Pang F, Wen Y, Zhang HF, Zhao Z, Hu JF. Antiproliferative and apoptotic activities of linear furocoumarins from *Notopterygium incisum* on cancer cell lines. *Planta Med*. 2010; **76**: 82-5.
- 227 Chien SC, Young PH, Hsu YJ, Chen CH, Tien YJ, Shiu SY, *et al*. Anti-diabetic properties of three common *Bidens pilosa* variants in Taiwan. *Phytochemistry*. 2009; **70**: 1246-54.
- 228 Jovel EM, Cabanillas J, Towers GHN. An ethnobotanical study of the traditional medicine of the Mestizo people of Suni Miraflores, Loreto, Peru. *Journal of Ethnopharmacology*. 1996; **53**: 149-56.

- 229 Elisabetsky E, Castilhos ZC. Plants Used as Analgesics by Amazonian Caboclos as a Basis for Selecting Plants for Investigation. *Int J Crude Drug Res.* 1990; **28**: 309-20.
- 230 Perdue GP, Blomster RN. South American plants III: Isolation of fulvoplumierin from *Himatanthus sucuuba* (M. Arg.) Woodson (apocynaceae). *Journal of Pharmaceutical Sciences.* 1978; **67**: 1322-23.
- 231 Abdel-Kader MS, Wisse J, Evans R, van der Werff H, Kingston DG. Bioactive iridoids and a new lignan from *Allamanda cathartica* and *Himatanthus fallax* from the Suriname rainforest. *J Nat Prod.* 1997; **60**: 1294-7.
- 232 Kuigoua GM, Kouam SF, Ngadjui BT, Schulz B, Green IR, Choudhary MI, *et al.* Minor secondary metabolic products from the stem bark of *Plumeria rubra* Linn. displaying antimicrobial activities. *Planta Med.* 2010; **76**: 620-5.
- 233 Bolzani Vda S, Young MC, Furlan M, Cavalheiro AJ, Araujo AR, Silva DH, *et al.* Search for antifungal and anticancer compounds from native plant species of Cerrado and Atlantic Forest. *An Acad Bras Cienc.* 1999; **71**: 181-7.
- 234 Castillo D, Arevalo J, Herrera F, Ruiz C, Rojas R, Rengifo E, *et al.* Spirolactone iridoids might be responsible for the antileishmanial activity of a Peruvian traditional remedy made with *Himatanthus sucuuba* (Apocynaceae). *Journal of Ethnopharmacology.* 2007; **112**: 410-14.
- 235 Zheng C, Yin Q, Wu H. Structural studies of NF- κ B signaling. *Cell Res.* 2010.
- 236 Kensler TW, Wakabayashi N, Biswal S. Cell Survival Responses to Environmental Stresses Via the Keap1-Nrf2-ARE Pathway. *Annual Review of Pharmacology and Toxicology.* 2007; **47**: 89-116.
- 237 Osburn WO, Kensler TW. Nrf2 signaling: An adaptive response pathway for protection against environmental toxic insults. *Mutation Research/Reviews in Mutation Research.* 2007; **659**: 31-39.
- 238 Banning A, Brigelius-Flohe R. NF- κ B, Nrf2, and HO-1 interplay in redox-regulated VCAM-1 expression. *Antioxid Redox Signal.* 2005; **7**: 889-99.
- 239 Nagarajan S, Doddareddy Mr, Choo H, Cho YS, Oh K-S, Lee BH, *et al.* IKKbeta inhibitors identification part I: Homology model assisted structure based virtual screening. *Bioorganic & Medicinal Chemistry.* 2009; **17**: 2759-66.

G. APPENDIX

G. APPENDIX

1. SUPPLEMENTARY DATA



Supplementary Figure 1. Validation of the bioassay using PPAR α agonist and antagonist. (a) Dose-dependent PPAR α activation in transfected cells by the PPAR α agonist GW7647. (b) Inhibition of GW7647-induced PPAR α activation by the PPAR α antagonist, GW6471. HEK-293 cells were transiently cotransfected with a plasmid encoding full-length PPAR α , a reporter plasmid containing PPRE coupled to a luciferase reporter, and EGFP as internal control. The cells were stimulated with the indicated concentrations of GW7647 (a) or GW6471 followed by GW7647 (b) for 18 hours. Luciferase activity was measured and normalized by the EGFP-derived fluorescence, and the result is expressed as fold induction compared to the control DMSO (Co). One experiment performed in a quadruplet is shown, out of two independently performed experiments with similar result.

Supplementary Table 1. List of plant extracts tested for a PPAR α and γ agonistic and NF- κ B inhibitor activity using luciferase reporter gene assay

Testing of plant extracts for PPAR γ activation and NF- κ B inhibition (Prof. Brigitte Kopp)							
	Plant species	Part	Solvent	PPAR α	PPAR γ	NF κ B	Code
1	<i>Agrimonia</i> sp.	HB	DCM	-	-	+	1
2	<i>Agrimonia</i> sp.	HB	DCM (CS)	-	-	+	2
3	<i>Agrimonia</i> sp.	HB	MeOH	-	-	-	3
4	<i>Agrimonia</i> sp.	HB	MeOH (TS)	-	-	-	179
5	<i>Agropyron repens</i>	RH	DCM	+	+	-	396
6	<i>Agropyron repens</i>	RH	MeOH	-	-	-	397
7	<i>Agropyron repens</i>	RH	MeOH (TS)	-	-	-	398
8	<i>Ajuga genevensis</i>	HB	DCM	-	-	-	257
9	<i>Ajuga genevensis</i>	HB	DCM (CS)	-	-	-	258
10	<i>Ajuga genevensis</i>	HB	MeOH (TS)	-	-	-	259
11	<i>Ajuga genevensis</i>	HB	MeOH	-	-	-	260
12	<i>Ajuga reptans</i>	HB	DCM	-	-	-	261
13	<i>Ajuga reptans</i>	HB	DCM (CS)	-	-	-	262
14	<i>Ajuga reptans</i>	HB	MeOH	-	-	-	263
15	<i>Ajuga reptans</i>	HB	MeOH (TS)	-	-	-	264
16	<i>Alnus viridis</i>	FO	DCM	-	-	-	330
17	<i>Alnus viridis</i>	FO	DCM (CS)	-	-	+	331
18	<i>Alnus viridis</i>	FO	MeOH	-	-	-	332
19	<i>Alnus viridis</i>	FO	MeOH (TS)	+	+	+	333
20	<i>Angelica archangelica</i>	RD	DCM	-	-	+	4
21	<i>Angelica archangelica</i>	RD	MeOH	-	-	-	5
22	<i>Angelica archangelica</i>	RD	MeOH (TS)	-	-	-	180
23	<i>Angelica sylvestris</i>	RD	DCM	-	-	-	399
24	<i>Angelica sylvestris</i>	RD	MeOH	-	-	-	400
25	<i>Angelica sylvestris</i>	RD	MeOH (TS)	+	+	+	401
26	<i>Bellis perennis</i>	FL	DCM	+	+	+	192
27	<i>Bellis perennis</i>	FL	MeOH	-	-	-	193
28	<i>Bellis perennis</i>	FL	MeOH (TS)	-	-	-	194
29	<i>Berberis vulgaris</i>	FR	DCM	-	-	-	6
30	<i>Berberis vulgaris</i>	FR	MeOH	-	-	-	7
31	<i>Berberis vulgaris</i>	FR	MeOH (TS)	+	+	-	181
32	<i>Beta vulgaris</i>	RD	DCM	-	-	-	189
33	<i>Beta vulgaris</i>	RD	MeOH	-	-	-	190
34	<i>Beta vulgaris</i>	RD	MeOH (TS)	-	-	-	191
35	<i>Betonica officinale</i>	HB	DCM	-	-	-	265
36	<i>Betonica officinale</i>	HB	DCM (CS)	-	-	-	266
37	<i>Betonica officinale</i>	HB	MeOH	-	-	-	267
38	<i>Betonica officinale</i>	HB	MeOH (TS)	-	-	-	268
39	<i>Calluna vulgaris</i>	HB	DCM	-	-	+	8
40	<i>Calluna vulgaris</i>	HB	DCM (CS)	-	-	+	9
41	<i>Calluna vulgaris</i>	HB	MeOH	-	-	-	10
42	<i>Calluna vulgaris</i>	HB	MeOH (TS)	-	-	-	182
43	<i>Capsella bursa-pastoris</i>	HB	DCM	+	+	+	402

44	<i>Capsella bursa-pastoris</i>	HB	DCM (CS)	+	+	-	403
45	<i>Capsella bursa-pastoris</i>	HB	MeOH	-	-	-	404
46	<i>Capsella bursa-pastoris</i>	HB	MeOH (TS)	+	+	+	405
47	<i>Circea lutetiana</i>	HB	DCM	-	-	-	334
48	<i>Circea lutetiana</i>	HB	DCM (CS)	+	+	-	335
49	<i>Circea lutetiana</i>	HB	MeOH	-	-	-	336
50	<i>Circea lutetiana</i>	HB	MeOH (TS)	-	-	-	337
51	<i>Epilobium angustifolium</i>	HB	DCM	-	-	-	14
52	<i>Epilobium angustifolium</i>	HB	DCM (CS)	-	-	-	15
53	<i>Epilobium angustifolium</i>	HB	MeOH	-	-	-	16
54	<i>Epilobium angustifolium</i>	HB	MeOH (TS)	+	+	-	184
55	<i>Epilobium montanum</i>	HB	DCM	-	-	-	406
56	<i>Epilobium montanum</i>	HB	DCM (CS)	-	-	-	407
57	<i>Epilobium montanum</i>	HB	MeOH	-	-	-	408
58	<i>Epilobium montanum</i>	HB	MeOH (TS)	+	+	-	409
59	<i>Epilobium parviflorum</i>	HB	DCM	-	-	+	11
60	<i>Epilobium parviflorum</i>	HB	DCM (CS)	+	-	-	12
61	<i>Epilobium parviflorum</i>	HB	MeOH	-	-	-	13
62	<i>Epilobium parviflorum</i>	HB	MeOH (TS)	-	-	-	183
63	<i>Equisetum arvense</i>	HB	DCM	-	-	+	338
64	<i>Equisetum arvense</i>	HB	DCM (CS)	+	+	+	339
65	<i>Equisetum arvense</i>	HB	MeOH	-	-	-	340
66	<i>Equisetum arvense</i>	HB	MeOH (TS)	-	-	-	341
67	<i>Equisetum palustre</i>	HB	DCM	-	-	-	338
68	<i>Equisetum palustre</i>	HB	DCM (CS)	-	-	+	339
69	<i>Equisetum palustre</i>	HB	MeOH	-	-	-	340
70	<i>Equisetum palustre</i>	HB	MeOH (TS)	-	-	-	341
71	<i>Euphrasia rostkoviana</i>	HB	DCM	-	-	-	342
72	<i>Euphrasia rostkoviana</i>	HB	DCM (CS)	+	+	-	343
73	<i>Euphrasia rostkoviana</i>	HB	MeOH	-	-	-	344
74	<i>Euphrasia rostkoviana</i>	HB	MeOH (TS)	-	-	-	345
75	<i>Euphrasia</i> sp.	HB	DCM	-	-	+	17
76	<i>Euphrasia</i> sp.	HB	DCM (CS)	+	-	-	18
77	<i>Euphrasia</i> sp.	HB	MeOH	-	-	-	19
78	<i>Euphrasia</i> sp.	HB	MeOH (TS)	-	-	+	185
79	<i>Filipendula ulmaria</i>	HB	DCM	-	-	+	20
80	<i>Filipendula ulmaria</i>	HB	DCM (CS)	+	+	+	21
81	<i>Filipendula ulmaria</i>	HB	MeOH	-	-	-	22
82	<i>Filipendula ulmaria</i>	HB	MeOH (TS)	-	-	+	186
83	<i>Filipendula ulmaria</i>	FO	DCM	-	-	-	346
84	<i>Filipendula ulmaria</i>	FO	DCM (CS)	+	+	-	347
85	<i>Filipendula ulmaria</i>	FO	MeOH	-	-	-	348
86	<i>Filipendula ulmaria</i>	FO	MeOH (TS)	-	-	-	349
87	<i>Filipendula vulgaris</i>	FL	DCM	-	-	-	273
88	<i>Filipendula vulgaris</i>	FL	MeOH	-	-	-	274
89	<i>Filipendula vulgaris</i>	FL	MeOH (TS)	-	-	-	275
90	<i>Gentiana punctata</i>	HB	DCM	-	-	-	350
91	<i>Gentiana punctata</i>	HB	DCM (CS)	-	-	-	351
92	<i>Gentiana punctata</i>	HB	MeOH	-	-	-	352
93	<i>Gentiana punctata</i>	HB	MeOH (TS)	-	-	-	353

94	<i>Gentiana punctata</i>	RD	DCM	-	-	-	354
95	<i>Gentiana punctata</i>	RD	MeOH	-	-	-	355
96	<i>Gentiana punctata</i>	RD	MeOH (TS)	+	-	-	356
97	<i>Geum montanum</i>	RD	DCM	-	-	+	414
98	<i>Geum montanum</i>	RD	MeOH	-	-	-	415
99	<i>Geum montanum</i>	RD	MeOH (TS)	-	-	-	416
100	<i>Geum urbanum</i>	HB	DCM	-	-	+	195
101	<i>Geum urbanum</i>	HB	DCM (CS)	+	+	+	196
102	<i>Geum urbanum</i>	HB	MeOH	-	-	-	197
103	<i>Geum urbanum</i>	HB	MeOH (TS)	-	-	+	198
104	<i>Geum urbanum</i>	RD	DCM	+	+	-	417
105	<i>Geum urbanum</i>	RD	MeOH	-	-	-	418
106	<i>Geum urbanum</i>	RD	MeOH (TS)	+	+	-	419
107	<i>Glechoma hederata</i>	HB	DCM	-	-	-	23
108	<i>Glechoma hederata</i>	HB	DCM	-	-	+	23
109	<i>Glechoma hederata</i>	HB	MeOH	-	-	-	25
110	<i>Glechoma hederata</i>	HB	MeOH (TS)	+	+	-	168
111	<i>Hippophae rhamnoides</i>	FR	DCM	-	-	-	357
112	<i>Hippophae rhamnoides</i>	FR	MeOH	-	-	-	358
113	<i>Hippophae rhamnoides</i>	FR	MeOH (TS)	-	-	-	359
114	<i>Hypericum maculata</i>	HB	DCM	-	+	+	360
115	<i>Hypericum maculata</i>	HB	DCM (CS)	+	-	-	361
116	<i>Hypericum maculata</i>	HB	MeOH	-	-	-	362
117	<i>Hypericum maculata</i>	HB	MeOH (TS)	+	+	-	363
118	<i>Linum usitatissimum</i>	SE	DCM	-	-	-	364
119	<i>Linum usitatissimum</i>	SE	MeOH	-	-	-	365
120	<i>Linum usitatissimum</i>	SE	MeOH (TS)	-	-	-	366
121	<i>Lycopodium</i> sp.	HB	DCM	-	-	+	26
122	<i>Lycopodium</i> sp.	HB	MeOH	-	-	-	27
123	<i>Lycopodium</i> sp.	HB	MeOH (TS)	+	+	-	169
124	<i>Majorana hortensis</i>	HB	DCM	-	-	-	367
125	<i>Majorana hortensis</i>	HB	DCM (CS)	-	-	+	368
126	<i>Majorana hortensis</i>	HB	MeOH	-	-	-	369
127	<i>Majorana hortensis</i>	HB	MeOH (TS)	+	+	-	370
128	<i>Malva neglecta</i>	HB	DCM	-	-	-	410
129	<i>Malva neglecta</i>	HB	DCM (CS)	+	+	-	411
130	<i>Malva neglecta</i>	HB	MeOH	-	-	-	412
131	<i>Malva neglecta</i>	HB	MeOH (TS)	-	-	+	413
132	<i>Malva</i> sp.	FO	DCM	-	-	+	28
133	<i>Malva</i> sp.	FO	DCM (CS)	+	+	-	29
134	<i>Malva</i> sp.	FO	MeOH	-	-	-	30
135	<i>Malva</i> sp.	FO	MeOH (TS)	-	-	+	170
136	<i>Melampyrum</i> sp.	HB	DCM	-	-	-	276
137	<i>Melampyrum</i> sp.	HB	DCM	-	-	-	277
138	<i>Melampyrum</i> sp.	HB	MeOH	-	-	-	278
139	<i>Melampyrum</i> sp.	HB	MeOH (TS)	-	-	+	279
140	<i>Melissa officinalis</i>	FO	DCM	-	-	+	199
141	<i>Melissa officinalis</i>	FO	DCM (CS)	+	+	+	200
142	<i>Melissa officinalis</i>	FO	MeOH	-	-	-	201
143	<i>Melissa officinalis</i>	FO	MeOH (TS)	-	-	+	202

144	<i>Origanum vulgare</i>	HB	DCM	-	-	-	371
145	<i>Origanum vulgare</i>	HB	DCM (CS)	-	-	-	372
146	<i>Origanum vulgare</i>	HB	MeOH	-	-	-	373
147	<i>Origanum vulgare</i>	HB	MeOH (TS)	+	-	-	374
148	<i>Petasites hybridus</i>	FO	DCM	-	-	-	420
149	<i>Petasites hybridus</i>	FO	DCM (CS)	-	-	-	421
150	<i>Petasites hybridus</i>	FO	MeOH	-	-	-	422
151	<i>Petasites hybridus</i>	FO	MeOH (TS)	-	-	-	423
152	<i>Peucedanum ostruthium</i>	FO	DCM	-	-	-	424
153	<i>Peucedanum ostruthium</i>	FO	DCM (CS)	-	-	-	425
154	<i>Peucedanum ostruthium</i>	FO	MeOH	-	-	-	426
155	<i>Peucedanum ostruthium</i>	FO	MeOH (TS)	+	+	+	427
156	<i>Peucedanum ostruthium</i>	RD	DCM	-	-	+	31
157	<i>Peucedanum ostruthium</i>	RD	MeOH	-	-	-	32
158	<i>Peucedanum ostruthium</i>	RD	MeOH (TS)	+	+	+	171
159	<i>Picea abies</i>	HB	DCM	-	-	+	280
160	<i>Picea abies</i>	HB	DCM (CS)	-	-	-	281
161	<i>Picea abies</i>	HB	MeOH	-	-	-	282
162	<i>Picea abies</i>	HB	MeOH (TS)	-	-	-	283
163	<i>Pimpinella major</i>	RD	DCM	-	-	-	428
164	<i>Pimpinella major</i>	RD	MeOH	-	-	-	429
165	<i>Pimpinella major</i>	RD	MeOH (TS)	-	-	-	430
166	<i>Plantago lanceolata</i>	FO	DCM	-	-	+	33
167	<i>Plantago lanceolata</i>	FO	DCM (CS)	-	-	+	34
168	<i>Plantago lanceolata</i>	FO	MeOH	-	-	-	35
169	<i>Plantago lanceolata</i>	FO	MeOH (TS)	+	+	+	172
170	<i>Potentilla anserina</i>	HB	DCM	-	-	+	36
171	<i>Potentilla anserina</i>	HB	DCM (CS)	+	+	-	37
172	<i>Potentilla anserina</i>	HB	MeOH	-	-	-	38
173	<i>Potentilla anserina</i>	HB	MeOH (TS)	-	-	-	173
174	<i>Prunella vulgaris</i>	HB	DCM	-	-	-	284
175	<i>Prunella vulgaris</i>	HB	DCM (CS)	+	+	+	285
176	<i>Prunella vulgaris</i>	HB	MeOH	-	-	-	286
177	<i>Prunella vulgaris</i>	HB	MeOH (TS)	-	-	-	287
178	<i>Ribes</i> sp.	FR	DCM	+	+	-	431
179	<i>Ribes</i> sp.	FR	MeOH	-	-	-	432
180	<i>Ribes</i> sp.	FR	MeOH (TS)	+	+	-	433
181	<i>Rosa canina</i>	FR	DCM	-	-	-	39
182	<i>Rosa canina</i>	FR	MeOH	-	-	-	40
183	<i>Rosa canina</i>	FR	MeOH (TS)	+	+	-	174
184	<i>Rumex alpinus</i>	FO	DCM	-	-	-	434
185	<i>Rumex alpinus</i>	FO	DCM (CS)	-	-	-	435
186	<i>Rumex alpinus</i>	FO	MeOH	-	-	-	436
187	<i>Rumex alpinus</i>	FO	MeOH (TS)	-	-	-	437
188	<i>Rumex alpinus</i>	RD	DCM	-	-	-	438
189	<i>Rumex alpinus</i>	RD	MeOH	-	-	-	439
190	<i>Rumex alpinus</i>	RD	MeOH (TS)	-	-	-	440
191	<i>Salvia officinalis</i>	FO	DCM	-	-	+	375
192	<i>Salvia officinalis</i>	FO	DCM (CS)	-	-	+	376
193	<i>Salvia officinalis</i>	FO	MeOH	-	-	-	377

194	<i>Salvia officinalis</i>	FO	MeOH (TS)	-	-	+	378
195	<i>Sambucus ebulus</i>	FR	DCM	-	-	-	441
196	<i>Sambucus ebulus</i>	FR	MeOH	-	-	-	442
197	<i>Sambucus ebulus</i>	FR	MeOH (TS)	-	-	-	443
198	<i>Sambucus nigra</i>	FL	DCM	-	-	-	379
199	<i>Sambucus nigra</i>	FL	MeOH	-	-	-	380
200	<i>Sambucus nigra</i>	FL	MeOH (TS)	+	+	-	381
201	<i>Sambucus nigra</i>	FR	DCM	-	-	-	41
202	<i>Sambucus nigra</i>	FR	MeOH	-	-	-	42
203	<i>Sambucus nigra</i>	FR	MeOH (TS)	+	+	+	175
204	<i>Sanicula europea</i>	RD	DCM	-	-	-	288
205	<i>Sanicula europea</i>	RD	MeOH	-	-	-	289
206	<i>Sanicula europea</i>	RD	MeOH (TS)	-	-	-	290
207	<i>Sorbus aucuparia</i>	FR	DCM	-	-	-	43
208	<i>Sorbus aucuparia</i>	FR	MeOH	-	-	-	44
209	<i>Sorbus aucuparia</i>	FR	MeOH (TS)	+	+	-	176
210	<i>Symphytum officinale</i>	CA	DCM	-	-	-	295
211	<i>Symphytum officinale</i>	CA	DCM	-	-	-	296
212	<i>Symphytum officinale</i>	CA	MeOH	-	-	-	297
213	<i>Symphytum officinale</i>	CA	MeOH (TS)	+	+	-	298
214	<i>Symphytum officinale</i>	FO	DCM	-	-	-	291
215	<i>Symphytum officinale</i>	FO	DCM (CS)	-	-	-	292
216	<i>Symphytum officinale</i>	FO	MeOH	-	-	-	293
217	<i>Symphytum officinale</i>	FO	MeOH (TS)	-	-	-	294
218	<i>Symphytum officinale</i>	RD	DCM	+	+	-	45
219	<i>Symphytum officinale</i>	RD	MeOH	-	-	-	46
220	<i>Symphytum officinale</i>	RD	MeOH (TS)	-	-	-	177
221	<i>Tilia</i> sp.	FL	DCM	+	+	-	47
222	<i>Tilia</i> sp.	FL	MeOH	-	-	-	48
223	<i>Tilia</i> sp.	FL	MeOH (TS)	-	-	+	178
224	<i>Tussilago farfara</i>	FO	DCM	-	-	+	382
225	<i>Tussilago farfara</i>	FO	DCM (CS)	+	+	+	383
226	<i>Tussilago farfara</i>	FO	MeOH	-	-	-	384
227	<i>Tussilago farfara</i>	FO	MeOH (TS)	-	-	-	385
228	<i>Urtica dioica</i>	FO	DCM	-	-	-	386
229	<i>Urtica dioica</i>	FO	DCM (CS)	+	+	-	387
230	<i>Urtica dioica</i>	FO	MeOH	-	-	-	388
231	<i>Urtica dioica</i>	FO	MeOH (TS)	-	-	-	389
232	<i>Vaccinium myrtillus</i>	FR	DCM	-	-	-	390
233	<i>Vaccinium myrtillus</i>	FR	MeOH	-	-	-	391
234	<i>Vaccinium myrtillus</i>	FR	MeOH (TS)	+	+	-	392
235	<i>Vaccinum vitis</i>	FR	DCM	-	-	-	444
236	<i>Vaccinum vitis</i>	FR	MeOH	-	-	-	445
237	<i>Vaccinum vitis</i>	FR	MeOH (TS)	+	+	-	446
238	<i>Verbascum</i> sp.	FL	DCM	+	+	-	393
239	<i>Verbascum</i> sp.	FL	MeOH	-	-	-	394
240	<i>Verbascum</i> sp.	FL	MeOH (TS)	-	-	-	395
241	<i>Verbena officinalis</i>	HB	DCM	-	-	+	49
242	<i>Verbena officinalis</i>	HB	DCM (CS)	-	-	-	50
243	<i>Verbena officinalis</i>	HB	MeOH	-	-	-	51

244	<i>Verbena officinalis</i>	HB	MeOH (TS)	-	-	+	179
245	<i>Veronica chamedrys</i>	HB	DCM	-	-	-	299
246	<i>Veronica chamedrys</i>	HB	DCM (CS)	+	+	-	300
247	<i>Veronica chamedrys</i>	HB	MeOH	-	-	-	301
248	<i>Veronica chamedrys</i>	HB	MeOH (TS)	-	-	-	302
249	<i>Veronica officinalis</i>	HB	DCM	-	-	-	303
250	<i>Veronica officinalis</i>	HB	DCM (CS)	+	+	-	304
251	<i>Veronica officinalis</i>	HB	MeOH	-	-	-	305
252	<i>Veronica officinalis</i>	HB	MeOH (TS)	-	-	-	306
253	<i>Veronica sp.</i>	HB	DCM	-	-	+	52
254	<i>Veronica sp.</i>	HB	DCM (CS)	+	+	-	53
255	<i>Veronica sp.</i>	HB	MeOH	-	-	-	54
256	<i>Veronica sp.</i>	HB	MeOH (TS)	-	-	-	188

**Testing of TCM plant extracts for PPAR α activation and NF- κ B inhibition
(Prof. Brigitte Kopp)**

	Plant species	Part	Solvent	PPAR α	PPAR γ	NF κ B	Code
1	<i>Albizia julibrissin</i>	BA	PE	-	-	-	203
2	<i>Albizia julibrissin</i>	BA	EtOAc	+	+	-	204
3	<i>Albizia julibrissin</i>	BA	MeOH	-	-	+	205
4	<i>Albizia julibrissin</i>	BA	H ₂ O	-	-	-	206
5	<i>Albizia julibrissin</i>	FL	PE	-	-	-	207
6	<i>Albizia julibrissin</i>	FL	EtOAc	+	+	+	208
7	<i>Albizia julibrissin</i>	FL	MeOH	-	-	-	209
8	<i>Albizia julibrissin</i>	FL	H ₂ O	-	-	-	210
9	<i>Arisaema sp.</i>	RH	PE	+	+	+	211
10	<i>Arisaema sp.</i>	RH	EtOAc	-	-	-	212
11	<i>Arisaema sp.</i>	RH	MeOH	-	-	-	213
12	<i>Arisaema sp.</i>	RH	H ₂ O	-	-	-	214
13	<i>Arnebia euchroma</i>	RH	PE	-	-	-	215
14	<i>Arnebia euchroma</i>	RH	EtOAc	-	-	-	216
15	<i>Arnebia euchroma</i>	RH	MeOH	-	-	-	217
16	<i>Arnebia euchroma</i>	RH	H ₂ O	-	-	-	218
17	<i>Atractylodes macrocephala</i>	RH	PE	-	-	-	219
18	<i>Atractylodes macrocephala</i>	RH	EtOAc	-	-	-	220
19	<i>Atractylodes macrocephala</i>	RH	MeOH	-	-	-	221
20	<i>Atractylodes macrocephala</i>	RH	H ₂ O	-	-	-	222
21	<i>Cnidium monnieri</i>	FR	PE	-	-	-	223
22	<i>Cnidium monnieri</i>	FR	EtOAc	+	+	+	224
23	<i>Cnidium monnieri</i>	FR	MeOH	-	-	-	225
24	<i>Cnidium monnieri</i>	FR	H ₂ O	-	-	-	226
25	<i>Dimocarpus longan</i>	AR	PE	-	-	-	227
26	<i>Dimocarpus longan</i>	AR	EtOAc	-	-	-	228
27	<i>Dimocarpus longan</i>	AR	MeOH	-	-	-	229
28	<i>Dimocarpus longan</i>	AR	H ₂ O	-	-	-	230
29	<i>Forsitia suspensa</i>	FR	PE	-	-	-	231
30	<i>Forsitia suspensa</i>	FR	EtOAc	-	-	+	232
31	<i>Forsitia suspensa</i>	FR	MeOH	-	-	-	233
32	<i>Forsitia suspensa</i>	FR	H ₂ O	-	-	-	234
33	<i>Juncus effuses</i>	MD(CA)	EtOAc	-	-	+	235

34	<i>Juncus effuses</i>	MD(CA)	MeOH	-	-	-	236
35	<i>Juncus effuses</i>	MD(CA)	H ₂ O	-	-	-	237
36	<i>Lilium brawonii</i>	BU	EtOAc	+	+	-	238
37	<i>Lilium brawonii</i>	BU	MeOH	-	-	-	239
38	<i>Lilium brawonii</i>	BU	H ₂ O	-	-	-	240
39	<i>Lophatherum gracile</i>	HB	PE	+	-	-	241
40	<i>Lophatherum gracile</i>	HB	EtOAc	+	-	-	242
41	<i>Lophatherum gracile</i>	HB	MeOH	-	-	-	243
42	<i>Lophatherum gracile</i>	HB	H ₂ O	-	-	-	244
43	<i>Nelumbo lucifera</i>	PL	PE	-	-	-	245
44	<i>Nelumbo lucifera</i>	PL	EtOAc	-	-	-	246
45	<i>Nelumbo lucifera</i>	PL	MeOH	-	-	-	247
46	<i>Nelumbo lucifera</i>	PL	H ₂ O	-	-	-	248
47	<i>Polygonum multiflorum</i>	CA	PE	-	-	-	249
48	<i>Polygonum multiflorum</i>	CA	EtOAc	-	-	-	250
49	<i>Polygonum multiflorum</i>	CA	MeOH	-	-	-	251
50	<i>Polygonum multiflorum</i>	CA	H ₂ O	-	-	-	252
51	<i>Tribulus terrestris</i>	FR	PE	-	-	-	253
52	<i>Tribulus terrestris</i>	FR	EtOAc	+	+	-	254
53	<i>Tribulus terrestris</i>	FR	MeOH	-	-	-	255
54	<i>Tribulus terrestris</i>	FR	H ₂ O	-	-	-	256

**Testing of ferns extracts for PPAR γ activation and NF- κ B inhibition
(Prof. Gottfried Reznicek)**

	Plant species	Part	Solvent	PPAR α	PPAR γ	NF κ B	Code
1	<i>Athyrium filix</i>	FO	PE	-	-	-	480
2	<i>Athyrium filix</i>	FO	MeOH	-	-	-	485
3	<i>Athyrium filix</i>	FO	EtOAc	-	-	-	490
4	<i>Athyrium filix</i>	FO	DCM	-	-	-	495
5	<i>Athyrium filix</i>	FO	H ₂ O	-	-	-	500
6	<i>Athyrium filix</i>	FO	EtOH(30%)				505
7	<i>Dryopteris dilatata</i>	FO	PE	-	-	-	479
8	<i>Dryopteris dilatata</i>	FO	MeOH	-	-	-	484
9	<i>Dryopteris dilatata</i>	FO	EtOAc	-	-	-	489
10	<i>Dryopteris dilatata</i>	FO	DCM	-	-	-	494
11	<i>Dryopteris dilatata</i>	FO	H ₂ O	-	-	-	499
12	<i>Dryopteris dilatata</i>	FO	EtOH(30%)	-	-	-	504
13	<i>Dryopteris filix</i>	FO	PE	-	-	-	477
14	<i>Dryopteris filix</i>	FO	MeOH	-	-	-	482
15	<i>Dryopteris filix</i>	FO	EtOAc	+	+	+	487
16	<i>Dryopteris filix</i>	FO	DCM	+	+	+	492
17	<i>Dryopteris filix</i>	FO	H ₂ O	-	-	-	497
18	<i>Dryopteris filix</i>	FO	EtOH(30%)	-	-	-	502
19	<i>Matteuccia struthiopteris</i>	FO	PE	-	-	-	481
20	<i>Matteuccia struthiopteris</i>	FO	MeOH	-	-	-	486
21	<i>Matteuccia struthiopteris</i>	FO	EtOAc	-	-	-	491
22	<i>Matteuccia struthiopteris</i>	FO	DCM	-	-	-	496
23	<i>Matteuccia struthiopteris</i>	FO	H ₂ O	-	-	-	501
24	<i>Matteuccia struthiopteris</i>	FO	EtOH(30%)	-	-	-	506

Testing of coffee extracts for PPARγ activation and NF-κB inhibition (Prof. Gottfried Reznicek)							
	Plant species	Part	Solvent	PPARα	PPARγ	NFκB	Code
1	<i>Coffea arabica</i> (Ethiopia, Green)	SE	PE	-	-	n.t.	450
2	<i>Coffea arabica</i> (Ethiopia, Green)	SE	MeOH	-	-	n.t.	456
3	<i>Coffea arabica</i> (Ethiopia, Green)	SE	EtOAc	-	-	n.t.	462
4	<i>Coffea arabica</i> (Ethiopia, Green)	SE	DCM	-	-	n.t.	468
5	<i>Coffea arabica</i> (Ethiopia, Green)	SE	H ₂ O	-	-	n.t.	474
6	<i>Coffea arabica</i> (Ethiopia, Roasted)	SE	PE	-	-	n.t.	448
7	<i>Coffea arabica</i> (Ethiopia, Roasted)	SE	MeOH	-	-	n.t.	454
8	<i>Coffea arabica</i> (Ethiopia, Roasted)	SE	EtOAc	-	-	n.t.	460
9	<i>Coffea arabica</i> (Ethiopia, Roasted)	SE	DCM	-	-	n.t.	466
10	<i>Coffea arabica</i> (Ethiopia, Roasted)	SE	H ₂ O	-	-	n.t.	472
11	<i>Coffea arabica</i> (Mexico, Green)	SE	PE	-	-	n.t.	449
12	<i>Coffea arabica</i> (Mexico, Green)	SE	MeOH	-	-	n.t.	455
13	<i>Coffea arabica</i> (Mexico, Green)	SE	EtOAc	-	-	n.t.	461
14	<i>Coffea arabica</i> (Mexico, Green)	SE	DCM	-	-	n.t.	467
15	<i>Coffea arabica</i> (Mexico, Green)	SE	H ₂ O	-	-	n.t.	473
16	<i>Coffea arabica</i> (Mexico, Roasted)	SE	PE	-	-	n.t.	447
17	<i>Coffea arabica</i> (Mexico, Roasted)	SE	MeOH	-	-	n.t.	453
18	<i>Coffea arabica</i> (Mexico, Roasted)	SE	EtOAc	-	-	n.t.	459
19	<i>Coffea arabica</i> (Mexico, Roasted)	SE	DCM	-	-	n.t.	465
20	<i>Coffea arabica</i> (Mexico, Roasted)	SE	H ₂ O	-	-	n.t.	471
21	<i>Coffea robusta</i> (Vietnam, Green)	SE	PE	+	-	n.t.	452
22	<i>Coffea robusta</i> (Vietnam, Green)	SE	MeOH	-	-	n.t.	458
23	<i>Coffea robusta</i> (Vietnam, Green)	SE	EtOAc	+	-	n.t.	464
24	<i>Coffea robusta</i> (Vietnam, Green)	SE	DCM	+	-	n.t.	470
25	<i>Coffea robusta</i> (Vietnam, Green)	SE	H ₂ O	-	-	n.t.	476
26	<i>Coffea robusta</i> (Vietnam, Roasted)	SE	PE	-	-	n.t.	451
27	<i>Coffea robusta</i> (Vietnam, Roasted)	SE	MeOH	-	-	n.t.	457

28	<i>Coffea robusta</i> (Vietnam, Roasted)	SE	EtOAc	-	-	n.t.	463
29	<i>Coffea robusta</i> (Vietnam, Roasted)	SE	DCM	-	-	n.t.	469
30	<i>Coffea robusta</i> (Vietnam, Roasted)	SE	H ₂ O	-	-	n.t.	475
Plants extracts containing compounds predicted as PPARγ agonists or NF-κB inhibitors (Prof. Judith Rollinger and Prof. Hermann Stuppner)							
	Plant species	Part	Solvent	PPARα	PPARγ	NFκB	Code
1	<i>Aruncus dioicus</i>	FL	MeOH	-	-	-	167
2	<i>Doronicum austriacum</i>	RD	DCM	+	+	-	165
3	<i>Doronicum austriacum</i>	RD	MeOH	-	-	-	166
4	<i>Ferula assa-fetida</i>	RS	DCM	-	-	-	307
5	<i>Gnoderma lucidum</i>	FR	EtOH	-	-	-	308
6	<i>Krameria lappacea</i>	RD	DCM	-	-	+	158
7	<i>Krameria lappacea</i>	RD	Me ₂ CO	-	-	+	159
8	<i>Magnolia officinalis</i>	CO	DCM	+	+	-	157
9	<i>Morus alba</i>	RD	MeOH	-	-	-	309
10	<i>Himatanthus sucuuba</i>	MeOH	MeOH	n.t.	n.t.	+	642
11	<i>Sideritis hyssopifolia</i>	HB	MeOH	-	-	n.t.	722
12	<i>Silybum marianum</i>	FR	MeOH	-	-	-	164
Testing of plant extracts for PPARγ activation and NF-κB inhibition (Prof. Rudolf Bauer)							
	Plant species	Part	Solvent	PPARα	PPARγ	NFκB	Code
1	<i>Achyranthis bidentata</i>	RX	DCM	-	-	-	62
2	<i>Achyranthis bidentata</i>	RX	MeOH	-	-	-	105
3	<i>Aconitum carmichaelii</i>	RX	DCM	-	-	-	82
4	<i>Aconitum carmichaelii</i>	RX	MeOH	-	-	-	125
5	<i>Acorus tatarinowii</i>	RH	DCM	-	-	-	66
6	<i>Acorus tatarinowii</i>	RH	MeOH	-	-	-	109
7	<i>Akebia</i> sp.	CL	DCM	-	-	-	83
8	<i>Akebia</i> sp.	CL	MeOH	-	-	-	126
9	<i>Allium macrostemon</i>	BL	DCM	-	-	-	88
10	<i>Allium macrostemon</i>	BL	MeOH	-	-	-	131
11	<i>Andrographis paniculata</i>	HB	DCM	-	-	-	97
12	<i>Andrographis paniculata</i>	HB	MeOH	+	+	+	140
13	<i>Angelica sinensis</i>	RX	DCM	-	-	-	61
14	<i>Angelica sinensis</i>	RX	MeOH	-	-	-	104
15	<i>Aquilaria sinensis</i>	RE	DCM	-	-	-	653
16	<i>Aquilaria sinensis</i>	RE	MeOH	-	-	-	677
17	<i>Aristolochia debilis</i>	FR	DCM	-	-	+	650
18	<i>Aristolochia debilis</i>	FR	MeOH	-	-	-	674
19	<i>Artemisia scoparia</i>	HB	DCM	-	-	-	95
20	<i>Artemisia scoparia</i>	HB	MeOH	-	-	-	138
21	<i>Asari</i> sp.	RX+RH	DCM	-	-	-	86
22	<i>Asari</i> sp.	RX+RH	MeOH	-	-	-	129
23	<i>Astralagus membranaceus</i>	RX	DCM	+	+	+	77
24	<i>Astralagus membranaceus</i>	RX	MeOH	-	-	-	120
25	<i>Belamcanda chinensis</i>	RH	DCM	+	+	-	656

26	<i>Belamcanda chinensis</i>	RH	MeOH	-	-	-	680
27	<i>Benincasa</i> sp.	SE	DCM	-	-	-	658
28	<i>Benincasa</i> sp.	SE	MeOH	-	-	-	682
29	<i>Broussonetia papyrifera</i>	FR	DCM	-	-	-	654
30	<i>Broussonetia papyrifera</i>	FR	MeOH	-	-	-	678
31	<i>Buddelja officinalis</i>	FL	DCM	-	-	-	96
32	<i>Buddelja officinalis</i>	FL	MeOH	-	-	-	139
33	<i>Bupleurum</i> sp.	RX	DCM	+	-	+	60
34	<i>Bupleurum</i> sp.	RX	MeOH	-	-	-	103
35	<i>Callicarpa bodinieri</i>	HB	DCM	-	-	+	652
36	<i>Callicarpa bodinieri</i>	HB	MeOH	-	-	-	676
37	<i>Carthamus tinctorius</i>	FL	DCM	-	-	-	72
38	<i>Carthamus tinctorius</i>	FL	MeOH	-	-	-	115
39	<i>Choerospondias axillaris</i>	FR	DCM	-	-	-	647
40	<i>Choerospondias axillaris</i>	FR	MeOH	-	-	-	671
41	<i>Chrysanthemum indicum</i>	FL	DCM	-	-	+	660
42	<i>Chrysanthemum indicum</i>	FL	MeOH	-	-	-	684
43	<i>Cimicifuga</i> sp.	RH	DCM	-	-	+	668
44	<i>Cimicifuga</i> sp.	RH	MeOH	-	-	-	692
45	<i>Codonopsis</i> sp.	RX	DCM	-	-	-	73
46	<i>Codonopsis</i> sp.	RX	MeOH	-	-	-	116
47	<i>Corydalis yanhusuo</i>	RH	DCM	-	-	-	85
48	<i>Corydalis yanhusuo</i>	RH	MeOH	-	-	-	128
49	<i>Crataegus pinnatifida</i>	FR	DCM	-	-	-	76
50	<i>Crataegus pinnatifida</i>	FR	MeOH	-	-	-	119
51	<i>Curcuma</i> sp.	RX	DCM	-	-	-	84
52	<i>Curcuma</i> sp.	RX	MeOH	-	-	-	127
53	<i>Cynanchum paniculatum</i>	RD	DCM	-	-	-	662
54	<i>Cynanchum paniculatum</i>	RD	MeOH	-	-	-	686
55	<i>Echinacea pallidia</i>	FL	Hex	-	+	n.t.	1426
56	<i>Evodia rutaecarpa</i>	FR	DCM	-	-	+	661
57	<i>Evodia rutaecarpa</i>	FR	MeOH	-	-	-	685
58	<i>Forsythia suspensa</i>	FR	DCM	-	-	-	71
59	<i>Forsythia suspensa</i>	FR	MeOH	-	-	-	114
60	<i>Gardenia jasminoides</i>	FR	DCM	-	-	-	65
61	<i>Gardenia jasminoides</i>	FR	MeOH	-	-	-	108
62	<i>Gastrodia elata</i>	RH	DCM	-	-	-	68
63	<i>Gastrodia elata</i>	RH	MeOH	-	-	-	111
64	<i>Gentiana macrophylla</i>	RD	DCM	-	-	-	657
65	<i>Gentiana macrophylla</i>	RD	MeOH	-	-	-	681
66	<i>Ilex pubescens</i>	CO	DCM	-	-	-	648
67	<i>Ilex pubescens</i>	CO	MeOH	-	-	-	672
68	<i>Isatis indigotica</i>	RD	DCM	+	+	-	659
69	<i>Isatis indigotica</i>	RD	MeOH	-	-	-	683
70	<i>Leonurus japonicus</i>	FR	DCM	-	-	-	67
71	<i>Leonurus japonicus</i>	FR	MeOH	-	-	-	110
72	<i>Ligusticum chuanxiong</i>	RH	DCM	-	-	-	75
73	<i>Ligusticum chuanxiong</i>	RH	MeOH	-	-	-	118
74	<i>Lindera aggregata</i>	RD	DCM	-	-	-	663
75	<i>Lindera aggregata</i>	RD	MeOH	-	-	-	687

76	<i>Lonicera japonica</i>	CL	DCM	-	-	-	93
77	<i>Lonicera japonica</i>	CL	MeOH	-	-	-	136
78	<i>Lycium barbarum</i>	FR	DCM	-	-	-	667
79	<i>Lycium barbarum</i>	FR	MeOH	-	-	-	691
80	<i>Lysimachia christinae</i>	HB	DCM	-	-	-	655
81	<i>Lysimachia christinae</i>	HB	MeOH	-	-	-	679
82	<i>Magnolia biondii</i>	FL	DCM	-	-	-	649
83	<i>Magnolia biondii</i>	FL	MeOH	-	-	-	673
84	<i>Notopterygium incisum</i>	RX+RH	DCM	-	+	-	90
85	<i>Notopterygium incisum</i>	RX+RH	MeOH	-	-	-	133
86	<i>Ophipogonis japonicus</i>	RX	DCM	-	-	-	58
87	<i>Ophipogonis japonicus</i>	RX	MeOH	-	-	-	101
88	<i>Paeonia lactiflora</i>	RD	DCM	+	+	-	646
89	<i>Paeonia lactiflora</i>	RD	MeOH	-	-	-	670
90	<i>Paeonia rubra</i>	RX	DCM	-	-	-	80
91	<i>Paeonia rubra</i>	RX	MeOH	-	-	+	123
92	<i>Panax notoginseng</i>	RX	DCM	-	-	-	55
93	<i>Panax notoginseng</i>	RX	MeOH	-	-	-	98
94	<i>Piper kadsura</i>	CL	DCM	-	-	+	666
95	<i>Piper kadsura</i>	CL	MeOH	-	-	-	690
96	<i>Platycodon gradiflorum</i>	RX	DCM	-	-	-	59
97	<i>Platycodon gradiflorum</i>	RX	MeOH	-	-	-	102
98	<i>Polygonatum odoratum</i>	RX	DCM	-	-	-	74
99	<i>Polygonatum odoratum</i>	RX	MeOH	-	-	-	117
100	<i>Polygonum multiflorum</i>	RX	DCM	-	-	+	57
101	<i>Polygonum multiflorum</i>	RX	MeOH	-	-	-	100
102	<i>Poria cocos</i>	RX	DCM	+	-	-	56
103	<i>Poria cocos</i>	RX	MeOH	-	-	-	99
104	<i>Prunella vulgaris</i>	FL	DCM	-	-	+	651
105	<i>Prunella vulgaris</i>	FL	MeOH	-	-	-	675
106	<i>Prunus sp.</i>	SE	DCM	-	-	-	69
107	<i>Prunus sp.</i>	SE	MeOH	-	-	-	112
108	<i>Rhemania glutinosa</i>	RX	DCM	-	-	-	70
109	<i>Rhemania glutinosa</i>	RX	MeOH	-	-	-	113
110	<i>Salvia miltiorrhiza</i>	RX	DCM	-	-	-	79
111	<i>Salvia miltiorrhiza</i>	RX	MeOH	-	-	-	122
112	<i>Santalum album</i>	LG	DCM	-	-	-	63
113	<i>Santalum album</i>	LG	MeOH	-	-	-	106
114	<i>Saposhnikovia divaricata</i>	RD	DCM	-	-	-	664
115	<i>Saposhnikovia divaricata</i>	RD	MeOH	-	-	-	688
116	<i>Sargentodoxa cuneata</i>	CL	DCM	-	-	-	87
117	<i>Sargentodoxa cuneata</i>	CL	MeOH	-	-	-	130
118	<i>Schisandra chinensis</i>	FR	DCM	-	-	-	94
119	<i>Schisandra chinensis</i>	FR	MeOH	-	-	-	137
120	<i>Scutellaria baicalensis</i>	RX	DCM	-	-	+	91
121	<i>Scutellaria baicalensis</i>	RX	MeOH	-	-	-	134
122	<i>Sophora japonica</i>	FL	DCM	+	+	-	665
123	<i>Sophora japonica</i>	FL	MeOH	-	-	-	689
124	<i>Spatholobus suberrectus</i>	CL	DCM	-	-	-	64
125	<i>Spatholobus suberrectus</i>	CL	MeOH	-	-	-	107

126	<i>Stephania tetrandra</i>	RX	DCM	-	-	+	81
127	<i>Stephania tetrandra</i>	RX	MeOH	-	-	-	124
128	<i>Trichosanthis</i> sp.	RX	DCM	-	-	-	89
129	<i>Trichosanthis</i> sp.	RX	MeOH	-	-	-	132
130	<i>Typha</i> sp.	PO	DCM	+	+	-	645
131	<i>Typha</i> sp.	PO	MeOH	-	-	-	669
132	<i>Zingiberis officinalis</i>	RX	DCM	-	+	+	78
133	<i>Zingiberis officinalis</i>	RX	MeOH	-	-	-	121
134	<i>Ziziphus spinosa</i>	SE	DCM	-	-	-	92
135	<i>Ziziphus spinosa</i>	SE	MeOH	-	-	-	135

NOTE

+	: active*	FR	: Fructus
-	: inactive	HB	: Herba
AR	: Arillus	LI	: Lignum
BA	: Bark	MD	: Medulla
BU	: Bulbus	PL	: Plumule
CA	: Caulis	RD	: Radix
CO	: Cortex	RH	: Rhizoma
CS	: Chlorophyll separated	RS	: Resin
FL	: Flower	SE	: Semen
MeOH	: Methanol	FO	: Folium
DCM	: Dicloromethane	PE	: Petroleum ether
Hex	: Hexane	EtOAc	: Ethyl acetate
MeOH (TS)	: Metanol (tannin separated)	Me ₂ CO	: Aceton
DCM (CS)	: Dicloromethane (chlorophyll separated)	EtOH	: Ethanol

* activity 50 % above control (DMSO treatment) at 10 µg/ml was considered active.

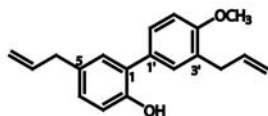
Supplementary Table 2. The activity of the magnolol derivatives towards all subtypes of human PPAR (α , β/δ , γ), as well as towards mouse PPAR α and γ , determined in luciferase reporter transactivation assay*.

DNTI Code:	Internal code:	PPAR α (maximal fold activation)	PPAR β/δ (maximal fold activation)	PPAR γ (maximal fold activation)	mPPAR α (maximal fold activation)	mPPAR γ (maximal fold activation)
Magnolol	727	n.d.	1.69	2.92	2.26	2.09
Honokiol	728	1.67	3.60	1.97	2.09	1.54
PP03-WS-1-A_1	752	n.d.	3.02	2.03	n.d.	2.09
PP03-WS-10-A_1	753	n.d.	2.15	3.21	n.d.	2.67
PP03-WS-101-A_1	754	n.d.	n.d.	3.21	n.d.	2.10
PP03-WS-102b-A_1	755	n.d.	n.d.	1.55	n.d.	n.d.
PP03-WS-103b-A_1	756	n.d.	n.d.	n.d.	n.d.	n.d.
PP03-WS-104-A_1	757	n.d.	n.d.	n.d.	n.d.	n.d.
PP03-WS-11-A_1	758	n.d.	n.d.	1.87	n.d.	1.57
PP03-WS-12-A_1	759	1.53	n.d.	1.96	n.d.	1.56
PP03-WS-15-A_1	760	n.d.	n.d.	n.d.	n.d.	n.d.
PP03-WS-16-A_1	761	n.d.	n.d.	n.d.	n.d.	n.d.
PP03-WS-19b-A_1	762	n.d.	2.46	1.83	2.11	2.34
PP03-WS-2-A_1	763	n.d.	1.89	2.16	1.94	2.45
PP03-WS-20a-A_1	764	n.d.	n.d.	n.d.	n.d.	n.d.
PP03-WS-21b-A_1	765	n.d.	n.d.	2.02	n.d.	1.58
PP03-WS-22a-A_1	766	n.d.	n.d.	1.59	1.65	1.95
PP03-WS-22b-A_1	767	n.d.	1.95	1.52	n.d.	1.53
PP03-WS-23a-A_1	768	n.d.	n.d.	n.d.	n.d.	n.d.
PP03-WS-23b-A_1	769	n.d.	n.d.	1.60	n.d.	1.61
PP03-WS-24a-A_1	770	n.d.	n.d.	n.d.	n.d.	n.d.
PP03-WS-25-A_1	771	n.d.	n.d.	1.99	n.d.	n.d.
PP03-WS-26bc-A_1	772	n.d.	n.d.	1.92	n.d.	1.74
PP03-WS-29c-A_1	773	n.d.	n.d.	n.d.	n.d.	n.d.

PP03-WS-31-A_1	774	n.d.	n.d.	1.51	n.d.	1.54
PP03-WS-32-A_1	775	n.d.	2.03	2.97	1.71	2.56
PP03-WS-33-A_1	776	n.d.	1.75	2.48	n.d.	1.67
PP03-WS-3a-A_1	777	n.d.	n.d.	2.05	1.68	1.90
PP03-WS-4-A_1	778	n.d.	n.d.	n.d.	n.d.	n.d.
PP03-WS-5-A_1	779	n.d.	n.d.	n.d.	n.d.	n.d.
PP03-WS-6-A_1	780	n.d.	n.d.	n.d.	n.d.	n.d.
PP03-WS-7a-A_1	781	1.58	3.02	2.27	2.15	2.05

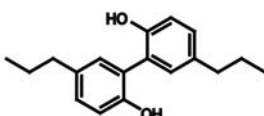
* HEK-293 cells were transiently cotransfected with a reporter plasmid containing PPRE coupled to the luciferase reporter, a respective PPAR subtype expression plasmid, and EGFP as internal control. Upon stimulation with the indicated concentrations of the respective compounds for 18 hours, luciferase activity was measured and normalized by the EGFP-derived fluorescence. The result is presented as fold induction compared to the DMSO vehicle control, and n.d. denotes not detected (up to 30 μ M). The data shown are means of three independent experiments performed in triplicate. Note: mPPAR (mouse PPAR), PPAR (human PPAR). All compounds were obtained from Prof. Judith Rollinger.

PP03-WS-1-A_1



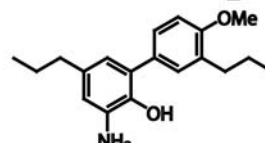
4'-Methoxy-5,3'-di-(2-propenyl)-biphenyl-2-ol

PP03-WS-10-A_1



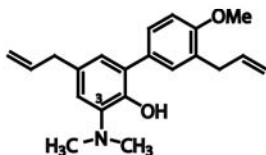
5,5'-Dipropyl-biphenyl-2,2'-diol

PP03-WS-101-A_1



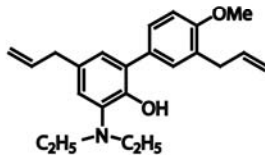
3-Amino-2'-methoxy-5,3'-dipropyl-biphenyl-2'-ol

PP03-WS-102b-A_1



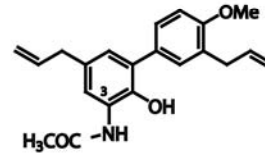
3-N,N-Dimethylamino-2'-methoxy-5,3'-di(2-propenyl)-biphenyl-2'-ol

PP03-WS-103b-A_11



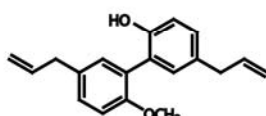
3-N,N-Diethylamino-2'-methoxy-5,3'-di(2-propenyl)-biphenyl-2'-ol

PP03-WS-104-A_1



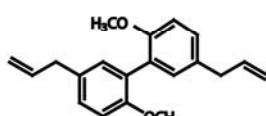
3-N-Acetylamino-2'-methoxy-5,3'-di(2-propenyl)-biphenyl-2'-ol

PP03-WS-11-A_1



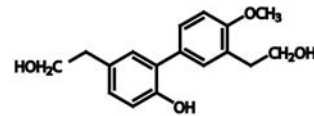
2-Methoxy-5,5'-di-(2-propenyl)-biphenyl-2-ol

PP03-WS-12-A_1



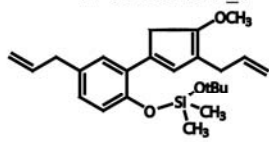
2,2'-Dimethoxy-5,5'-di-(2-propenyl)-biphenyl

PP03-WS-15-A_1



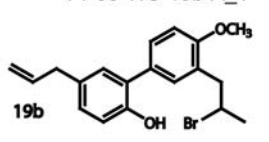
4'-Methoxy-5,3'-bis-(2-hydroxyethyl)-biphenyl-2-ol

PP03-WS-16-A_1



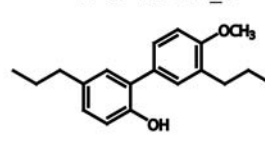
tert-Butyl-(5,3'-diallyl-4'-methoxy-biphenyl-2-yl)oxy-dimethylsilane

PP03-WS-19b-A_1



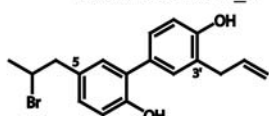
4'-Methoxy-5-(2-propenyl)-3'-(2-bromopropyl)-biphenyl-2-ol

PP03-WS-2-A_1



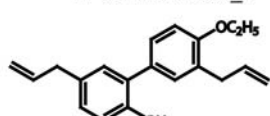
4'-Methoxy-5,3'-dipropyl-biphenyl-2-ol

PP03-WS-20a-A_1



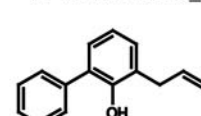
5-(2-Bromopropyl)-3'-(2-propenyl)-biphenyl-2,4'-diol

PP03-WS-21b-A_1



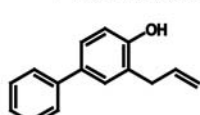
5,3'-Di-(2-propenyl)-4'-ethoxy-biphenyl-2-ol

PP03-WS-22a-A_1



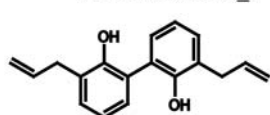
3-(2-Propenyl)-biphenyl-2-ol

PP03-WS-22b-A_1



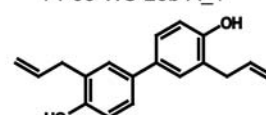
3-(2-Propenyl)-biphenyl-4-ol

PP03-WS-23a-A_1

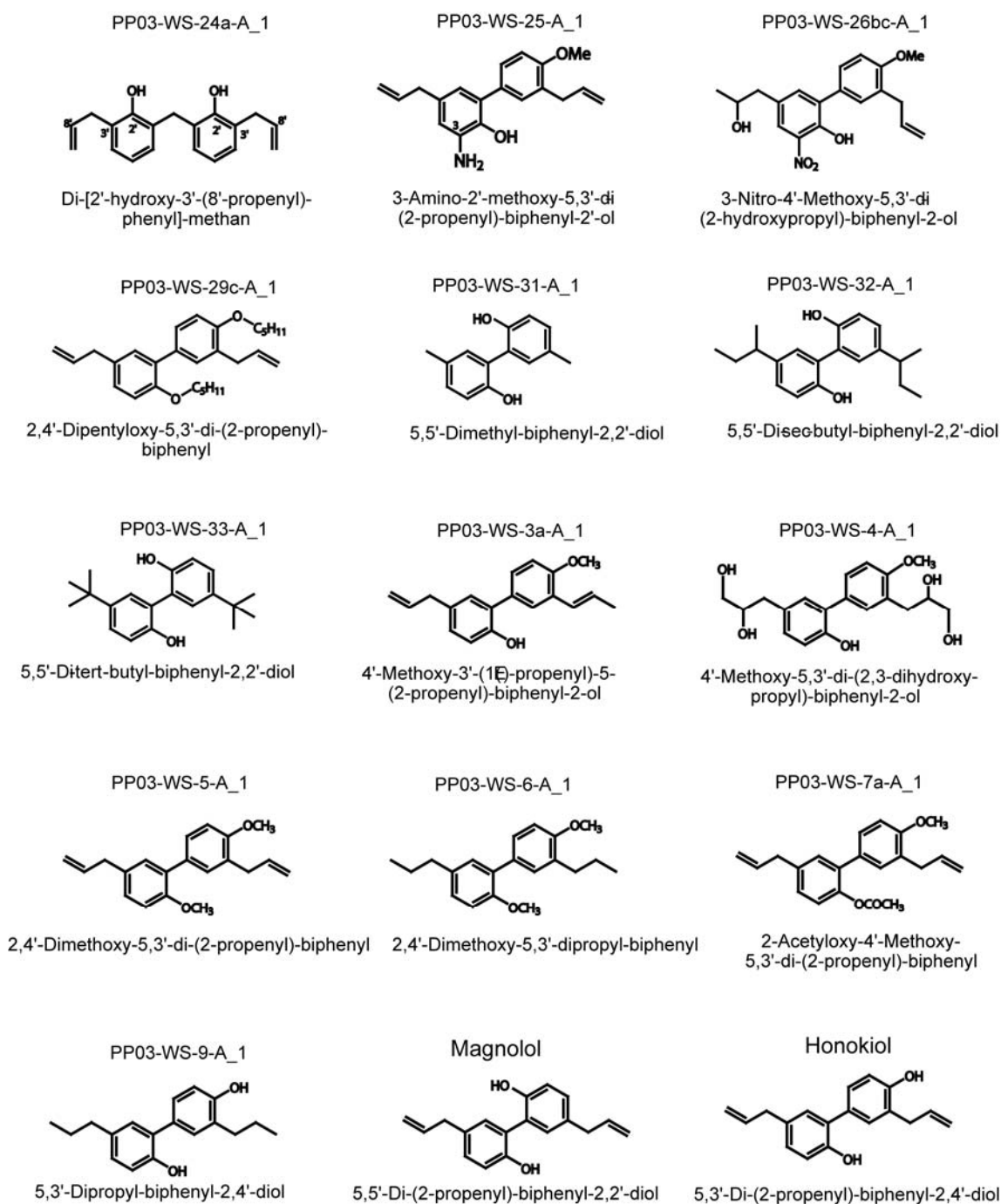


3,3'-Di-(2-propenyl)-biphenyl 2,2'-diol

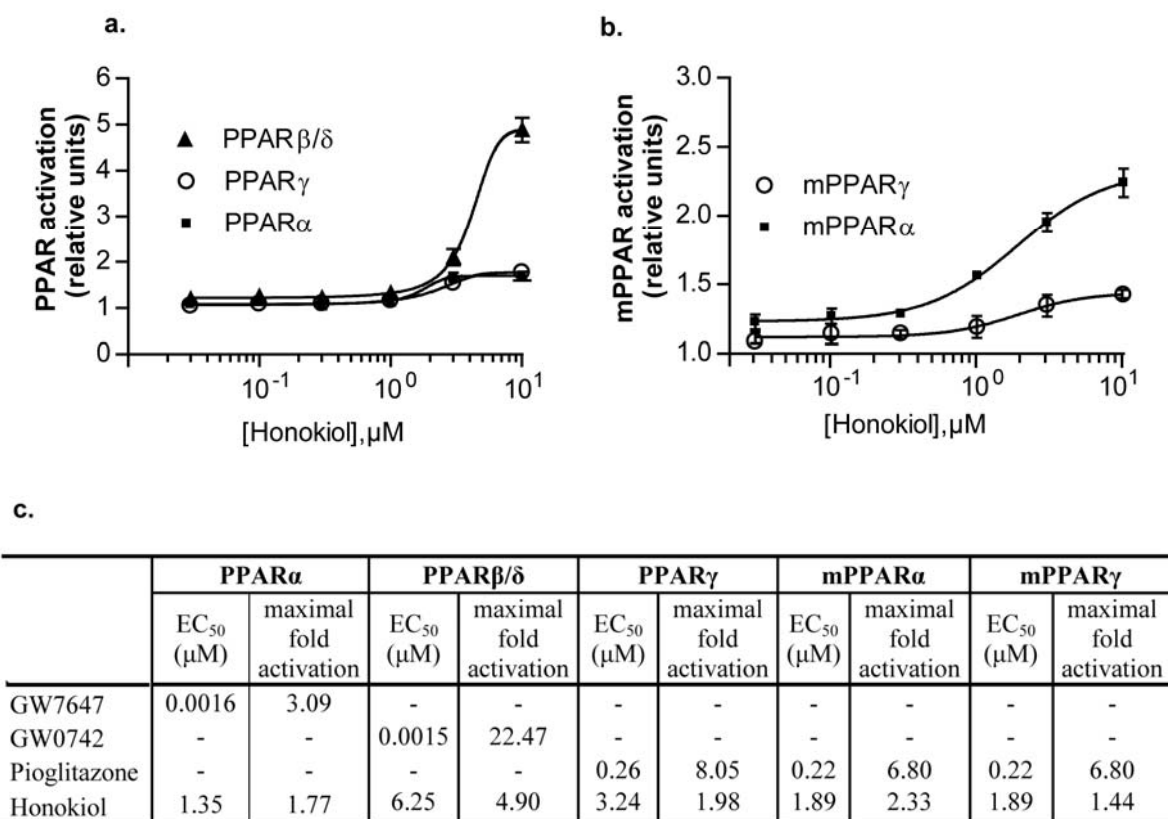
PP03-WS-23b-A_1



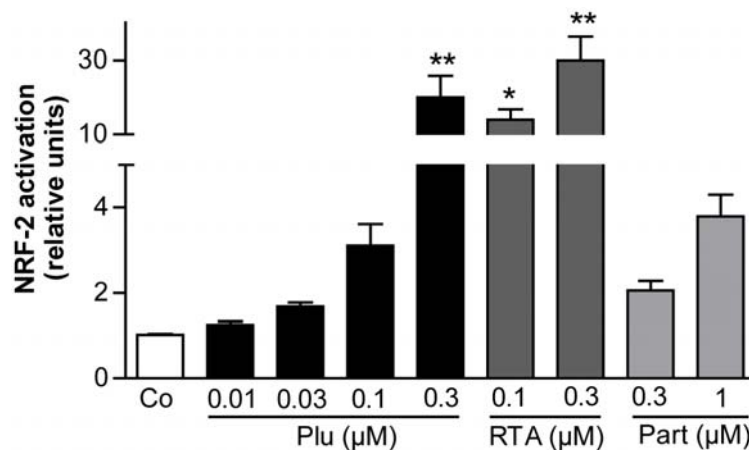
3,3'-Di-(2-propenyl)-biphenyl 4,4'-diol



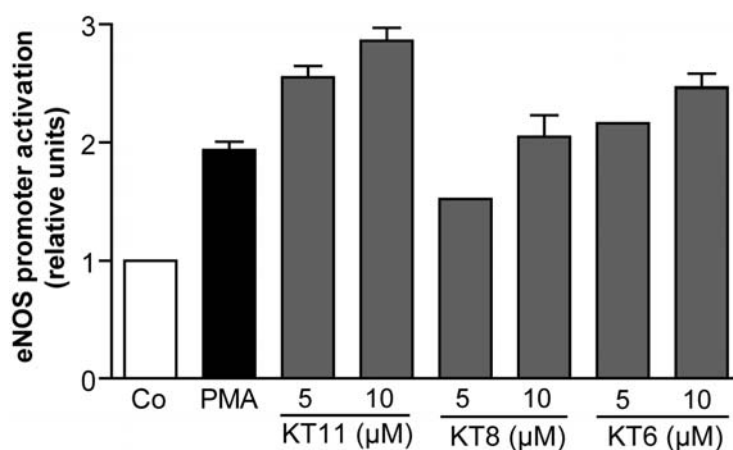
Supplementary Figure 2. The synthesis compounds derived from magnolol.



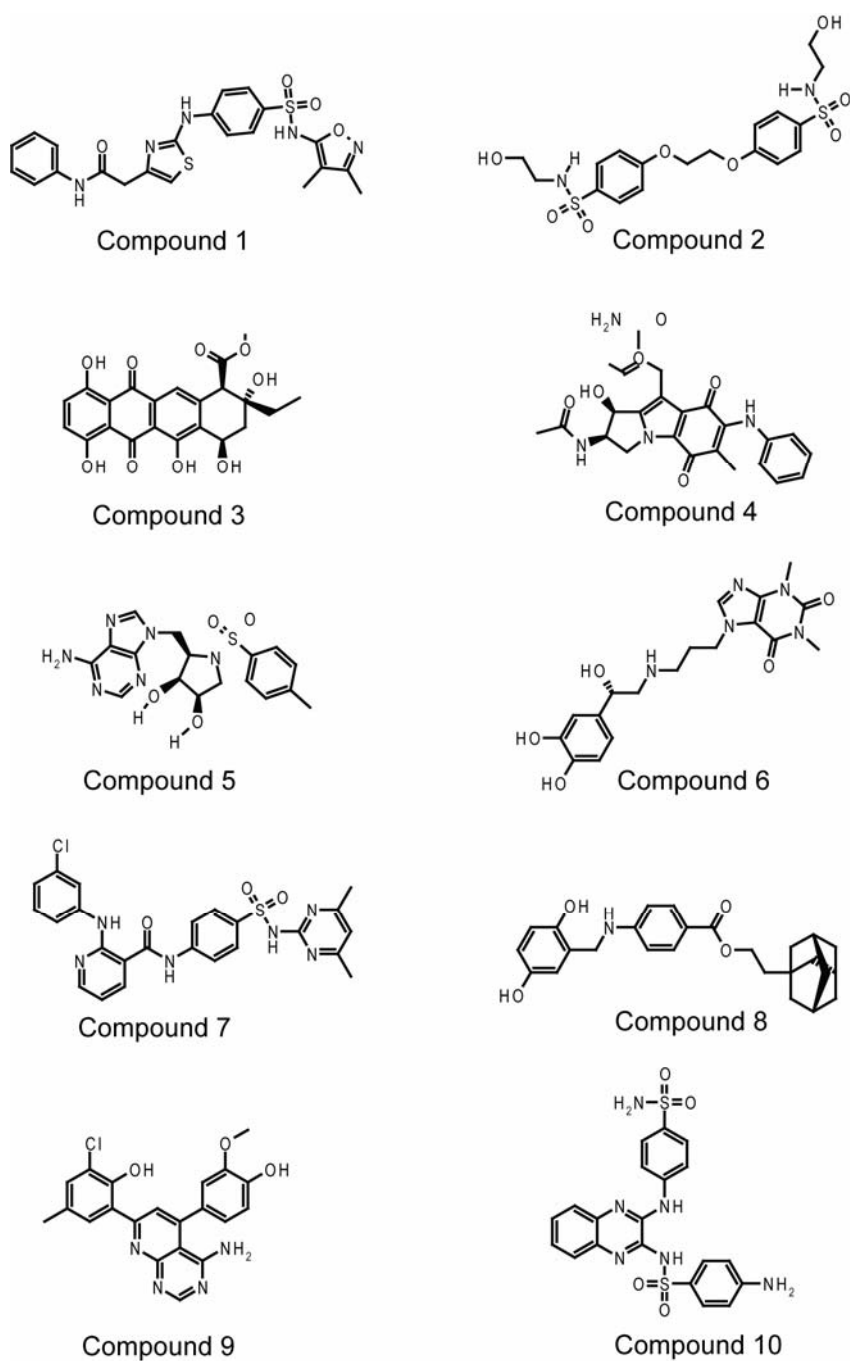
Supplementary Figure 3. The activity of honokiol towards PPARs in the luciferase reporter transactivation assay. a) and b) show the activity of honokiol towards human PPARs and mouse PPARs, respectively. c) The table showing the EC₅₀ of honokiol in the respective PPAR subunits. HEK-293 cells were transiently cotransfected with a reporter plasmid containing PPRE coupled to the luciferase reporter, the respective PPAR expression plasmids, and EGFP as internal control. Upon stimulation with the indicated concentrations of the respective compounds for 18 hours, luciferase activity was measured and normalized by the EGFP-derived fluorescence. The result is presented as fold induction compared to the DMSO control. The data shown are means \pm SEM from three independent experiments performed in quadruplet. The data were analyzed with GraphPad Prism software using settings for nonlinear regression with sigmoidal dose response and variable slope. PPAR and mPPAR denotes human and mouse PPAR, respectively.



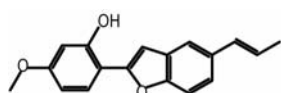
Supplementary Figure 4. The potential of plumericin to activate Nrf2 as assessed in a luciferase reporter gene assay. HEK-293 cells were transiently cotransfected with a plasmid containing an antioxidant response element (ARE) coupled to a luciferase reporter gene and EGFP expression plasmid as internal control. Upon treatment with the indicated concentrations of the respective compounds for 15 hours, luciferase activity was measured and normalized by the EGFP-derived fluorescence. The result was presented as fold induction compared to the DMSO control (Co). The data shown are means \pm SEM, of three independent experiments performed in a triplicate. The bars are means \pm SEM; * $p < 0.05$; ** $p < 0.01$ (one-way ANOVA followed by Dunnett's post-test).



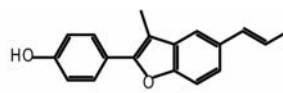
Supplementary Figure 5. The influence of the three benzofuran inhibitors of NF- κ B on eNOS promoter activity assessed in a luciferase reporter gene assay. EA.hy926 cells containing human eNOS promoter coupled to a firefly luciferase reporter gene were incubated with the indicated concentrations of the respective compounds for 18 hours. Luciferase activity was measured and normalized by the total protein content measured by the Bradford method. The result is presented as fold induction compared to the DMSO control. The data shown are means \pm SEM ($n=1-3$), performed in a triplicate.



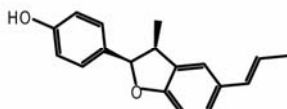
Supplementary Figure 6. Ten virtual hits selected for biological evaluation on IKK- β enzyme activity *in vitro* and NF- κ B activation induced by TNF- α in 293/NF- κ B-luc cells.



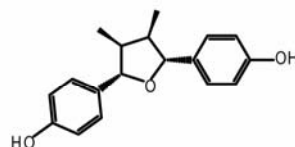
ratanhiaphenol I
CAS:79214-54-3
KT10



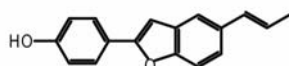
ratanhiaphenol II or
eupomatenoid 6
CAS: 41744-26-7
KT11



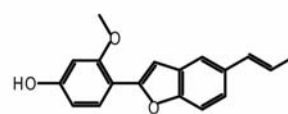
(+)-conocarpan
CAS:56319-02-9
KT7



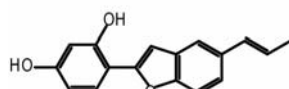
Meso-3,3'-didemethoxy-nectandrin B
CAS:130325-40-5
KT3



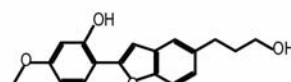
2-(4-hydroxy-phenyl)-5-(E)-
propenyl-benzofuran
CAS:109194-69-6
KT8



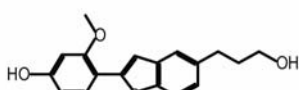
2-(2-methoxy-4-hydroxyphenyl)-5-(E)-
propenyl-benzofuran
CAS:91432-06-3
KT9



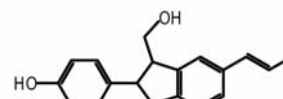
2-(2,4-dihydroxy-phenyl)-5-(E)-
propenyl-benzofuran
CAS:109194-71-0
KT6



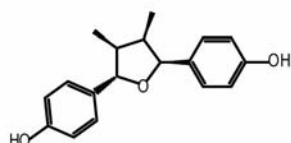
2-(2-hydroxy-4-methoxyphenyl)-5-
(3-hydroxypropyl)-benzofuran
CAS:119321-98-1
KT5



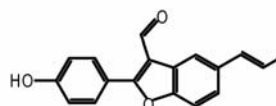
5-(3-hydroxy-propyl)-2-(2-methoxy-4-
hydroxyphenyl)-benzofuran
CAS:119321-96-9
KT1



(2S,3S)-2,3-dihydro-3-hydroxymethyl-2-
(4-hydroxyphenyl)-5-(E)-propenyl-benzofuran;
CAS:119322-04-2
KT4



(-)-larreatricin
CAS:130062-03-2
KT12



3-Formyl-2-(4-hydroxyphenyl)-5-(E)-
propenyl-benzofuran
CAS:119322-02-0
KT2

Supplementary Figure 7. The benzofurans isolated from *Krameria lappacea*

2. ABBREVIATIONS

15d-PGJ2	: 15-Deoxy-delta-12,14-prostaglandin
ABP	: Actin-binding proteins
Akt	: Protein kinase B (PKB)
ANOVA	: Analysis of variance
AP-1	: Activator protein-1
ARE	: Antioxidant responsive element
Asp	: Aspartic acid
ATP	: Adenosine triphosphate
BADGE	: Bisphenol A-diglycidylether
Blys	B lymphocyte stimulator
BMS-345541	: N-(1,8-Dimethylimidazo[1,2-a]quinoxalin-4-yl)-1,2-ethanediamine hydrochloride
BSA	: Bovine serum albumin
C3H10T1/2	Mouse embryonic fibroblasts cell line
CAS	: Chemical abstracts service
CBP	: CREB-binding protein
CD	: Cluster of differentiation
CDK	: Cyclin dependent kinase
CHM	Chinese herbal medicine
COX-2	: Cyclooxygenase 2
Cys	: Cystein
ddH ₂ O	: Double distilled water
DHMEQ	: Dehydroxymethylepoxyquinomicin
DMSO	: Dimethylsulfoxide
DTT	: Dithiothreitol
EDTA	: Ethylenediaminetetraacetic acid
ELISA	: Enzyme linked immunosorbent assay
eNOS	: Endothelial nitric oxide synthase
FDA	: Food and drug administration
FITC	: Fluorescein isothiocyanate

FOXO3	: Forkhead box class O 3 transcription factor
Glu	: Glutamic acid
GLUT	: Glucose transporter
Gly	: Glycine
GST	Glutation-S-transferase
GW0742	: 4-[2-(3-Fluoro-4-trifluoromethyl-phenyl)-4-methyl-thiazol-5-ylmethylsulfanyl]-2-methyl-phenoxy}-acetic acid
GW501516	: 2-methyl-4(((4-methyl-2-(4-trifluoromethylphenyl)-1,3-thiazol-5-yl)methyl)sulfanyl)phenoxy)acetic acid
GW6471	[(2S)-2-[[[(1Z)-1-Methyl-3-oxo-3-[4-(trifluoromethyl)phenyl]-1-propenyl]amino]-3-[4-[2-(5-methyl-2-phenyl-4-oxazolyl)ethoxy]phenyl]propyl]-carbamic acid ethyl ester
GW7647	: 2-methyl-2-[[4-[2-[[[(cyclohexylamino)carbonyl](4-cyclohexylbutyl)amino]ethyl]phenyl]thio]-propanoic acid
GW9662	: 2-chloro-5-nitro-N-phenylbenzamide
HDAC3	: Histone deacetylase 3
HEK 293	: Human embryonic kidney 293 cells
HETEs	: Hydroxyeicosatetraenoic acid
HLH	: Helix loop helix
HODE	: Hydroxyoctadecadienoic acid
HRP	: Horse radish peroxidase
HUVECtert	: human umbilical vein cell expressing telomerase reverse transcriptase
ICAM-1	: Inter-cellular adhesion molecule 1
IFN- γ	: Interferon γ
IKK	: Inhibitor κ B kinase
IKK- β inh IV	IKK- β inhibitor IV or 2-[(aminocarbonyl)amino]-5-(4-fluorophenyl)-3-thiophenecarboxamide
iNOS	: Inducible nitric oxide synthase
I κ B	: Inhibitor κ B
JNK	: C-Jun N-terminal kinase
JTT-501	: 4-[4-[2-(5-methyl-2-phenyl-4-oxazolyl)ethoxy]benzyl]-3,5-

	isoxazolidinedione)
KD	: Kinase domain
Ki	: Inhibition constant
L165041	: [4-[3-(4-Acetyl-3-hydroxy-2-propylphenoxy)propoxy]phenoxy]acetic acid
LB	: Lysogeny broth
LBD	: Ligand binding domain
LDL	: Low density lipoprotein
LOX	: Lipooxygenase
LT α / β	Leukotriene α / β
LTB4	: Leukotriene B4
LZ	: Leucine zipper
MCP-1	: Monocyte chemotactic protein-1
mRNA	: Messenger RNA
NBS	New born bovine serum
NCoR	: Nuclear-receptor corepressor
NEMO	: NF- κ B essential modulator
NF- κ B	: Nuclear factor- κ B
NIK	: NF- κ B-inducing kinase
NLS	: Nuclear localization signal
NO	: Nitric oxide
Nrf2	: NF-E2-related factor 2
oxoODE	: Oxidized octadecadienoic acid
PBS	: Phosphate buffered saline
PDGF-BB	: Platelet-derived growth factor with two B (-BB) chains
PIAS1	: Protein inhibitor of activated STAT1
PMSF	: Phenylmethylsulphonylfluoride
PPAR	: Peroxisome proliferator-activated receptor
PPRE	: PPAR response element
PVDF	: Polyvinylidene fluoride
RAW264.7	: Mouse leukaemic monocyte macrophage cell line

RHD	: Rel homology domain
RXR	: Retinoid X receptor
SD	: Standard deviation
SDS	: Sodium dodecyl sulphate
SDS-PAGE	: Sodium dodecyl sulphate polyacrylamide gel electrophoresis
SEM	: Standard error of the mean
Ser	: Serine
SOC	: Super optimal broth
SRC-1	: Steroid receptor coactivator-1
STAT	: Signal transducer and activator of transcription
T0070907	: 2-chloro-5-nitro-N-(4-pyridyl)benzamide
Tab2	: TAK1-binding proteins 2
TBL1	: Transducin- β -like 1
TBLR1	: TBL1-related protein
TBS-T	: Tris-buffered saline containing tween 20
TCM	: Traditional chinese medicine
TEMED	: N,N,N',N'-tetramethylethylene diamine
TNF- α	: Tumor necrosis factor alpha
TRADD	: Tumor necrosis factor receptor type 1-associated death domain
TRAF2	: TNF receptor-associated factor 2
TRAP220	: Thyroid hormone receptor-associated protein 220
TR-FRET	: Time-resolved fluorescence energy transfer
TRIS	: Tris(hydroxymethyl)aminomethane
UBD	: Ubiquitin-binding domain
VCAM	: Vascular cell adhesion molecule
VSMC	: Vascular smooth muscle cells
WY14643	: N-(3-[2-quinolinylmethoxy] phenyl)-trifluoromethanesulphonamide

3. PUBLICATIONS

Publications in peer-reviewed journals

- Fakhrudin, N., Ladurner, A., Atanasov, A.G., Heiss, E.H., Baumgartner, L., Markt, P., Schuster, D., Ellmerer, E.P., Wolber, G., Rollinger, J.M., Stuppner, H., and Dirsch, V.M., (2010), Computer-aided discovery, validation, and mechanistic characterization of novel neolignan activators of peroxisome proliferator-activated receptor γ , *Molecular Pharmacology* 77(4):559-566.
- Noha, S.M., Atanasov, A.G., Schuster, D., Markt, P., Fakhrudin, N., Heiss, E.H., Schrammel, O., Rollinger, J.M., Stuppner, H., Dirsch, V.M. and Wolber, G., (2011), Discovery of a novel IKK- β inhibitor by ligand-based virtual screening techniques. *Bioorganic & Medicinal Chemistry Letters* 21(1):577-583

Submitted manuscripts

- Helge Joa, H., Vogl S., Atanasov A.G., Zehl M., Nakel T., Fakhrudin N., Heiss E.H., Picker P., Urban E., Wawrosch C., Saukel J., Reznicek G., Kopp B., and Dirsch V.M., Identification of ostruthin from *Peucedanum ostruthium* rhizomes as an inhibitor of vascular smooth muscle cell proliferation (submitted).

Manuscripts in preparation

- In vivo and in vitro antiinflammatory properties of lignan derivatives isolated from *Ratanhiae radix*.
- Discovery of novel polyacetylenes activators of PPAR γ from *Notopterygium incisum*.

- Antidiabetic potential of fatty acids from the Chinese traditional medicines Tiān nán xīng and Bàn xià by activation of PPAR α , PPAR γ and AMPK
- Modulation of endothelial nitric oxide synthase activity by a benzofuran derivative isolated from *Krameria lappacea*

Oral presentation

- Fakhrudin, N., Ladurner, A., Atanasov, A.G., Heiss, E.H., Baumgartner, L., Markt, P., Schuster, D., Ellmerer, E.P., Wolber, G., Rollinger, J.M., Stuppner, H., Dirsch, V.M., Neolignans as novel PPAR-gamma agonists: a computational guided discovery, *International Symposium: Drugs from Nature Targeting Inflammation*, April 8th - 10th, 2010, Innsbruck, Tyrol, Austria.

Poster presentations

- Fakhrudin, N., Ladurner, A., Atanasov, A., Heiss, E., Baumgartner, L., Markt, P., Schuster, D., Ellmerer, E., Wolber, G., Rollinger, J., Stuppner, H., and Dirsch, V., Discovery and mechanistic characterization of neolignans as PPAR γ agonists, 35th Congress of the Federation-of-European-Biochemical-Societies, Gothenburg, Sweden, June 26th - July 1st, 2010.
- Fakhrudin, N., Vogl, S., Picker, P., Heiss, E.H., Saukel, J., Reznicek, G., Kopp, B., Atanasov, A.G., Dirsch, V.M., 2009, Luciferase reporter gene assays for discovery of peroxisome proliferator-activated receptor- α and - γ agonists and nuclear factor- κ B inhibitors from medicinal plants. *The International Conference on Pharmacy and Advance Pharmaceutical Sciences*, October 5th-6th, 2009, Gadjah Mada University, Yogyakarta, Indonesia.
- Fakhrudin, N., Vogl, S., Picker, P., Heiss, E.H., Saukel, J., Reznicek, G., Kopp, B., Atanasov, A., Dirsch, V.M., Screening for discovery of novel

peroxisome proliferator-activated receptor-alpha and -gamma agonists and nuclear factor- κ B inhibitors by luciferase reporter gene assays, *21st Scientific Congress of the Austrian Pharmaceutical Society*, April 16th-18th, 2009, Vienna, Austria

- Baumgartner, L., Sosa, S., Fakhrudin, N., Ladurner, A., Atanasov, A.G., Heiss, E.H., Widowitz, U., Schuster, D., Rollinger, J.M., Wolber, G., Bauer, R., Dirsch, V., Tubaro, A., Stuppner, H., Evaluation of the antiinflammatory properties of secondary metabolites from *Ratanhiae radix*, *International Symposium: Drugs from Nature Targeting Inflammation*, April 8th- 10th, 2010, Innsbruck, Tyrol, Austria.
- Rozema, E., Fakhrudin, N., Atanasov, A.G., Schuster, D., Heiss, E.H., Sonderegger, H., Krieg, C., Gruber, C.W., Huck, C.W., Urban, E., Dirsch, V.M., Bonn, G.K., Kopp, B. Bioactive fatty acids and cerebrosides from the TCM drug *Arisaema* sp., *7th Tannin Conference / 58th International Congress and Annual Meeting of the Society-for-Medical-Plant-and-Natural-Product-Research*, August 29th - September 2th, 2010, Berlin, Germany.
- Rozema, E., Fakhrudin, N., Atanasov, A.G., Schuster, D., Heiss, E.H., Sonderegger, H., Krieg, C., Gruber, C.W., Huck, C.W., Urban, E., Dirsch, V.M., Bonn, G.K., Kopp, B., Bioactive fatty acids and cerebrosides from the TCM drug *Arisaema* sp., *Metabolomics 2010*, June 27th - July 1st, 2010, Amsterdam, The Netherlands.
- Picker, P., Vogl, S., Fakhrudin, N., Atanasov, A., Heiss, E., Reznicek, G., Saukel, J., Wawrosch, C., Dirsch, V.M., Kopp, B., Screening of 35 plants used in Austrian folk smedicine for PPAR α and γ activation and NF- κ B inhibition, *57th International Congress and Annual Meeting of the Society for Medicinal Plant and Natural Product Research*, August 16th-20th, 2009, Geneva, Switzerland.

- Vogl, S., Picker, P., Fakhrudin, N., Atanasov, A., Heiss, E., Reznicek, G., Saukel, J., Wawrosch, C., Dirsch, V.M., Kopp, B., Influence of chlorophyll and tannins from plant extracts on cell-based luciferase reporter gene assays, *57th International Congress and Annual Meeting of the Society for Medicinal Plant and Natural Product Research*, August 16th–20th, 2009, Geneva, Switzerland.
- Baumgartner, L., Fakhrudin, N., Atanasov, A., Heiss, E., Schwaiger, S., Ellmerer, E.P., Rollinger, J.M., Dirsch, V.M., Stuppner, H., Discovery of benzofuran derivatives in *Ratanhiae radix* as novel inhibitors of NF-κB activation, *57th International Congress and Annual Meeting of the Society for Medicinal Plant and Natural Product Research*, August 16th–20th, 2009, Geneva, Switzerland.

4. CURRICULUM VITAE

Personal information

Full name : Nanang Fakhrudin.
Birth date : 20 February 1980, in Klaten, Indonesia
Nationality : Indonesian

Educational background

08/1998-02/2003, Bachelor of Pharmacy, Faculty of Pharmacy, Gadjah Mada University, Yogyakarta, Indonesia.

03/2003-02/2004, Pharmacist (licence), Faculty of Pharmacy, Gadjah Mada University, Yogyakarta, Indonesia.

03/2004-02/2006, Master of Science, Faculty of Pharmacy, Gadjah Mada University, Indonesia.

Since 11/2007, PhD thesis at the Molecular Target Group, Department of Pharmacognosy, University of Vienna, under the direction of Prof. Verena Dirsch.

Scientific stays

08/2000-02/2003, Assistant for practical training for students in Faculty of Pharmacy, Gadjah Mada University, Yogyakarta, Indonesia

03/2003-08/2010, Junior lecturer in the Department of Pharmaceutical Biology, Faculty of Pharmacy, Gadjah Mada University, Yogyakarta, Indonesia.

Since 09/2010, Permanent the lecturer in Department of Pharmaceutical Biology, Faculty of Pharmacy, Gadjah Mada University, Yogyakarta, Indonesia.

Professional memberships

Since 2009, Austrian Association of Molecular Life Sciences and Biotechnology (ÖGMBT)

Since 2004, Indonesia Pharmacists Association (ISFI)

Other activities

Winter semester 2009-2010 and summer semester 2010, laboratory training for diploma students in the Department of Pharmacognosy, University of Vienna.

5. ACKNOWLEDGMENTS

First and foremost, I owe my deepest gratitude to my supervisor, Prof. Dr. Verena Dirsch, for excellent supervision and support during my study in Vienna. She gambled by accepting me as a Doctorate student in her group. I am very grateful for the trust given to take part in the NFN project

Sincere thanks to Dr. Atanas Atanasov and Dr. Elke Heiss for their support, expert guidance, helpful discussion, and also for the critical reading of this manuscript with insightful comments and suggestions. Their presence in the laboratory has been meaningful for me throughout the research period.

I would like to thank Prof. Dr Hermann Stuppner, Prof. Dr. Brigitte Kopp, Prof. Dr. Rudolf Bauer, Prof. Dr. Judith Rollinger, Prof. Dr. Gottfried Reznicek, and their groups within NFN project for performing phytochemical work; Prof. Dr. Johannes Saukel for correct botanical identification and collection of the tested plants, as well as Prof. Dr. Gerhard Wolber and his group for performing computational studies.

Special thanks to Prof. Dr. Oliver Werz and Prof. Dr. Irmgard Merfort as official reviewers of this dissertation.

It would not have been possible to write this doctoral thesis and get the meaningful data without the help and support of the kind people around me whom I would like to thank at this point: Mario Kumerz, for the introduction to the basic cell culture techniques when I started to work in the laboratory; Renate Baumgartner, for the meaningful friendship and for the kind introduction to the Austrian and western culture; Helge Joa for every fun given to live up our laboratory and for the unforgettable tea time; Angela Ladurner for working together in the first publication; and other members of “molecular target” group: Yvonne

Schilder, Christoph Schmitt, Cornelia Schreiner, Irene Sroka, Matthias Kramer, Andrea Schwaiberger and Tina Oberan for the wonderful and friendly atmosphere.

I am very much obliged to Judith Benedict and Elisabeth Geiger for their kind help in performing the screening assays; Daniel Schachner, Hortenzia Beres and Rebecca Leitner for excellent technical assistance; and Andrea Szabo who keeps everything in order and manages administrative stuff. I would also thank to all diploma students who contributed to this work: Olivia Schrammel and Anna Grzywacz for the contribution to the NF- κ B inhibitor assays, Christian Maier and Ursula Bauer for the contribution to the PPAR assays.

In addition, I thank all colleagues at the Department of Pharmacognosy (Phytochemistry and Botany group) for enjoyable times and beautiful memories built during our interaction.

It is a pleasure to thank the Austrian Federal Ministry for Science and Research, The Austrian Science Fund (FWF), OeAD (Österreichische Austauschdienst), Directorate General of Higher Education, Ministry of National Education, Indonesia, for the granted scholarships and support.

As a lecturer, I would like to thank Prof. Dr. Marchaban, DEA., Apt., Dean of Faculty of Pharmacy, Gadjah Mada University, and Prof. Ir. Sudjarwadi, M. Eng., Ph.D., Rector of Gadjah Mada University, Indonesia; for giving me the opportunity and permission to take part in a Doctorate program in Vienna.

I am heartily thankful to my lovely wife for the trust given, the fidelity in the bad and good situations, the great patience at all times, and most importantly, for taking care of our children. I acknowledge my children: Fatiya Izzati and Fauzia Ulinuha for sacrificing their golden time for me, I love you all. I am also indebted to my parents and my sisters who always pray for me and have given me their unequivocal support throughout.

Lastly, I offer my regards and blessings to all of those who contributed to this work and help me in any respect.

Vienna, February 2011

Verily, along with hardship is relief
(Q.S. Ash-Sharh).